Building Integrated Low Impact ICT Networks

Matthew Stewart B.Eng., M.Sc.

A thesis submitted for the

Degree of Doctor of Philosophy

BRE Centre of Excellence in Energy Utilisation

Department of Mechanical and Aerospace Engineering

University of Strathclyde

October 2011

COPYRIGHT DECLARATION

This thesis is the result of the author's original research. It has been composed by the author and has not been previously submitted for examination which has led to the award of a degree.

Signed: Date:

Simplicity is the ultimate form of sophistication

Leonardo Da Vinci

ACKNOWLEDGEMENTS

I would like to express my sincere gratitude to my supervisor, Professor John Counsell for his guidance and never ending enthusiasm throughout the course of this work and for proofreading the resulting thesis.

I am also very grateful to the BRE Trust who funded this research.

My thanks also go to fellow BRE centre researchers for their feedback and discussions on the many aspects of this field. Thanks also go to the ESRU and university staff and researchers. In particular, I would like to thank Cameron Johnstone for his early advice on how to approach problems of pachyderm proportions and Dr Jun Hong for introducing me to the many subtle issues in this area.

Many thanks also go to Ian Porter for his effort in professionally coding up the software to implement the control and to Chris-Haughton Brown in raising the commercial profile of the concept early on.

I would also like to thank many BRE Group staff throughout the organisation for their continuing encouragement, support and discussions; Rufus Logan and Andrew Williams in particular for sharing their viewpoints and experience. These and many others have brought a commercial aspect to the work and helped guide the focus and evolution of the system.

I am also grateful to BRE for including me as co-inventor in the application for patent of the resultant new knowledge and for continuing to fund my involvement in future exploitation of the work.

Finally, I would like to thank my family, whose patience and understanding were invaluable to me throughout this period. Without their support, this thesis would not have been completed.

TABLE OF CONTENTS

LIST OF FIGURES

LIST OF TABLES

NOMENCLATURE

Symbol	Definition
q	Fundamental charge (C)
k	Boltzmann constant (J/K)
σ	Stephan Boltzmann constant $\left(W \cdot K^4/m^2\right)$
ε	Emissivity
α	Absorptivity
β	Reflectance
γ	Transmittance
ρ	Ground reflectance
I	Current (A)
I_0	Diode saturation current (A)
I_{ph}, I_{SC}	Photon induced short circuit current (A)
I_{SCref}	Rated short circuit current (A)
I_{mp}	Maximum power current (A)
I_{mp}	Rated maximum power current (A)
I_d	Total appliance current (A)
I_L	Appliance load current (A)
I_C	Appliance battery charging current (A)
i	Instantaneous current (A)
V	Voltage (V)
V_{OC}	Open circuit voltage (V)
V_{OCref}	Rated open circuit voltage (V)

V_{mp}	Maximum power voltage (V)
V_{mpref}	Rated maximum power voltage (V)
V_t	Thermal voltage (V)
V_g	Band gap voltage (V)
V_d	Appliance voltage (V)
v	Instantaneous voltage (V)
n	Diode factor
R_{pc}	Parallel resistance per PV cell (Ω)
R_{Sc}	Series resistance per PV cell (Ω)
G	Irradiance $\left(W/m^2\right)$
G_{ref}	Reference irradiance $\left(W/m^2\right)$
G_{DN}	Direct normal irradiance $\left(W/m^2\right)$
G_{DH}	Diffuse horizontal irradiance $\left(W/m^2\right)$
$T, T_c, T_{\text{module}}$	Cell or module temperature (K)
T_{ref}	Reference cell temperature (K)
T_{amb}	Ambient Temperature (K)
a_i	Coefficient of current
N_s	Series connected cells
C_{FF}	Fill factor coefficient
C_{module}	Module heat capacity (J/K)
C_m	Module specific heat capacity (J/kgK)
ρ_m	Module density $\left(kg/m^3\right)$
d_m	Module depth (m)

A	Module area $\left(m^2\right)$
q_{sw}	Short wave energy transfer rate $\left(J/s\right)$
q_{lw}	Long wave energy transfer rate $\left(J/s\right)$
q_{conv}	Convective energy transfer rate $\left(J/s\right)$
P_{out}, P_{PV}	PV output $\left(W\right)$
P_G	Power transfer across system boundary $\left(W\right)$
P_D	Total demand power $\left(W\right)$
h_c	Heat transfer coefficient $\left(W/m^2K\right)$
$h_{c,\,free}$	Free convective heat transfer coefficient $\left(W/m^2K\right)$
$h_{c,\,forced}$	Forced convective heat transfer coefficient $\left(W/m^2K\right)$
θ	Angle of incidence $\left(\text{degrees}\right)$
τ	Angle of tilt $\left(\text{degrees}\right)$
η_{inv}	Inverter efficiency
$\eta_{\max}$	Rated inverter efficiency
pL	Percent loading
CE	Carbon Emissions $\left(kgCO2\right)$
CI	Carbon intensity $\left(gCO2/J\right)$
E	Energy $\left(J\right)$
t	Time $\left(s\right)$

Abbreviations

AC	Alternating Current
AMR	Automatic Meter Reading
AWG	American Wire Gauge
BAPV	Building Applied Photovoltaics
BIOS	Basic Input/output System
BIPV	Building Integrated Photovoltaics
CAT	Cable Category
CM	Condition Monitoring
CO2	Carbon Dioxide
CO2e	Carbon Dioxide Equivalent
CRC	Carbon Reduction Commitment Scheme
DC	Direct Current
DM	Demand Management
DNO	Distribution Network Operator
DSM	Demand Side Management
DSR	Demand Side Response
FiT	Feed-in Tariff
GPS	Global Positioning System
GSM	Global System for Mobile Communications
GUI	Graphical User Interface
HVAC	Heating Ventilation Air Conditioning
ICT	Information and Communications Technologies
IP	Internet Protocol
LAN	Local Area Network
LED	Light Emitting Diode

LCD	Liquid Crystal Display
MIB	Management Information Base
MPP	Maximum Power Point
MPPT	Maximum Power Point Tracker
PD	Powered Device
PDF	Pseudo Derivative Feedback
PID	Proportional Integral Derivative
PoE	Type 1 Power over Ethernet
PoE+	Type 2 Power over Ethernet
PSE	Power Source Equipment
PSU	Power Supply Unit
PTZ	Pan Tilt Zoom
RAM	Random Access Memory
RE	Renewable Energy
ROC	Renewable Energy Certificate
RPS	Redundant Power Supply
RTP	Real Time Pricing
SISO	Single Input Single Output
SME	Small medium enterprise
SOC	Battery State of Charge
STP	Shielded Twisted Pair Cable
TOU	Time of Use
UPS	Uninterruptible Power Supplies
USB	Universal Serial Bus
UTP	Unshielded Twisted Pair Cable
UHF	Ultra High Frequency
VoIP	Voice over Internet Protocol
WOL	Wake-on LAN

ABSTRACT

Urban renewable energy systems are being deployed at an increasing rate in the UK and worldwide as corporations and homeowners alike respond to legislation and incentives to reduce their carbon emissions in mitigation of climate change.

However, the uncertain nature in time and magnitude of building integrated renewable energy generation coupled with an equally uncertain building level demand means that local matching and utilisation of this potentially high value low carbon electricity resource is difficult to achieve with any reliability at short timescales and so not only is the full value of the renewable asset not realised but neither is the potential value of flexible demand assets. The research undertaken in this thesis centres on increasing the potential for exploitation of building integrated resources to address this issue.

This thesis is focused on development of a novel form of building integrated asset management controller which takes these real world uncertainties into account in matching flexible demand with an intermittent renewable supply with the twin objectives of minimising carbon emissions and unnecessary import/ export of electrical energy and hence reducing the overall impact of demand for electricity. The proposed controller is aimed at control of fleets of appliances at the building level and can operate independently of any third party.

The network design characteristics and deployment technologies of this novel control strategy are detailed with focus on application to industry standard networks of low power mobile computing devices and other flexible demands in office buildings.

Finally, a case study demonstration of the control as integrated within an ICT network shows how the control operates in practice to minimise the cost and carbon emissions impact of electricity consumption by actively matching renewable generation with demand in a consistent and reliable manner.

The thesis concludes with suggestions for further work and potential applications of the control method.

CHAPTER 1 - ELECTRICITY AND CARBON IN BUILDINGS

This chapter presents the findings of the initial literary review by way of background and introduction. The review looks at electricity consumption and carbon dioxide emissions in commercial office buildings, focusing on the impact of a specific category of appliances. Methods of managing these appliances in energy networks are discussed. A framework of interventions is highlighted to reduce waste of and dependence on the incumbent expensive and carbon intensive electricity supply structure. The proposed solution aims to incentivise owners of renewable generators through increasing the value of total ownership by utilising building integrated appliance assets within a controlled and bounded environment to minimise carbon dioxide (CO2) impact.

1.1. INTRODUCTION

We live in interesting times. At no previous point in human history has our impact on the environment we live in been so acutely in conflict with the harsh economics of supplying our ever increasing demand for energy, nor has our ability to influence this complex balance been so critical to future generations. Neither however, has our awareness and understanding been greater or the options available to us in pursuing the goal of a sustainable, low-carbon future through effective utilisation of the resources available.

The now infamous ‘hockey stick’ graph (Figure 1-1) of CO2 concentrations in our atmosphere over time needs little introduction [IPCC 2007]. This is almost certainly a man-made environmental consequence of our relatively recent progress – what we define as modern civilisation. It represents our preference and shift towards urban dwelling with all of the comforts and conveniences that living and working in cities can provide. We concentrate much of our energy and resources in providing these services

within buildings. Finding a sustainable balance in this relationship between buildings, energy and the environment will perhaps be our greatest achievement.

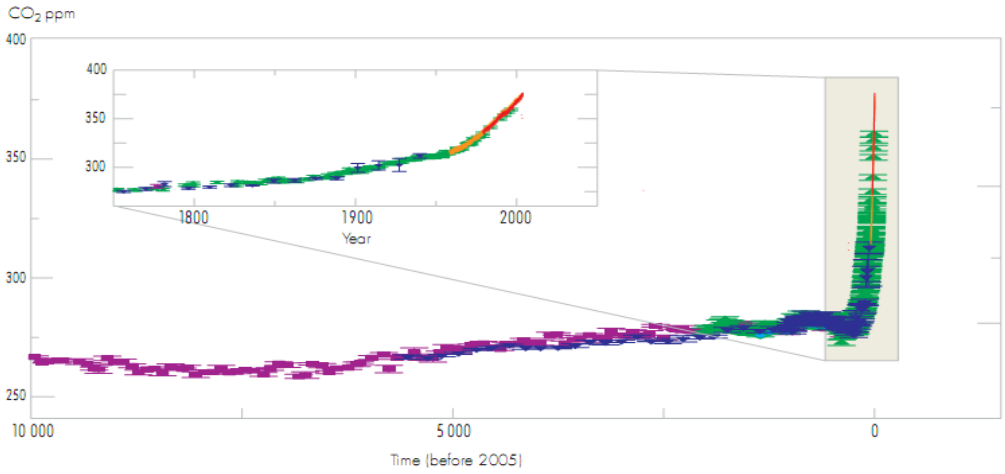

Figure 1-1 Atmospheric CO2 Concentrations over Time [Source: IPCC]

1.2. ELECTRICITY DEMAND AND EMISSIONS IN OFFICES

The UK's Department of Energy and Climate Change (DECC) states that carbon dioxide emissions resulting from energy use in the service sector represented 16% of the UK's total emissions in 2009, equating to around 110MtCO2e emissions [DECC 2011].

Although there has been a recent and rapid decline in the energy used for heating particularly in new build commercial buildings due to regulation and improving building standards, figures from the Carbon Trust state that electrical energy consumption of the UK service sector has doubled since 1990 to a present figure of 85,000,000 MWh per annum and is predicted to double again by 2020 [Carbon Trust 2010]. There are many reasons and assumptions behind this statement but two key and related trends identified for high and rising demand for electrical energy in commercial, other offices and buildings in general are the increasing ownership and use of consumer electronics equipment, computers and other information and communications technologies (ICT) and an explosion in using ubiquitous communications networks. The

incredible value of ICT and consumer electronics equipment to users in the home, workplace and to the economy has gone in tandem with increasing saturation of local data networks interconnecting ICT devices within a building (LAN) and connecting the building to ICT devices in other buildings across the globe. Since opening its domains for public use in 1994, the internet in 2011 reaches 2 billion users worldwide and the communications and data services that this group of technologies provide are now so entrenched that most businesses and many other services would simply cease to function without it. According to ITU statistics, domestic access to this service in the UK has rapidly grown from around 15 million users in 2000 to 50 million in 2010, representing over 80% of households with effectively total saturation in office buildings [ITU 2011]. From almost zero 20 years ago, energy consumption of the ICT sector in the UK in 2009 stood at an estimated 7% of total UK electricity demand and around 4% of total CO2 emissions [DECC 2009]. Although the majority of ICT energy is cited by DECC as being used in the home and might suggest a continuing primary strategic focus of targeting domestic energy use, the assertion is that by virtue of its already present connectivity, demand management of appliances in the ICT sector offers a softer target and perhaps focus should shift more towards how power to growing numbers of ICT and digital equipment in these buildings is delivered and managed. As discussed at length in later chapters, the ICT industry themselves already have a potential solution deployed in almost every commercial building worldwide.

1.2.1. ICT Networks and Appliances in Buildings

Design of a modern office building will include provision for ICT equipment at the early design stage. This process will include reservation of space (and power requirement) for switch rooms and routing through a building for perhaps many hundreds of kilometres of dedicated cabling connecting ICT devices to equipment in the switch room. Network or Ethernet switches represent a critical point of failure in the flow of information between devices both internally and externally and are therefore preferably located in dedicated, climate controlled rooms or areas. Such is the importance of these devices that owners also often invest significant additional capital

in dedicated cooling, back-up generation, so-called uninterruptible power supplies (UPS) and perhaps several other layers of power and data redundancy, monitoring and control to ensure continuity. The hardware cost alone of ensuring this level of security can be several hundreds of pounds for each individual port and there may be thousands of ports in an office building. These ancillary systems also contribute to the energy consumption of the switch room. In operation, Gartner states that the average switch room in a medium sized small-medium enterprise (SME) commercial building, including its cooling energy requirement, accounts for around 5% of the total electricity consumption for the building [Gartner 2009]. This figure is proportional to the number of networked devices and can be much higher depending on the business type.

Globally, from around 400 million devices in 2000, worldwide ownership of personal computers passed the 1 billion mark in 2007 and 2 billion in 2010, giving the ICT sector as a whole its fourth trillion dollar industry after televisions, mobile phones and the internet itself. Present revisions on the rate of expansion of this market predict that as China and India continue to develop, PC ownership worldwide will top 4 billion machines by 2016 [Forrester 2010]. This high rate of saturation is reflected in the numbers of employees who use these devices in their daily work. The percentage of workers in an office building who regularly use a personal computer (PC) to do their work has rapidly grown to 80% or around 17 million employees in the UK alone, comparing with 31 million employees in Germany and 108 million employees in the US. This high level of penetration is assumed at least echoed, if not surpassed, in Japan, Korea and other developed economies [Gartner 2009]. In terms of energy consumption, a report by BERR puts computing on the office floor at 15% of the total electricity demand for a typical commercial building and also states that of this figure; 40% (6% of total building electricity demand) is explicitly due to appliances on the office desk; the PC and monitor [BERR 2010].

Such high penetration of these devices in offices is not without its drawbacks however. If the not unreasonable assumption is made that computing contributes to heating the office environment by its energy use of 15%, and that half of total cooling energy is also due to the use of office ICT, the total impact of ICT equipment plus the server room is approaching 50% of the total consumption of the building. Obviously, the proportions

used to arrive at the figures used above vary by office, location and more than a few other factors but the fact remains that energy consumption of heating and cooling plant in offices is geared in some proportion around the use of computers on the office desk.

In the last few years, the increase in density of ICT equipment in modern office buildings (plus a fashion for large areas of glazing) has been blamed for causing overheating in an increasing number of cases; the 'Gherkin' building in London being a well-publicised example where working conditions can be such during summer months that productivity in some zones stops due to health and safety restrictions despite the cooling plant operating at maximum. The energy density of the building is so high during these times that voltage sag occurs along the entire local distribution network which then impacts on the quality of electricity delivered to neighbouring buildings and also causes further upstream problems for the utility.

1.3. POLICY TRENDS IMPACT

Public and private sector buildings in the UK have been set a target 39% reduction in present emissions levels by 2020 through the CRC Energy Efficiency Scheme. The intention of the CRC scheme is to financially incentivise building owners to reduce their carbon emissions based on consumption levels relative to a previous recorded level (through an Energy Performance Certificate, EPC) and also relative to other businesses, in theory creating a transparent league table of polluters [DECC]. Through this mechanism, energy reductions are expected to continue due to improvements in the building fabric and design but also in use through informed appliance procurement policies, active management of energy waste and other control opportunities.

Given previous success in driving efficiency in white goods, the ICT and consumer electronics industries are also adopting clear low carbon market drivers for their products in the form of similar voluntary energy labelling initiatives such as Energy Star and the EC's all-encompassing mandatory Energy using Products (EuP) directive on an increasing number and range of ICT and consumer electronics devices. In conjunction with the related WEEE, RoHS and other directives, the result is a drive away from

products with high embodied carbon and over-specification of functionality towards a streamlined device fit for purpose and of lower energy consumption and lighter CO2 footprint.

Among the simplest and more obvious operational efficiency measures is for users to switch devices off when not needed. Analysts 1E highlighted a 2007 survey whose results indicated that of the UK's employees who use a computer at work, 50% do not switch the device off when they go home for various reasons. The poll also noted that of those UK respondents who do power down at night, only 20% do so through company policy; less than the 27% who cited personal ethical reasons [1E 2007]. However, the potential savings accrued by switching off should not be underestimated. Using figures from the UK's Market Transformation Programme, the Carbon Trust concluded that up to 70% of office ICT energy consumption is wasted energy due to the devices being left on and in idle mode. These figures and associated emissions are summarised in Table 1-1 for single devices.

Working from home or elsewhere outside the office can potentially solve a number of problems; alleviating pressure in a cramped office or perhaps fitting better with an employee's preferred lifestyle. Present trends in computing devices are reflecting these changes with increasing sales of laptop, notebook and tablet class devices over fixed desktop PCs in the workplace.

Item	Average Daily Energy Consumption (kWh)	Annual Energy Consumption (kWh/yr)	Active Hours Run per day (hrs)	Average Annual Cost per Device	Carbon Emission Equivalent per device
Laptop(1)	0.960	350	24	£38.5	188kg CO_2
PC	1.12	411	24	£45	221kg CO_2
Monitor	0.936	341	24	£38	183kg CO_2
Multi-Function Device (Thermal)	2.8	1022	5.2	£112	548kg CO_2
Multifunction Device	0.72	261	9	£29	140kg CO_2
Photocopiers	5.1	1,861	24	£204.8	999kg CO_2

Table 1-1 Office ICT Energy Consumption and Emissions [Source: Carbon Trust]

Although not classed in the same way (and not yet compared to laptops or notebooks in any detail), recent trends in ownership and capabilities of smart phones are also significant. The smart-phone market in 2010/11 was almost 50% of all mobile phones sold, representing 1 billion handsets. The capabilities of these devices are also improving at pace; so much so that the defining line between a notebook or thin client class PC and a high end mobile phone is fast becoming blurry and in the next few years will likely become irrelevant. Several manufacturers have released products in 2011 which feature a dual core processor with clock speeds over 1GHz with one already announcing a dual core 2GHz device on sale by 2012, putting the computing and communications capabilities of a smart phone device almost on a par with low end enterprise class PCs but at a power rating of 2W maximum.

The defining feature of a mobile device is a battery and is a strong selling point for manufacturers. The trend towards mobile devices is therefore placing significant amounts of high grade energy storage on the office desk, typically enough to power the devices for around 5 hours untethered. Fixed UPS devices in the switch room also add to the potential ICT capacity by a few hours.

Although these and many similar trends indicate a resounding success for the ICT and consumer electronics industries, it would appear that the impact on the office working environment may end up going from one extreme to the other. Jenkins researched the effect of the predicted trends in ICT equipment energy consumption and dissipation as heat in well insulated office buildings and included the assumed effects of warming of the UK climate on heating and cooling system energy consumption through to 2030. The research also assumed nominal figures for power consumption and usage of the most common ICT devices and that power saving controls would be used in future networks. A significant conclusion from this work is the implication that due to drastically reduced energy dissipation as heat in the office due to low power ICT, energy requirement for cooling will decrease by 50% by 2030 but that energy for heating will almost triple in the same time with the overall result being a significant increase in the total electricity consumption of an office building, particularly in the north [Jenkins et al 2007]. An additional and at least as important conclusion from this

work is that sensitivity of environmental controls to occupancy is greatly increased. The effect is that gains in the office will be much more dynamic which then impacts on the relevance of present environmental control strategies.

If anything, Jenkins has likely underestimated the magnitude of this change and rate at which change will occur. For example, Jenkins critical assumption (in 2007) that an average 2030 PC would only require 60W was already surpassed for enterprise class machines by 2009. The recent trend for cloud computing and use of thin client machines also represents an additional dynamic. By shifting data processing off the machine to a central mainframe, the power consumption of PCs on the desk can be as low as 15W with a growing number of devices less than 10W, in 2010. Further, the potential effect of being absent from the office altogether through mobile working practices was not considered.

Perhaps an important lesson from this and other studies on the ICT impact on buildings is that product evolution, new devices, power consumption and therefore impact on a building cannot be predicted by more than a few years at most. There is, therefore, a bit of a dilemma facing architects and designers of office buildings regarding sizing of heating and cooling plant necessary to maintain comfort given the trends in ICT identified as well as a dilemma for building operators on how to control plant to maintain comfort. This is perhaps offset somewhat by the increased potential for control of high grade energy storage in ICT intensive environments.

1.4. CARBON INTENSITY OF ELECTRICITY SUPPLY

Reducing the energy use, waste and subsequent emissions inside the building is only one half of the problem however and in theory, there could be zero emissions from electricity use if there were none attached to generation and delivery of this energy in the first place. Although an idealistic statement, the fact remains that the set-point carbon intensity of electricity on which emissions penalties in buildings are based is not determined by the consumer but by plant investment decisions made by private companies in the power sector.

The UK's grid operator (National Grid) publishes an annual carbon intensity (CI) figure based on usage proportions of the different generator types, efficiency, utilisation ratio, part loading factors and includes pumped hydro and interconnectors with other countries. Nominal carbon emissions figures from each main generator type by fuel are summarised in Figure 1-2 and for 2010 resulted in an annual average figure of 0.536kg/kWh from which calculation of carbon emissions across all electricity users is based.

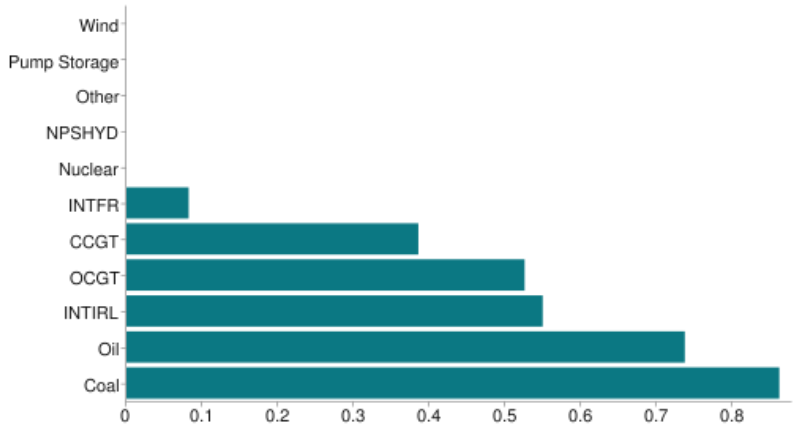

Figure 1-2 Nominal Carbon Intensity of Large Generating Plant in UK (2010) [Source: DECC]

DECC puts total emissions solely from the UK electricity supply sector at 34% of all generation in 2009, representing around 250MtCO2 equivalent and by far the largest share of emissions by sector [DECC 2011].

1.4.1. Integration of Large Scale Renewables

In contribution to reduction in emissions from electricity generation, the UK's Committee on Climate Change (CCC) have recommended that emissions from the power sector including generation, transmission and distribution of electrical energy need to reduce by 40% from current levels by 2020 in order that the UK meet its EU agreed reduction in CO2 emissions [CCC CH4, 2009]. In terms of generation mix, this

figure represents a shift from 6% (4GWe) renewables penetration in 2009 to over 30% (23GWe) by 2020. Should the forecast by the CCC prove accurate, the carbon intensity of the UK electricity network is predicted to drop from its present annual average value of 0.536kg/kWh to 0.33kg/kWh by 2020. This might, at first, sound like good news but there are many issues to address before this low carbon vision can become a reality. These issues relate to the intermittent nature of renewable generation and how the resulting uncertainty is managed.

In a well-publicised study of Danish wind, Sharman states that despite being distributed, wind fleets function effectively as one power station with rapid power transients and extended periods of zero or near zero output across the whole country [Sharman et al 2005]. This scenario is already familiar to the UK; on 6th September 2010, the combined output of the UKs wind generation fleet peaked at a (then) record 1.86GW, accounting for 4.7% of total UK generation at that moment and a capacity factor of 40% [BWEA 2010]. On 29th March 2011, the combined output was 20MW [ELEXON 2011]. Modelling by Oswald et al of a 25GW wind fleet in and around the UK concluded that even a 25GW wind power fleet would contribute little or no reliable capacity [Oswald et al 2008]. The effect for the utilities is that spot prices will be highly volatile which in turn forces the remaining fossil plants to run at lower efficiency. Bach et al goes on to conclude that such high levels of wind generators can therefore only realistically become viable in an EU supergrid context – a network which will be decades before becoming a reality [Bach et al 2009]. The strong suggestion from Bach and others is that excess low carbon wind will be treated as an unwanted disturbance on the network which will be exported. An alternative to export proposed by MacDonald et al uses embedded energy storage on the network to absorb both intermittency and any other sources of fluctuation in the power network using grid frequency [MacDonald et al 2005].

This apparently low relative value of excess wind energy is also seen in a mechanism recently and increasingly forced into use by the operator which removes unwanted excess generation by paying wind farm operators substantially more than their energy is otherwise worth to disconnect from the network [BWEA 2011] rather than pay even more to scheduled generators in contract cancellation fees. Although this may change in

the future with an anticipated rise in the market value of carbon, it will only be reversed since conventional gas generators will then be asked to disconnect but remain on standby or run at part load , utilising both the plant and primary fuel inefficiently. Management of intermittency is therefore key to reducing the carbon intensity of electricity but due to the inflexibility of the present settlement system, utilities require heavy and sustained investment in back-up conventional plant and strengthening and extending the infrastructure to deal with the problem. Price, Waterhouse & Cooper (PWC) in 2010 states that the UK is likely to miss the 2020 target by a significant margin and highlights annual roll out of wind is presently less than half of the rate needed, concluding that an estimated investment of £10 billion per annum over the next decade is required to put the sector (and emissions reductions from generation) back on track [PWC 2010]. This widely accepted figure represents a 10% annual increase in electricity costs to the consumer for the next decade. However, bearing in mind that there is only coincidental correlation between low carbon wind generation and demand [POYRY 2009], are consumers making the right investment choice in continuing to support a system and infrastructure which, by its nature, cannot readily give the customer the low cost low impact product desired?

1.4.2. Building Integrated Renewables

Carbon intensive electricity consumption in buildings can also be off-set by investing in a local renewable source of power. Over 75 countries, states and provinces around the world are presently offering some sort of feed-in tariff (FiT) as a financial incentive to encourage ownership of a building integrated renewable supply [NREL 2010]. According to the NREL report, these various FiT mechanisms are responsible for 75% of all solar PV and 45% of all wind developments worldwide, indicating the importance of this mechanism in stimulating a new market.

Until recently, the UK's policy mechanisms on renewable energy were only geared towards utilities and large investors through the Renewables Obligation (RO) scheme. This rather complex scheme is primarily aimed at the seemingly dubious business

strategy of trading emissions through RO certificates (ROCs) in an EU trading market (EU ETS). Through the 2008 Energy Act and 2009 Renewable Energy Strategy, the UK's Feed-in Tariff (FiT) or Clean Energy Cashback scheme is aimed at encouraging businesses and individuals to invest in a local low carbon generating technology by providing a financial return on a long term contract of 25 years and tied to inflation [DECC 2011]. A range of plant is covered by the FiT with return on investment based on a weighting for each type of plant and scale of installation. Delivery of the FiT is via the Micro-generation Certification Scheme (MCS), administered on behalf of the government by BRE and specifies compliance with component quality standards, safety and quality of installation. This is seen as a natural progression by micro-renewable technologies indicating shift towards a more commercial and systems oriented market structure.

1.5. DEMAND MANAGEMENT

Management and control of devices and appliances in buildings to reduce energy waste or optimise cost is a well-researched and increasingly active area and many mechanisms and system solutions exist with more proposed each year. Demand management methods can be separated broadly into two categories; emergency load restriction strategies where the consumer is financially reimbursed for accepting an agreed level of disruption and on-going load management strategies which aim to incentivise longer term behavioural changes and consumption patterns [IEA 2005]. The aim of system design in longer term demand management has therefore concentrated on minimising impact on consumers by utilising some form of energy storage within the building.

A breakdown of electricity consumption by appliance type for domestic and commercial buildings is given in Figure 1-3 and Figure 1-4 using recent data from DECC and BERR and indicates significant potential for appliance level control in these two building types.

Traditionally, only storage heating, hot water and wet storage heating were of sufficient capacity to be worth the investment but latterly, researchers and commercial systems

have become available which control capacity in cold appliances, wet appliances and even using the thermal capacity of the building structure itself. Significantly for this study, note the relative scales of ICT, computing and consumer electronics in these charts to other identified demand management (DM) targets.

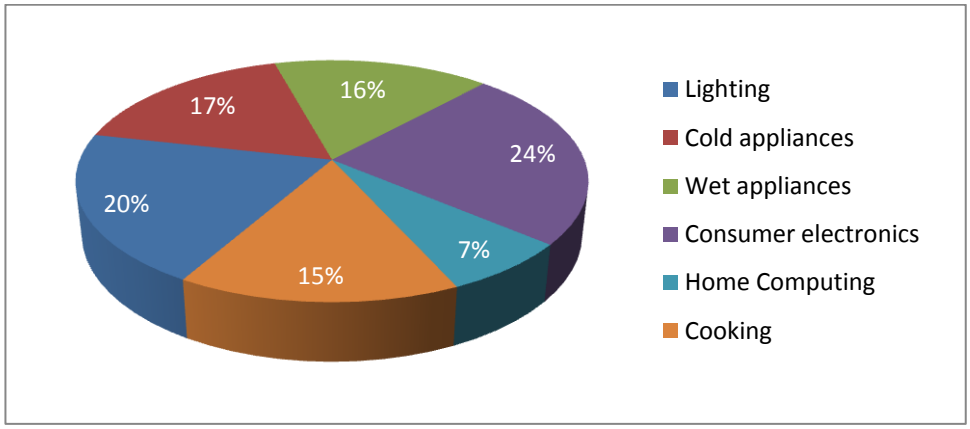

Figure 1-3 Electricity Consumption in UK Domestic Buildings by Appliance Category

Source: DECC Energy Consumption in the UK, Domestic data tables, 2009 Update

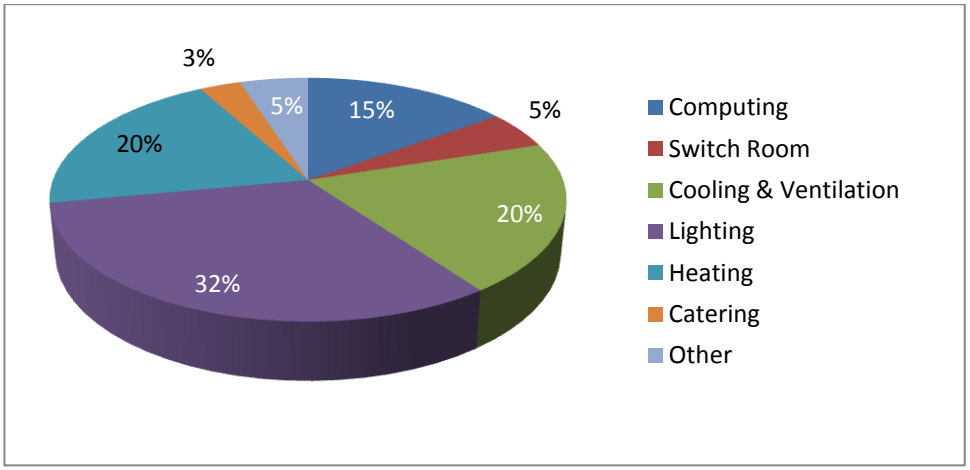

Figure 1-4 Electricity Consumption in UK Commercial Buildings by Appliance Category

Energy consumption in the United Kingdom, 2008 Update Pub URN 08/456 – Department for Business Enterprise & Regulatory Reform

1.5.1. Utility Driven Demand Management

The UK's Carbon Emissions Reduction Target (CERT) programme is aimed at incentivising utilities to reduce emissions from demand in domestic dwellings [DECC 2010]. This seemingly contradictory task intends to use a number of measures to encourage electricity users to reduce and adjust their consumption patterns, including raising the awareness of users to the fuel cost of poor insulation and electrical appliance waste, to providing technical advice on low energy product replacement. Active appliance control also falls under the CERT remit.

The latest incarnation of utility driven demand side management is known as demand side response (DSR). The wholesale price of electricity bought by distribution suppliers (DNO's) is usually most expensive (and least profitable) when demand is highest. These peaks in demand usually occur in early evening and to a lesser extent in the morning on a daily basis and are much more pronounced during winter months. A stated objective of DSR is to re-shape the demand profile such that these peaks are reduced. Although several options for manipulating network load shape are possible, the focus of present and likely future utility driven DSR programmes is perhaps not too surprisingly on load deferment away from peak times rather than demand reduction strategies [OFGEM 2010].

Typically, the control signal in DSR programmes is price. Static time of use (TOU) tariff structures such as E7 and E10 have been in use in the UK for decades and encourage consumers to use electricity at off-peak times rather than at peak through behaviour or by use of simple timers on appliances. Remotely controlled loads such as storage heaters, hot water boilers, underfloor heating and large capacity thermal stores are typically used with these tariffs in conjunction with dedicated signalling equipment such as the radio teleswitch. According the DECC, almost 2 million customers in the UK participate in E7 and E10 schemes. Other commercial systems such as CELECT, aim to optimise energy cost to the consumer within the limits set by a pricing signal from the utility however systems which attempt to bridge this gap are rare [Counsell et al 1997].

With the anticipated roll-out of automated meter reading (AMR) technology however, utilities in the UK are increasingly looking at implementing dynamic TOU pricing or real time pricing (RTP) [Roscoe et al 2010]. RTP involves varying the tariff cost of electricity to consumers throughout the day by tracking the varying wholesale cost to the utility over the same period. Several pilot schemes of this type are underway in a number of other countries to test consumer sensitivity to pricing strategies versus benefits to the utility. Hybrid tariffs incorporate elements of the above primary structures.

1.5.2. Controlled Integration of Renewables

Integration and management of uncertainty from specifically building integrated renewables using a form of appliance control in networks is a relatively new field and few published papers are available.

The ‘deeming’ mechanism given in the FiT document is common to other FiTs and illustrates the base case and present status of best practice in passive grid-connected building integrated low carbon energy supply. According to the FiT exactly 50% of generation is deemed as off-setting local consumption with the remaining 50% deemed exported to the network. It is important to note that under the FiT structure, the demand does not have to ‘do’ anything to shape its consumption profile to that of the renewable to be deemed to have utilised 50% of the generated low carbon energy (hence passive, at present). The trade-off for owners of grid-connected generators under the FiT is that in exchange for a significant portion of the annual returns, the utility takes responsibility and risk in completely managing any uncertainty associated with the source in addition to its normal task of absorbing risk from variations in the demand. This method of ‘deeming’ a proportion of generation used on-site is stated in the FiT as being a compromise to simplify metering requirements which would otherwise increase cost but the implications are far reaching for any alternative integration applications by setting a minimum bar for such systems of 50% renewable utilisation with the use of 50Hz grid frequency being implied.

Infield proposes explicit use of grid frequency to actively control appliances [Infield et al]. For purely traditional demand side management purposes which optimise cost or function of the network, the use of frequency control may be both sufficient and appropriate. However, supply side cost optimisation or the deeming method mentioned above is about the limit of this signal; grid frequency cannot be used in wholesale price based DSR schemes to indicate low carbon availability from either grid connected wind or similarly grid-connected building integrated photovoltaics (BIPV) or retro-fitted building applied photovoltaics (BAPV) for several reasons. The nature of wind or solar generation variability is managed such that it predominantly affects spot market prices rather than wholesale. Further, frequency variation represents network imbalance only and cannot differentiate between the many sources of this imbalance on the network, including variation in demand (which is already paid for through tariff mechanisms). More significantly, given the fundamental control principle of one master, any future proposed implementation of frequency control as standard in building integrated 'smart' networks is therefore unethical because it prohibits use of any prospective alternative system which proposes appliance control through some other signalling mechanism.

Given the highly restrictive nature of grid-connection, the benefits for prospective 3rd party systems designers have historically been severely restricted with the most common solution simply to take renewable energy, and control, off-grid altogether and a niche market mentality.

1.6. DYNAMIC CARBON MANAGEMENT

The material presented indicates that present policies are starting to have a significant impact on the energy consumption of ICT appliances in the workplace and elsewhere and will continue to do so. However, the suggestion is also that the overall electricity consumption of office buildings will likely increase anyway either due to cooling requirement for high density of high power ICT equipment or, more likely, heating requirement for high (or low) density of low power equipment.

In addition to increased electricity bills, there will be added cost through the carbon reduction commitment (CRC) scheme since emissions will also increase. In parallel, the cost of electricity will also rise due to utility investments while CO2 passed on to the consumer from the present and future predicted generation mix stagnates at high levels. Although these levels can be offset somewhat at the building level by investing in a low carbon renewable, the full value and potential of the investment in both low power ICT and a building integrated source is not realised under present integration strategies, proposed DSR programmes or 3rd party solutions due to separate and conflicting control strategies and a lack of appropriate signal.

1.7. RESEARCH OBJECTIVES

In light of the above summary analysis, the objective of this thesis is to research, design and develop a utility-independent building level control strategy capable of managing both embedded energy storage within assets and a building integrated renewable energy stream with the primary aim of minimising the impact of electricity supply to a building integrated ICT network.

1.8. LAYOUT

This chapter has set out to define the scope of the problem, introducing the concept of uncertainty in both supply of energy and use of that energy. The impact of policy measures on office buildings in terms of technology and management are highlighted. The focus of this thesis is identified in the context of delivering a sustainable low carbon solution with the primary benefits being to the primary stakeholder and asset owner.

Chapter 2 identifies photovoltaics as the renewable technology of choice for deployment on buildings and reviews the key issues and limitations in predicting dynamic performance of this intermittent zero carbon source in a control context. The impact on system design and control are discussed.

Chapter 3 describes the assumptions, methodology and development of a closed loop feedback controller suited to the application of managing uncertainty in building integrated power networks at the appliance level. Simulation results indicate that robustness of the proposed control is sensitive to scales of PV to load to energy storage capacity.

Chapter 4 investigates enabling technologies and other requirements necessary to implement this form of control using IT industry standard unified data and power infrastructures.

Chapter 5 presents case study results, demonstrating deployment using industry standard components and implementation of the controller within a standard ICT network infrastructure. The value of interoperability is highlighted.

Chapter 6 summarises the implications for the work done in this thesis and concludes with further work identified in this field.

1.9. REFERENCES

1E, *PC Energy Report*, press release, 2009

4th CCC Report – *Delivering Low Carbon Power*, http://www.theccc.org.uk/sectors/power , 2010

Bach P, *Wind Power and Spot Prices: German and Danish Experience 2006-2008*, Renewable Energy Foundation, London, 2009

British Wind Energy Association, press release, 2010, 2011

Carbon Emissions Reduction Target (CERTS) Programme, http://certs.lbl.gov/certs-der-pubs.html

Counsell J, Reeves J, *Heating Apparatus Controlled to Utilize Lower Cost Energy*, Patent Publication: US5700993 (A), EC: G05D23/20G4C2, 1997

Department for Energy and Climate Change, *Statistical Release – 2009 Greenhouse Gas Emissions*, 2011

DECC, *The UK's Clean Energy Cashback Scheme*, http://www.decc.gov.uk , 2011

Department for Business Enterprise & Regulatory Reform - *Energy consumption in the United Kingdom*, 2008 Update Pub URN 08/456

Energy Star Programme Requirements for Computers Version 5, 2010

European Commission, *Framework Directive for the Eco-design of Energy using Products*, 2009

Foote C, Roscoe A, Currie R, Ault G, MacDonald J, *Ubiquitous Energy Storage*, Conference on Future Power Systems, Amsterdam 2005

IEA DSM TASK XI, *Final Report – Time of Use Pricing and Energy Use for Demand Management Delivery*, 2007

Infield, D, Short, J, Home, C, Ferris, L, *Potential for Dynamic Demand Side Management in the UK*, Power Engineering General Meeting, 2007

ITU, *Internet Access in the UK*, online statistics, 2011, http://www.itu.int/ITU-D/ict/statistics/index.html

Jenkins D, Liu Y, Peacock A. *Climate and Internal Factors Affecting Future UK Office Heating and Cooling Energy Consumption*, Energy and Buildings, Vol 40, pp874-881, 2008

NREL, *A Policymakers Guide to Feed-in Tariff Policy Design*, http://t.ymlp20.com/mwbapamjjarahbmuaxabss/click.php , 2011

OFGEM, *Demand Side Response*, Public Consultation Paper, 2010

Oswald J, *Will British Weather Provide Reliable Electricity*, Energy Policy No36, pp3202-3215, 2008

POYRY, *The Impact of Intermittency*, press release, 2009

POYRY, *The Challenges of Intermittency in North West European Power Markets*, press release, 2011

PWC, *Meeting the 2020 Renewable Energy Targets: Filling the Offshore Wind Financing Gap*, public resource, retrieved 2010.

Roscoe A, Ault, G, *Supporting high penetrations of renewable generation via implementation of real-time electricity pricing and demand response,* IET Renewable Power Generation, pp. 369-382, 2010

Sharman H, *Why UK Wind power should not exceed 10GW*, Civil Engineering, 158, pp161-169, 2005

UK Office of National Statistics, *PC Ownership Trends*, http://www.statistics.gov.uk/cci/nugget.asp?id=868, retrieved 2009

CHAPTER 2 - DYNAMIC PERFORMANCE ASSESSMENT OF PHOTOVOLTAIC GENERATORS

This chapter details current state of the art in photovoltaics (PV) performance assessment and systems integration of this renewable energy stream. The review looks at the issues in present building integrated or applied photovoltaic (BIPV/BAPV) modelling methods as well as highlighting the implications of model based prediction for control purposes. Methods of optimising a renewable stream of energy are explored with the aim of defining these requirements for use in the proposed demand control scheme detailed in Chapter 3.

2.1. BACKGROUND

Smaller scale on-site low carbon and renewable generation (micro-generation) has significant potential to contribute to carbon dioxide (CO2) emissions reductions by directly producing high grade electrical energy close to the demand while also reducing emissions and energy waste through conventional generation, transmission and distribution of electricity.

Of the potential micro-renewable technologies available, emphasis is given in this chapter to PV systems as this type of generator is recognised as presently being best rewarded, is most technologically developed and is far more suited to smaller scale deployment in urban areas than alternatives. Photovoltaics can be applied to buildings post-build as a retro-fit solution, known as building applied photovoltaics (BAPV), or integrated within the building fabric during construction, known as building integrated photovoltaics (BIPV), replacing conventional cladding or roofing materials on the exterior; installed as a facade providing a secondary function as a prime mover for passive ventilation [Clarke, Johnstone et al] or potentially replacing glazing with semi-transparent PV [Lunt et al 2011]. Although the predominant emphasis in this work

relates to retro-fitted photovoltaics (BAPV), the terms BIPV and BAPV are used interchangeably unless explicitly stated otherwise. Besides more obvious benefits such as a lack of moving parts, zero noise pollution, long life and utilising perhaps a previously unused area of roof or wall, PV arrays generate zero carbon electricity at a time aligned with average daytime demand and in particular alignment with average demand profiles of commercial and office buildings as is illustrated in Figure 2-1.

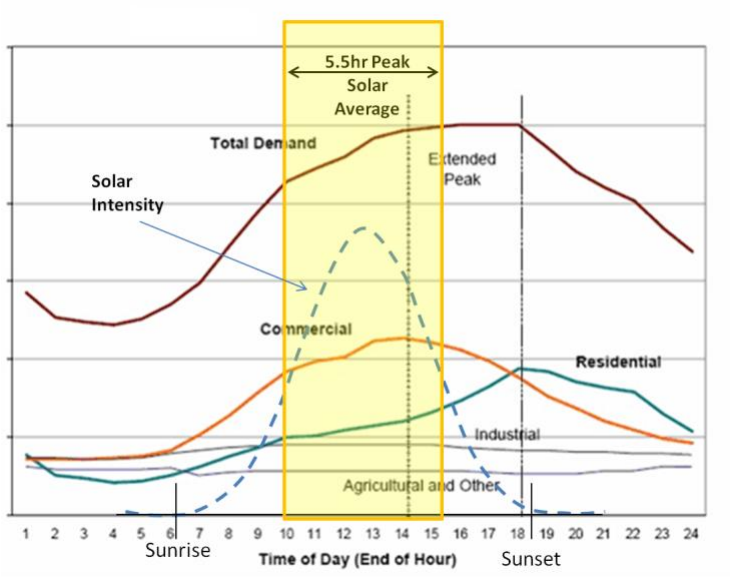

Figure 2-1 Natural Alignment of Solar PV Generation with Demand

As noted in Chapter 1 however, the utility presently has no incentive to utilise this energy source in anything more than a general sense while the owner of a building integrated PV system, who has an incentive, presently lacks the ability to do so. One of several mechanisms necessary in providing this ability is knowledge of renewable generation.

Condition monitoring (CM) is the name given to the practice of measuring an externally available parameter in a system and using it to infer the state of another internal parameter which is indicative of health or performance or other defined state. As a form of prediction, CM therefore relies primarily on the models and knowledge of the plant being an accurate representation of behaviour as well as knowing the limits of

confidence in any inferred relationship. Within this confidence level, the number and choice of independent parameter measurements made and the frequency at which these are monitored also plays a large part in the overall accuracy, quality and value of CM.

It is perhaps indicative to find that although a car battery is deemed suitable for routine continuous monitoring including remedial action when supply is limited, a PV array perhaps representing tens of thousands of pounds of capital investment is typically monitored only a few times per year and output is not actively utilised by the owner. There is however, presently little added value in monitoring PV generation of smaller building integrated arrays at short time intervals outside of academic research or keen interest since, unlike a car battery, a BIPV generator has little or no direct value as a power supply asset to the building.

By comparison to the single method of connection to the grid, there are a number of off-grid, semi-off grid and pseudo off-grid system topologies which use combinations of renewable generating technologies, batteries, thermal storage, back-up generators or other resources in an effort to reduce dependence on grid supply or to utilise a renewable or both but the vast majority of these are far from ideal in being overly complex for function, inflexible in operation and typically expensive to deploy.

A root cause of these problems in BIPV system design relates to limitations of predictive modelling for both initial sizing of components and for operational condition assessment of the system and the subsequent effect of these limitations have on controller design and hence value. The proposed demand control algorithm for BIPV systems presented in Chapter 3 of this thesis presents an opportunity to re-evaluate the value and limitations of CM in a more dynamic setting as background knowledge to development of an appropriate control strategy.

2.2. CONDITION ASSESSMENT OF BIPV

As a general rule of thumb for the UK, the annual yield of an optimally oriented, grid-connected 1kWp rated PV array is typically in the region of 700-800kWh with an

average 10% variation in output between London and Edinburgh [DECC 2008]. This general value is less than the installed rated capacity due to numerous meteorological and environmental influences on behaviour such as ambient temperature, relative wind speed and direction, mounting conditions, aging through natural degradation and soiling and dirt build-up on the array over time. Partial shading effects from surrounding structures and vegetation also greatly influence performance. Variations in manufacture of individual modules in an array also result in degraded performance, as does the use of protection diodes and inevitable wiring loss.

A summary of the extent and impact of the main annual loss factors in grid connected mono-crystalline silicon PV systems are presented in Figure 2-2 from [King 1992] as measured against manufacturer's rated output at Standard Test Conditions (irradiance of $1000 W/m^2$, cell temperature of 25°C, air mass modifier of 1.5 and ASTM Standard Spectrum) and figures obtained in the field. Note that the models used to arrive at these figures are diode based steady state models and as such may not be relevant to dynamic performance of an array.

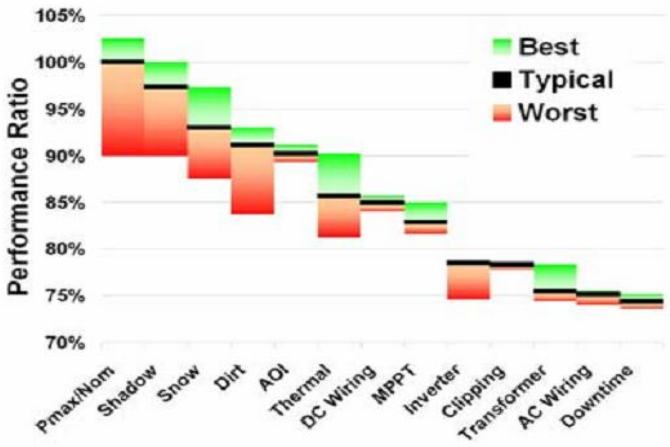

Figure 2-2 Annual Performance Loss Factors in PV Generation [Source: King]

A similar summary is also given by others such as Xantrex (2001), Thevenard (2005) and King (1992). As is shown, a reasonable 25% overall reduction from rated system output is a common figure cited although others such as SAP; the UK's Standard

Assessment Procedure for measuring the energy rating of residential dwellings, gives a generous 20% average reduction in output from manufacturer's ratings in its calculations, perhaps representing recent advances in balance of system elements [Anderson 2009].

Presently available estimation and simulation programs differ in the complexity and interaction between the model groups represented in Figure 2-2 in some fashion and are, on average, accurate to within 20% in predicting future nominal system performance ratio and yield on an annual basis from historic input data [Klise et al]. However, a defining feature of estimation tools is the use of steady state or quasi steady state models to describe the system. These models are used based on the assumption that the system dynamics can be ignored at the monitoring timescales involved. Moving towards more dynamic modelling, simulation and performance prediction of PV and PV systems at shorter timesteps however invalidates most if not all of the above summary with the realisation that all of the loss categories considered are actually time varying to greater and lesser degrees and with the further complication that there is strong coupling between many of the groups as is described in the following section.

2.3. MODELLING PHOTOVOLTAIC GENERATORS

Although the physical phenomenon of conversion of energy from light to electricity was first observed by Becquerel some 172 years ago, the physics of this process owes its fundamental understanding to Einstein. Until then, classical electromagnetic theory based on continuous representations of Maxwell's Equations and the laws of thermodynamics could not fully explain this phenomenon. Experiments on frequency response of dissimilar metallic junctions (Hertz 1877) and fundamental research on the discrete nature of electromagnetic radiation (Plank 1900) formed the observational foundations of Einstein's seminal treatise on the photovoltaic effect (Einstein 1905), for which he later received the Nobel Prize in 1920. Einstein's succinct formula coupling Plank's constant with electromagnetic frequency to describe the energy content of a discrete 'quanta' of electromagnetic radiation was contentious, revolutionary and

provided the theoretical basis for later development of the entirely new field of quantum physics.

The emissive power intercepted by the earth from the sun is therefore described as being frequency dependant with an average of around $1357 W / m^2$ striking the upper atmosphere at a wavelength of around $0.5 \mu m$. This value is reduced by a number of effects, resulting in a sea level, solar noon global irradiance of $1000 W / m^2$. As is shown in Figure 2-3, most of the energy content is concentrated in the visible spectrum and just outside from 0.4 to around $1.1 \mu m$. This is also the bandwidth of silicon.

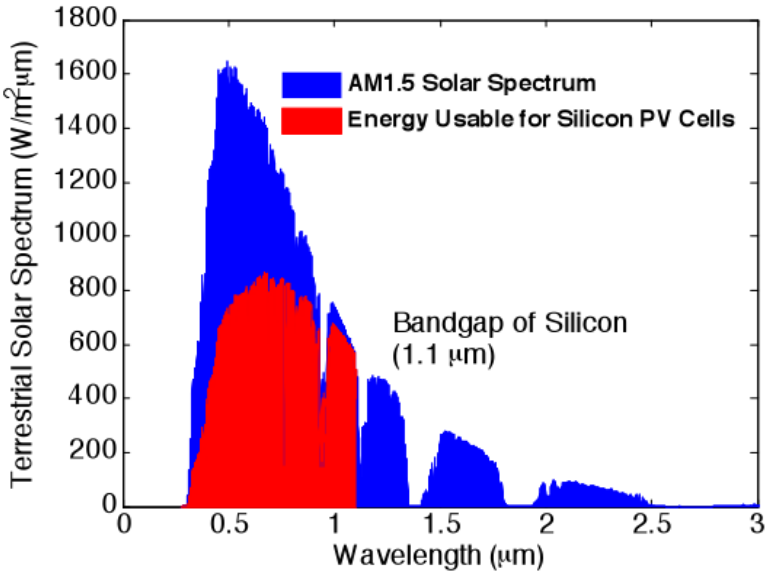

Figure 2-3 Solar Spectrum

Based on this knowledge, modern silicon wafer based photovoltaic cells are designed and constructed from at least one p-n junction fabricated from a thin layer of semiconductor material whose electrical conduction characteristics are modified and magnified by adding impurities to create a surplus or deficit of electrons across the junction. Under conditions of thermal equilibrium and in the absence of light, the electrostatic tension generated by these dissimilar materials, also known as the band-gap voltage prevents migration of electrons hence no charge is transferred under these

conditions. When exposed to light however, photons which have greater energy than the band-gap energy of the junction are absorbed causing charge to flow in exchange of thermally excited electrons, giving rise to a frequency dependant, photon-induced current.

Variation of generated current with voltage is regarded as an exponential with behaviour similar to that of at least one diode in parallel with a source of current as shown in Figure 2-6 and approximated by the Shockley equation (Equation 2-1); named after transistor co-inventor and 1956 Nobel winner W. Shockley [Shockley et al 1952].

$$I = I_0 \cdot \left(e^{\left(V / n \cdot V_t \right)} - 1 \right)$$ Equation 2-1

Under illumination and short-circuit conditions, Kirchhoff's Law states that induced current will flow in an external circuit and when open-circuited, the induced current is shunted internally within the cell. Between these two conditions at the function maxima, electrical power generating capacity is at its theoretical optimum.

The current voltage characteristic of a Shockley p-n diode is shown in Figure 2-4 and illustrates that diode forward bias is non-linear and results in energy dissipation.

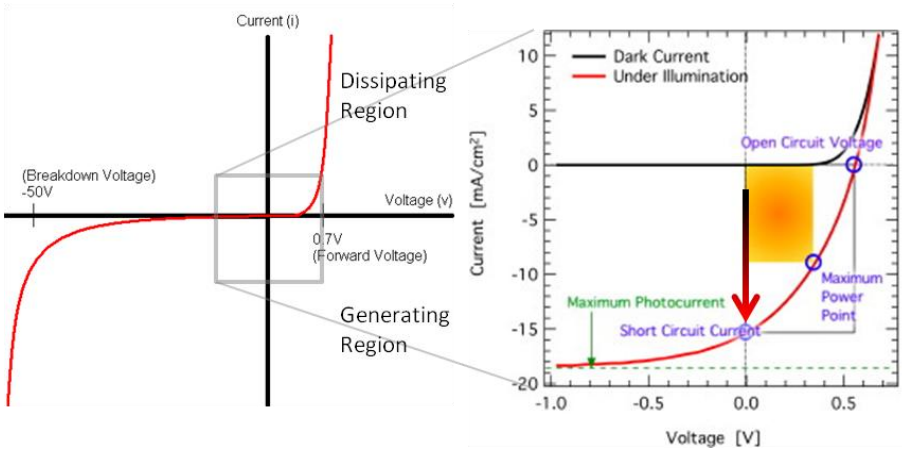

Figure 2-4 Photo-diode Characteristic Response to Illumination

The exploded section of the figure shows that in parallel with a light dependant source of current, the diode characteristic curve moves downwards into a generating region with generated power output (orange area) a function of temperature and illumination against thermal voltage and dark current reference values.

Post-production, PV modules are sorted according to steady state performance under ASTM specified Standard Test Conditions of uniform irradiance of $1000 W/m^2$ at an equivalent sea level frequency spectra defined by an air mass modifier of AM1.5 in a tightly controlled thermal environment. Example plots of typical I-V curves illustrate this relationship as determined by modelling software PVSYST for a typical 36-cell poly silicon PV module model (BP350J), shown in Figure 2-5 a and b [PVSYST].

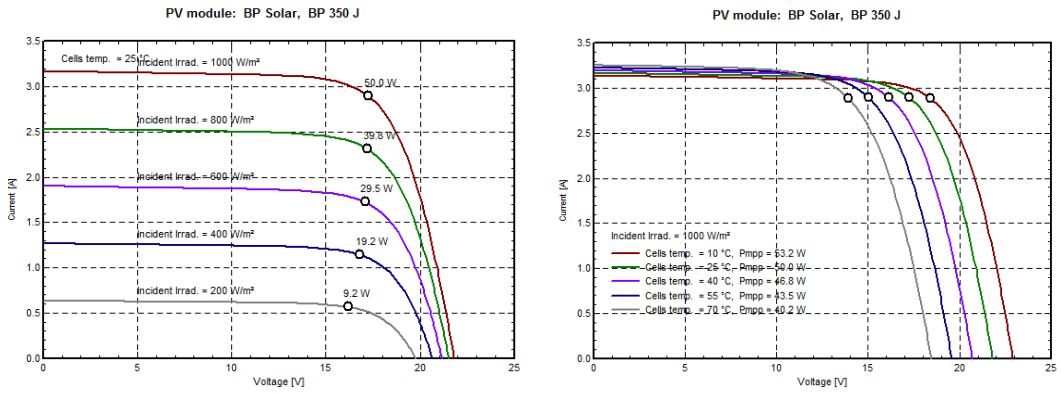

Figure 2-5 Typical PV Datasheet I-V Curves [Source: PVSYST]

Note that the shape of the rated curve is technology specific, for example amorphous modules exhibit a gentler curve through greater sensitivity to temperature.

In addition to rated short circuit current and open circuit voltage, a typical datasheet for a PV module or cell also specifies the maximum power output of the module, thereby giving a third performance indicator at rated conditions which then allows modelling of the process based on the relation given above. Coefficients are also usually given in a module datasheet which suggests a linear dependence of current and voltage on module temperature.

Determining the correct position of operating points by augmenting the modelled Shockley equation in some way to represent observed or other operational behaviour forms the basis for the field of PV modelling. This is a very challenging field since internal malfunction or variation of individual cells in a module can profoundly affect module and string performance and externally, overall system behaviour is not only dependent on the dynamics of the load and output conditions and perhaps changeable site specific or mounting parameters, but PV operational behaviour is obviously highly sensitive to weather and other meteorological conditions which are themselves highly complex and dynamic.

2.3.1. Standard PV Models

Given the similarity of operation to that of a diode, there is naturally a large body of research in the field of modelling photovoltaic generators as an equivalent electrical circuit. These models are derived from decades of observational and empirical evidence and have benefited from the precise knowledge of the physics of semiconductor behaviour and diode characteristics.

At one extreme, very detailed models intended for cell research and development purposes evaluate the current and voltage distributions at individual cell level under controlled laboratory lighting and thermal conditions to a very high degree of accuracy. Such models require literally dozens of parameter details not specified by the manufacturer's datasheet and are far too complex for any other purpose [Klise et al, 2009].

The 2-diode equivalent circuit model with 7 unknowns intends to address a specific inaccuracy with the less parameter intensive 1-diode model in that two diodes can therefore include recombination opportunities within the photodiode, allowing better modelling of the curve shape and so increase accuracy [Mullejans et al 2004]. However, this level of complexity requires knowledge of particular diode characteristics and uses information rarely freely available in public literature.

The 1-diode model [De Soto et al 2007] and its variations with 5 unknowns are most popular in publications and are typically the electrical models used in yield estimation software utilities such as PVSYST, TRYNSYS and PVGIS as summarised by Klise in 2009 [Klise et al 2009]. Besides the three operating points calculated from the datasheet for the module, the fourth and fifth parameters in these models are internal cell series and shunt resistances. Modelling of series resistance gives a better representation of the shape of the curve between maximum power point and open circuit voltage. Likewise, inclusion of a shunt resistance better models the relationship between maximum power point and short circuit current. A typical 1-diode model is shown below. The figure also highlights the difference between models for a real cell and an ideal Shockley based cell.

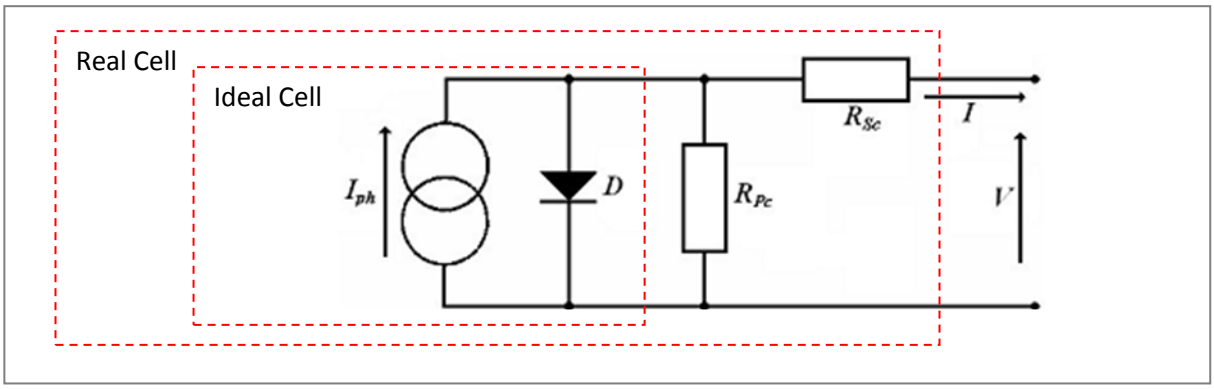

Figure 2-6 1 Diode Representation of a PV Cell

The describing equation for the standard one diode model in Figure 2-6 is given as;

$$I = I_{ph} - I_0 \cdot \left[\exp\left(\frac{q \cdot (V + I \cdot R_{Sc})}{n \cdot k \cdot T} \right) - 1 \right] - \frac{V + I \cdot R_{Sc}}{R_{Pc}} \qquad \text{Equation 2-2}$$

Where $V_t = \frac{n \cdot k \cdot T}{q}$ is defined as the thermal voltage.

However, the necessary inclusion in the model of a diode introduces numerical solving problems linked to the implicit nature of the equations for D. This can be shown using bond graph formalism where the causal stroke indicates the direction in which effort is imposed (voltage in electrical terms). In Figure 2-7, the PV cell is represented by flow source $S_f = I_{ph}$ in parallel with two resistors R_D and R_{Pc}, followed by a series resistance R_{Sc}. The diode resistance is non-linear and also therefore its current-voltage relation (as given previously). The PV cell bond graph is completed by inclusion of a load resistance R_L.

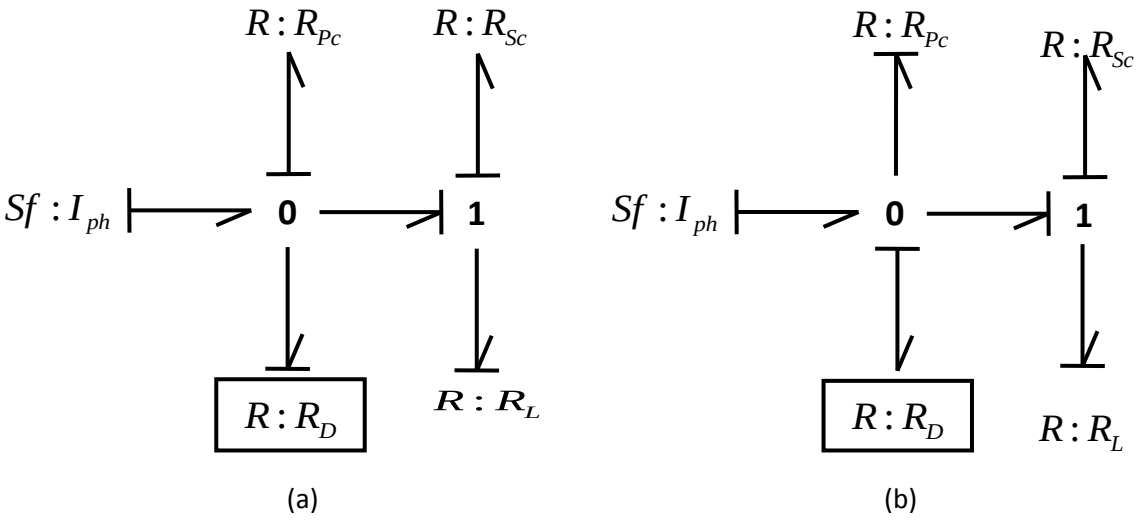

Figure 2-7 Bond Graph Representation of a 1 Diode Model PV Cell

Figure 2-7a shows conductance causality for R_D while Figure 2-7b shows resistance causality, illustrating both diode states and the origin of the algebraic loop in the numerical solution of the describing equation. Further, the inclusion of internal series and parallel resistances also increases complexity in solving the describing equations for current and voltage output as is shown.

For performance assessment of BIPV, these standard diode based models are considered by many far too complex when only the operating point giving power output is desired.

Further, temperature dependence of the system to numerous influences are not easily integrated into the model with the result is that this structure of model tends to be better suited to steady state performance estimation and simulation of PV systems at longer timescales.

A number of researchers have proposed numerous variations such as omitting one or both resistances in an effort to reduce, rather than increase, model complexity. At its most basic, a PV cell can be represented as shown in Figure 2-8.

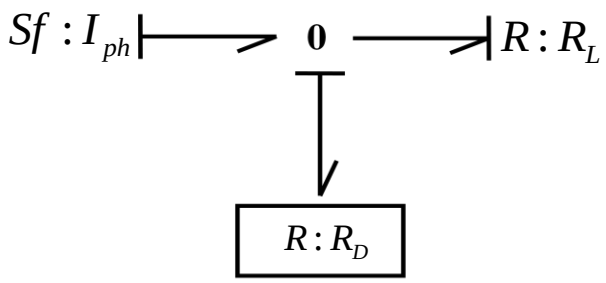

Figure 2-8 Reduced Bond Model of a PV Cell

Given previous statements indicating that the current is photon induced and that the diode characteristic is temperature dependent, the global bond graph of a PV cell is shown in Figure 2-9 as having irradiance and temperature inputs with output correctly associated with a resistive load as is the case in a real system.

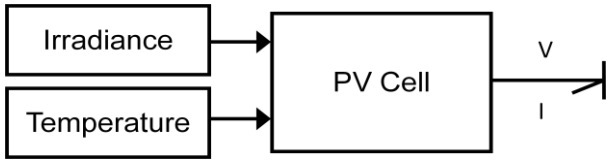

Figure 2-9 Global Bond Graph of a PV System

For purposes of systems integration and control, reduced models can therefore be much more useful than highly detailed models. However, the trade-off is usually reduced accuracy.

2.3.2. Efficiency Models

Kelly proposes a simplified model for BIPV systems by omitting internal resistances and introducing an experimentally derived curve fitting parameter in an effort to reduce complexity and unknowns but the resultant model is not widely regarded as generically applicable due to this empirically determined parameter [Kelly 2001]. As a further simplification, a generic diode factor suggested by Thevenard for the simplified 1-diode model results in reasonable accuracy at high levels of insolation but is known to become increasingly unreliable at lower intensities, particularly below $400 W / m^2$ [Thevenard 2005]. King notes that this adaptation to the 1-diode model incorrectly assumes that cell efficiency is independent of solar intensity [King et al 2008]. However, by reducing the diode to a linear resistance, the method greatly simplifies the PV electrical model by eliminating the need for an iterative solution in calculating current and voltage. The resultant model is known as a fill factor or efficiency model and can be implemented solely using irradiance and ambient temperature input parameter values in addition to those readily available on a manufacturer's datasheet to give electrical power output directly.

The result of these simplifications is a model whose sensitivities are shifted from internal to external parameters. Based on the global bond graph of Figure 2-9 and an ideal representation of a PV cell as given in Figure 2-6, light generated current in a fill factor model is dominated by irradiance but only weakly dependant on temperature as given by:

$$I_{sc} = \frac{G}{G_{ref}} \cdot I_{scref} \left(1 + \alpha_i \left(T - T_{ref}\right)\right) \qquad \text{Equation 2-3}$$

The diode current I_o is introduced as an approximation of the reverse transport mechanisms within the cell junction. There have been several methods proposed to calculate this so-called dark current; Kelly uses an experimentally derived parameter while Jones and Underwood suggest a fixed value based on array area [Jones et al]. Dependence of the diode saturation current on cell temperature can also be given explicitly as:

$$I_0 = C_3 \cdot T^3 \cdot \exp\left(\frac{-q \cdot V_g}{k \cdot T}\right) \qquad \text{Equation 2-4}$$

Where coefficient C_3 can be calculated from datasheet values plus knowledge of the band gap voltage of the material:

$$C_3 = \frac{I_{scref} \cdot \exp\left(\frac{q \cdot V_g}{n \cdot k \cdot T_{ref}}\right)}{T_{ref}^3 \cdot \left(\exp\left(\frac{q \cdot V_{ocref}}{n \cdot k \cdot T_{ref}}\right) - 1\right)} \qquad \text{Equation 2-5}$$

Array open circuit volts are then calculated from:

$$V_{oc} = Ns \cdot \left(\frac{n \cdot k \cdot T}{q}\right) \cdot \ln\left(1 + \frac{I_{sc}}{I_0}\right) \qquad \text{Equation 2-6}$$

Thus far, the ranges of current and voltage have been defined based on conditions denoted by irradiance and temperature. Theoretical maximum power voltage is then

calculated by assuming a linear reduction from open circuit volts with temperature near maximum operating conditions:

$$V_{mp} = V_{oc} \cdot \frac{V_{mpref}}{V_{ocref}} \qquad \text{Equation 2-7}$$

Theoretical maximum power point current is calculated from a standard ideal cell voltage/current relation:

$$I_{mp} = I_{sc} - I_0 \left(\exp\left(\frac{qV_{mp}}{nkT} \right) - 1 \right) \qquad \text{Equation 2-8}$$

The fill factor coefficient C_{FF} is defined as the ratio of maximum power to ideal power as shown below:

$$C_{FF} = \frac{I_{mp} \cdot V_{mp}}{I_{sc} \cdot V_{oc}} \qquad \text{Equation 2-9}$$

In simplified form, the array power generating capacity is therefore given as a fill factor model:

$$P_{out} = C_{FF} \cdot \frac{G \cdot \ln(k_1 \cdot G)}{T_{module}} \qquad \text{Equation 2-10}$$

Where k_1 is defined as $k_1 = \left(\frac{I_{scref}}{G_{ref} \cdot I_0} \right)$.

A great many researchers have compared the various PV electrical models found in literature and many (e.g. King, Thevenard) highlight that each has its own area of application; diode based steady state models can be accurate to within 15-20% on average and are well suited to estimation and simulation programs while simple efficiency based models are far easier to implement but at a lesser accuracy of 20-25% on average. The application area for efficiency based models is aimed more towards dynamic modelling where the accuracy previously lost can be regained to a degree by better representation of the specific physics of the system. However, in contrast to the widely accepted structure of diode-based PV models given previously, there is no general agreement among researchers as to the precise structure of a dynamic efficiency based PV model.

2.4. Dynamic Modelling of BIPV Systems

State of the art in dynamic modelling of photovoltaic generators incorporates the fill factor electrical model above and includes representation of the dynamics of temperature dependence of the system. Under dynamic operating conditions, the rate of change of temperature of a PV cell with time is non-zero and therefore should be included to maintain a reasonable degree of model accuracy. The schematic below, Figure 2-10, illustrates the main energy transfer paths to and from a system (PV module) to include front and rear convective and radiative transfers in addition to the energy taken from the system in the form of electrical power. These energy flows must balance.

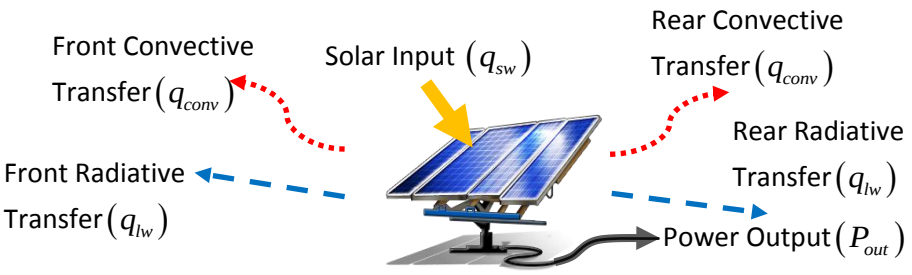

Figure 2-10 Energy Balance for a PV Array

Based on this schematic, the rate of change of module temperature with time is given by explicit calculation of the fundamental differential equation;

$$C_{module}\frac{dT_c}{dt} = q_{sw} + q_{lw} + q_{conv} - P_{out} \qquad \text{(Equation 2-11)}$$

Module heat capacity C_{module} is a critical parameter and can be calculated from knowledge of the module material properties as given by

$$C_{module} = \sum_m A \cdot d_m \cdot \rho_m \cdot C_m \qquad \text{(Equation 2-12)}$$

Example values for calculating heat capacity are recopied from Jones et al as Equation 2-12, the authors arriving at a figure of 2918 *J/K* for the heat capacity of a BP585 36-cell mono-crystalline PV module [Jones & Underwood 2001].

BP585 module heat capacity				
Element	ρ_m (kg/m$^{3)}$	C_m (J/kgK)	d_m (m)	A x d_m x C_m x ρ_m (J/K)
Monocrystalline silicon PV cells	2330	677	0.0003	241
Polyester/ Tedlar trilaminate	1200	1250	0.0005	382
Glass facing	3000	500	0.003	2295
Total				**2918**

Table 2-1 PV Module Thermal Parameters (Source: Jones, Underwood 2001)

The value of 2918J/K is considered fairly representative given the construction of silicon wafer based modules of this scale. The table also shows that the majority of thermal mass is contained in the protective glass facing. An alternative method is to assume a constant U-value for a generic module. For example, the sizing and simulation utility PVSYST presently uses a constant U-value of $29 W/m^2 K$ in its calculations for silicon based cells.

Theoretical description of convective energy exchange from a panel surface to a surrounding fluid (air) is proportional to the temperature difference between the two as given by Newton's Law of Cooling:

$$q_{conv} = -h_c \cdot A \cdot (T_{module} - T_{amb}) \qquad \text{Equation 2-13}$$

The convection heat transfer coefficient h_c is the summation of free and forced convective effects as shown in Figure 2-11.

Holman gives an approximation for turbulent, buoyancy driven free convection from a vertical plane in air [Holman 1992].

$$h_{c,\,free} = 1.31 \cdot (T_{module} - T_{amb})^{1/3} \qquad \text{Equation 2-14}$$

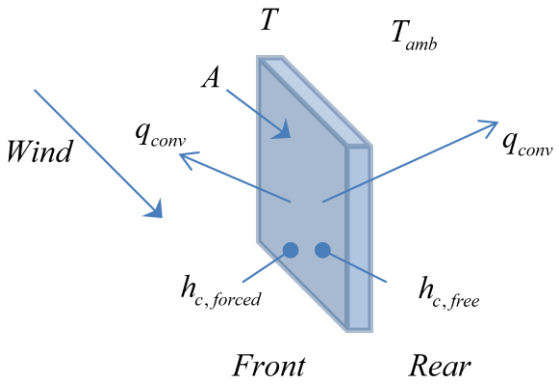

Figure 2-11 Convection from a Heated Vertical Surface

The summation of free convection from the rear of the panel and forced convection from the front gives an overall convection loss:

$$q_{conv} = -A \cdot \left(h_{c,\,forced} + h_{c,\,free} \right) \cdot \left(T_{module} - T_{amb} \right) \qquad \text{Equation 2-15}$$

The magnitude of heat transfer from the front of the panel is therefore sensitive to wind speed. However, assigning a function to describe the forced convection coefficient, $h_{c,\,forced}$ in terms of an effect on module temperature is challenging, particularly in urban areas. Although some authors suggest a linear relation between forced convection and wind speed [Schott 1985], this parameter is not usually measured at a PV site and so its impact on module temperature cannot be easily verified. Various constant forced convection coefficients from literature would suggest a value of between $1.2\,W/m^2K$ [ASHRAE] to $9.6\,W/m^2K$ [Pratt 1981] for a wind speed of $1\,m/s$.

The theoretical basis for long wave radiative energy exchange between two bodies is given by the Stefan-Boltzmann Law:

$$q_{lw} = \sigma \cdot \varepsilon \cdot T^4$$ Equation 2-16

Holman defines the fraction of radiation leaving one surface that reaches another as the view factor [Holman 1992]. If two surfaces x and y are considered, the net long wave transfer is given by:

$$\begin{aligned} q_{lw_{xy}} &= A_x \cdot F_{xy} \cdot (L_x - L_y) \\ &= A_y \cdot F_{yx} \cdot (L_y - L_x) \end{aligned}$$ Equation 2-17

A common simplification in modelling building integrated PV systems is that the rear panel temperature is the same as the temperature of the building fabric facing the back of the array; hence there is negligible long wave transfer via this path. Lui and Jordan describe the view factor of a tilted surface at angle τ from horizontal as $\left(1+\cos\left(\tau\right)\right)/2$ for the sky and $\left(1-\cos\left(\tau\right)\right)/2$ for the ground [Lui & Jordan 1963]. Inclusion of these coefficients and combining Equations 2-16 and 2-17 gives the general form below for net long wave transfer between the panel and its surroundings.

$$q_{lw} = A \cdot \sigma \cdot \left(\frac{\left(1+\cos\left(\tau\right)\right)}{2} \cdot \varepsilon_{sky} \cdot T_{sky}^4 + \frac{\left(1-\cos\left(\tau\right)\right)}{2} \cdot \varepsilon_{ground} \cdot T_{ground}^4 - \varepsilon_{module} \cdot T_{module}^4 \right)$$ Equation 2-18

A schematic of this energy transfer path is given in Figure 2-12, showing the fractions of ground and sky thermally conducive to energy transfer.

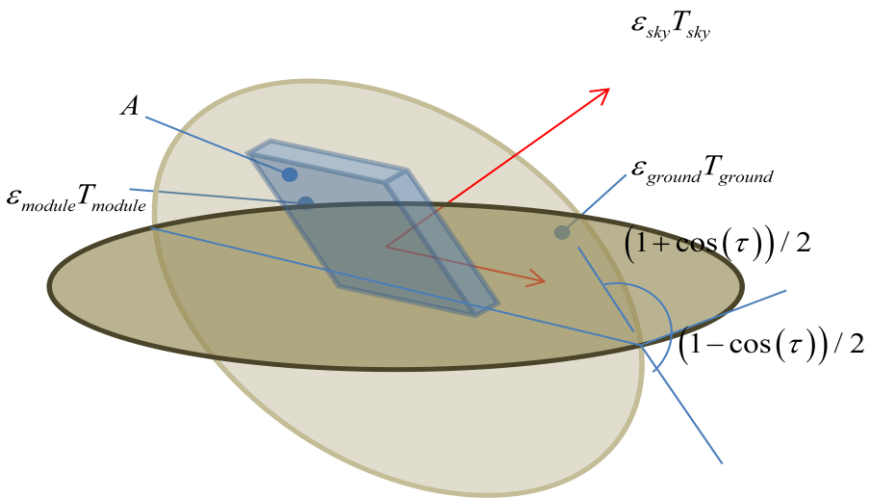

Figure 2-12 Solar Geometry and Radiative loss

The form of Equation 2-18 therefore suggests that the sky is considered to be exchanging long wave radiant energy with the PV module with the rate of exchange dependent on geographical location and array aspect, time of day and climatic conditions. Sky emissivity and sky temperature are therefore important external dynamic parameters since these include the fraction of indirect cloud cover seen by an array and therefore to a significant extent, the surrounding ambient temperature. There are several methods of determining a fictitious sky temperature depending on the data available and the reference calculation is done for clear skies. Cooper suggests a generic empirical relation coupling ambient temperature to incorporate the range of T_{sky} with cloud cover in one equation [Cooper et al 1980]. Relative to a black body of equal temperature, Schott gives constant values of $\varepsilon_{sky} = 0.95$ for clear sky conditions and $\varepsilon_{sky} = 1$ for cloudy conditions and varies a sky temperature describing function according to $T_{sky} = (T_{amb} - \delta T)$ where $\delta T = 20$ for clear sky conditions and $\delta T = 0$ for cloudy conditions. Correct calculation of long wave exchange is therefore dependent on cloud cover fraction.

From Equation 2-11 short wave radiant energy input to the system q_{sw} is given by:

$$q_{sw} = G \cdot A \cdot \alpha \qquad \text{Equation 2-19}$$

The absorptivity parameter α is known as a function of the angle of incidence as well as the absorptive and reflective properties of the laminating materials, glass and the cell material as given by Snell's and Bouger's laws. The reflectance parameter can be calculated from Fresnel's relationship [Duffie Beckman 1974]. Fundamentally, the relation between absorptivity, reflectance and transmittance properties of a PV cell is given by the identity:

$$\alpha + \beta + \gamma = 1 \qquad \text{Equation 2-20}$$

Proportions of each property in the relation above depends heavily on angle of incidence with reflectance losses as much as 80% at low solar elevations as shown in Figure 2-13, also resulting in a 20-30% reduction in alpha at low solar elevations than that during full sun [Schott, 1985].

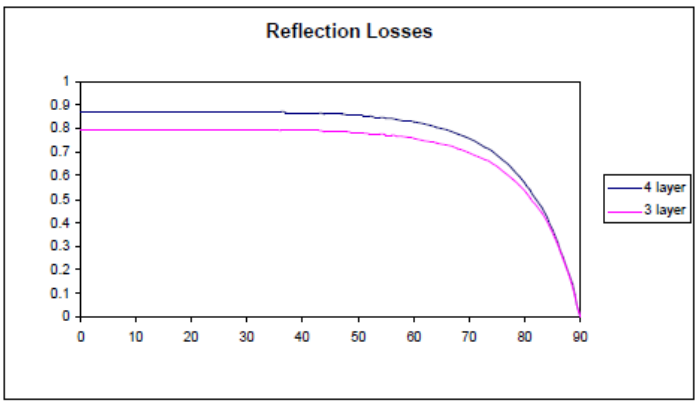

Figure 2-13 Reflection Losses with Varying Angles of Incidence [Source: Born]

Although it is known that variations in spectral composition also take place during dynamic weather conditions altering absorptivity and reflectance ratios to some degree, it is usual in PV modelling to approximate this parameter using a constant value. For silicon, around 77% of the photons striking the cell surface during peak solar intensity around noon are absorbed and of those around 10% are lost in reflection, resulting in a nominal absorptivity constant of 0.7 for crystalline PV cells. This is one of several primary simplifications in solar modelling which directly affects performance assessment of the generator.

The full dynamic PV model can then be expressed as a relatively simple first order system by:

$$C_{module} \cdot \frac{dT_c}{dt} = \sigma \cdot A \cdot \left(\varepsilon_{sky} \cdot \left(T_{amb} - \delta T \right)^4 - \varepsilon_{module} \cdot T_{module}^4 \right) + G \cdot A \cdot \alpha - \frac{C_{FF} \cdot G \cdot \ln\left(k_1 \cdot G \right)}{T_{module}} \cdot \eta_{inv} - A \cdot \left(h_{c,\,forced} + h_{c,\,free} \right) \cdot \left(T_{module} - T_{amb} \right)$$

Equation 2-21

Experimental validation of this and similar models has been performed by several authors showing reasonable accuracy between modelled and actual values as measured on-site and short timescales of 1min sampling [Jones et al]. A noted result from Jones is the time constant of a BP585 module given as ~7mins. This value is taken as representative of the module type, scale, mass and construction in general and strongly suggests that at least minutely data is required to capture the effects of temperature on array performance. An issue highlighted by Jones is that this model, in common with every other presently defined model, does not perform well at low levels of irradiance and tends to underestimate production during changeable conditions. This is mainly due to absorptivity and reflectance parameters being deemed constant as highlighted above but there are other important influences as discussed below.

The present form of this model is generally accepted as requiring refinement before being suitable for continuous monitoring or monitoring at short timesteps due to the model inaccuracies identified above coupled to a lack of a calibration reference parameter, resulting in model drift particularly during erratic conditions [Jones et al]. The latter requirement is also therefore a strong area of research but as is shown below, provision of a model reference parameter for smaller PV arrays is not easy to achieve in any cost effective manner.

2.5. PREDICTING SOLAR AVAILABILITY

The level of irradiance incident on an array naturally varies with season and with time of day due to changing position of the sun in the sky. This, at least, can be calculated to high degree of accuracy. The reference in modelling solar availability is a model of a clear sky. In passing through the atmosphere, irradiance is reduced by effects which scatter sunlight, creating a diffuse global light source in addition to a direct or beam source. A tilted surface will also experience light reflected from the ground or nearby structures. The useful irradiance seen by an array is therefore a function of its constituent time varying beam, diffuse and reflected components. Figure 2-14 illustrates the origins of these components.

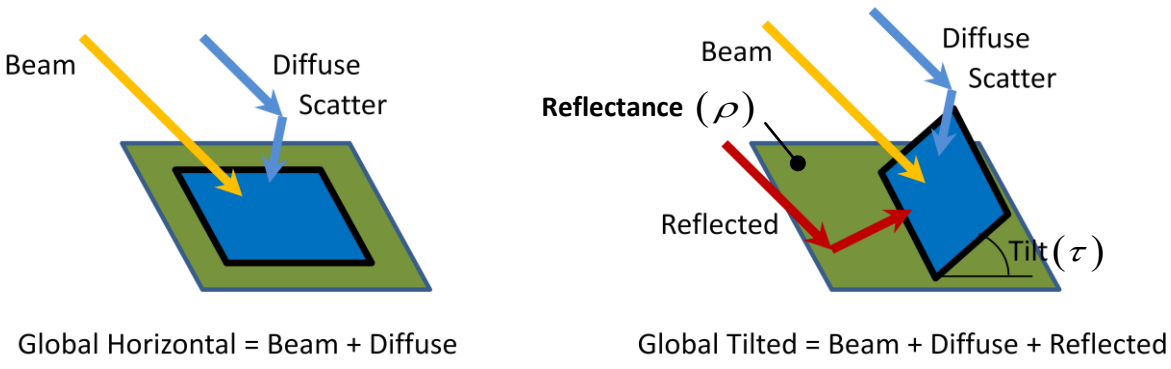

Figure 2-14 Illustration of Distinct Components in Irradiance

The mathematical relation between beam, diffuse and reflected components of global tilted or in-plane irradiance can be estimated for clear sky conditions from Lui and Jordan:

$$\begin{aligned} G &= G_{DN} \cdot \cos(\theta) \\ &+ G_{DH} \cdot \left(\frac{1+\cos(\tau)}{2} \right) \\ &+ \left(G_{DN} \cdot \cos(\theta) + G_{DH} \cdot \left(\frac{1+\cos(\tau)}{2} \right) \right) \cdot \left(\frac{1-\cos(\tau) \cdot \rho}{2} \right) \end{aligned}$$

Equation 2-22

Where the three terms are beam, diffuse and reflected contributions respectively.

The number of unknowns in this relationship is normally reduced to one (at an accuracy cost) by assuming a constant value for ground reflectance ρ and assuming a relationship between direct normal and diffuse horizontal components based on a single primary parameter (global horizontal or global tilted irradiance). This is achieved through calculating an atmospheric clearness index and using this to relate beam to diffuse fractions. However this is a nonlinear process given that an apparent sky brightening occurs around the sun and at the horizon, increasing the diffuse component and authors such as Perez propose sophisticated models to include these phenomena in prediction of overall global tilted radiation [Perez 2004]. These so called anisotropic diffuse sky models are used in many PV estimation utilities and software sizing programs to better model a non-uniform but otherwise clear sky.

In general, a common figure cited and used is roughly 80% beam and around 20% diffuse with reflected contribution only a few per cent and often omitted altogether. The magnitude limits of hourly solar variability therefore vary between an upper limit of around 80% (there is always at least 20% diffuse) during bright periods and 20% during heavily overcast periods, giving a magnitude range of around 60% of array rated values due to the effect of clouds. This range however represents steady state variability and not the full dynamic range.

The frequency and duration of cloud events against sampling rate is also of importance in the clearness index modelling approach. In an early paper, Suerhke et al identified the fundamental differences in wide bandwidth (minutely) irradiance data against low bandwidth (hourly) data typically found in historic meteorological archives. The main difference verified was that the frequency distribution of short term irradiance during variable conditions is much more bi-polar than hourly sampling [Suerhke et al 1989]. Clearness index (and consequent beam fraction) therefore tends to be either very low or very high during erratic weather (cloud type during erratic weather is predominantly well defined low altitude cumulus or strato-cumulus) with fewer values falling between. An example modelled clearness index curve against actual hourly data over a year is given in Figure 2-15.

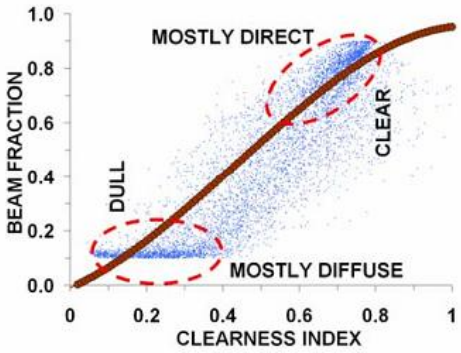

Figure 2-15 Clearness Index Vs Beam Fraction [Source: Ransome]

During highly changeable weather, instantaneous PV performance is dominated by the bright sky periods where apparent irradiance is seen to increase by up to 40% over clear sky conditions due to the so called ‘edge of cloud effect’ which creates fast transient peaks in power just before and after a ‘cloud event’ [Ransome et al 2005]. This basic dynamic behaviour is seen in Figure 2-16 in data gathered at 15s intervals on an increasingly cloudy day in Glasgow. The figure also highlights the bi-polar nature of incident insolation during erratic weather conditions.

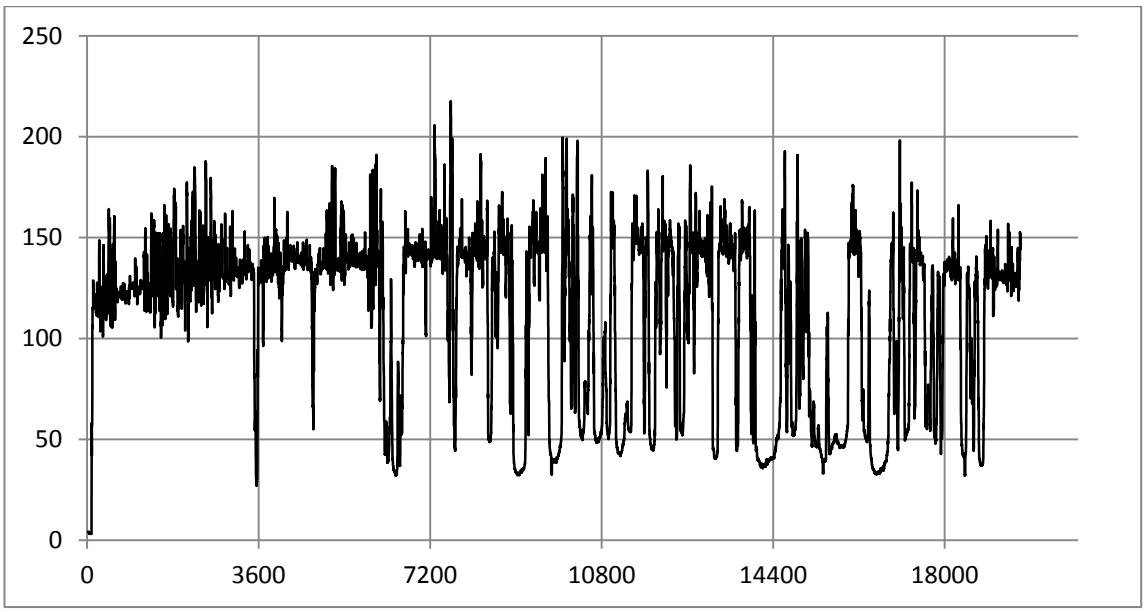

Figure 2-16 PV Power Plot at 15s Intervals

The duration of cloud events relates to wind speed at cloud level in addition to the scale, number and water content (reflectance) of the clouds themselves – none of which are easily measured or modelled. Although the types of clouds seen during changeable weather are fairly consistent (fluffy clouds), accounting for cross-winds and cloud cohesion over time makes prediction of cloud duration a continuing research challenge. Ransome reports that the difference in modelled performance and dynamic performance under erratic weather conditions increases below around 400W/m2 by around 5% underestimation at 200W/m2 and 10% underestimation at 100W/m2 in addition to nominal model inaccuracy. It is therefore concluded for the present work that it is not possible using present models and modelling methods to accurately assess PV performance at very short timesteps for dynamic energy control purposes.

2.5.1. Present Status of CM of BIPV Systems

Irradiance is obviously the primary desired parameter in modelling of PV systems. However, irradiance sensors remain very expensive items with costs varying between

several hundreds to over a thousand pounds for silicon cell based devices and pyranometer (thermopile based) devices respectively. Measurement of direct in-plane irradiance is most common as this is easiest to infer and can be cheapest but more expensive systems may measure global horizontal instead as this can be done at higher accuracy.

Further, the second desired parameter in modelling PV, panel temperature, is not easy to ascertain with any accuracy. This is due to thermal variations across the panel (a particular issue in roof mounted systems) making direct sensory measurements highly sensitive to sensor mounting position. Individual cell temperature is also highly sensitive to shading and soiling and the sensor itself after fitting will likely be unable to be calibrated with any accuracy. In fitting a temperature sensor to the rear of a panel, the local mass of that particular area is then increased which itself can cause a hot-spot, invalidating any measurements. Hot-spots in PV panels are to be avoided since the uneven mechanical stresses induced can cause accelerated degradation and even crack the cell. An available solution is proposed in including a calibrated reference temperature within some irradiance sensors instead of directly on the panel but the necessary assumption is that this measured temperature is representative of the array or panel temperature which may not be the case.

The quality of data gathered is of high importance and although many authors have proposed local measurement [Koutroulis 2001], most monitoring systems are proprietary and unable to be verified in their entirety. Signal conditioning hardware, data acquisition hardware, processing hardware and data storage or display all add significantly to the cost of CM as does ensuring sensor calibration and maintenance at high overall quality. This cost is presently unjustified for all but very large arrays or to satisfy particular needs. There is therefore strong research interest in inferring reference parameters from nearby locations in an effort to reduce these costs.

In terms of prediction, a paper by Skarveit et al first proposed that distribution of sub-hourly irradiances within a sample could be modelled and inferred as a function of hourly clearness index [Skarveit et al 1992]. Woyte et al stated that clearness index is insensitive to seasonal variations and location but highly sensitive to insolation conditions [Woyte 1996].

The simplest and most cost effective method of inferring an insolation reference and perhaps temperature at an unmonitored site to predict output is to assume that weather conditions 'here' are the same as 'there' with some distance between. This method may well be accurate on the percentage of days where steady weather conditions, either clear or cloudy, cover large regions but on days where cloud cover is patchy, inferred values are much higher risk due to the unknown position of transient clouds across the area represented between time intervals. Given its maritime climate, most days in the UK for example are patchy to some degree.

Present research interest in multiple sites modelling predominantly relates to predicting the magnitude of what is termed the smoothing effect; the supply side equivalent of diversity which is assumed to occur during partially or intermittently cloudy days over a PV fleet connected by a single distribution network [Kawasaki et al 2006]. Spatial correlation between sites therefore depends mainly on the cloud type, wind conditions at cloud level, cloud cohesion over time and the area being represented.

Murata et al simulated a network of 52 PV systems using historic hourly weather data and analysed relative worst case variability against average variability for the group and suggests that the number of PV systems is not a factor in this ratio. An additional important result was that the correlation between two sites is almost zero unless the separating distance was very short or time interval very long [Murata et al 2009]. This suggests a clustered approach.

Hoff et al proposes using hourly satellite data in a method by which cloud effects are predicted for the next time interval through what is described as a dispersion factor; a mathematical description coupling cloud direction and transit speed (through present and previous values) with the distance between sites [Hoff et al 2009]. The further suggestion from Hoff is that there may be an optimum density of PV over an area which minimises relative aggregate output variability seen. However, actual existence of this 'sweet spot' is not intuitive and is disputed by Lave.

Lave et al proposes using 1-minute sky temperature imaging sensory data with analysis using wavelet decomposition techniques to identify cloud events in terms of their frequency characteristics before propagating calculated cloud motion vectors across a

fleet [Lave et al 2010]. The result is a frequency dependant ‘trigger’ which oscillates the model between clear sky and cloudy sky modelled values of irradiance. However, assigning specific frequencies to represent clear or cloudy conditions relies again on cloud cohesion being consistent. Further, since the method uses rates of change rather than magnitude, there is risk of the model being caught in the wrong state or over-compensating, resulting in false positives.

Spatially correlated predictive models are a relatively new area and the basic assumptions made by the authors above are critical at their early stage of development. These include that there can be an accurate correlation between hourly values and future sub-hourly conditions at a high enough confidence level to be valuable. This is presently disputed. In an important early paper, Gansler identified fundamental model stability problems in inferring sub-hourly conditions from hourly data using models which necessarily have operational limits and proposed a far shorter sampling rate than hourly [Gansler et al 1995]. This observation has been supported by a number of authors already cited with some (Jones, Lave) suggesting 1min sample rate.

2.6. OUTPUT POWER CONDITIONING

Output from an array is almost always regulated via an inverter, converter or charge controller device. An inverter is a device which produces AC power output through a multi-stage process typically consisting of an input filter, DC/AC switching converter, output filter and transformer. The transformer stage is known and accepted as a significant source of conversion efficiency loss and newer high frequency solid state inverter models do not have this component. DC/DC conversion and battery charging devices are more efficient through having no need for a transformer in the first place and so are simpler, more robust machines.

Both wind and solar PV inverter devices continuously consume power through wake-on-power and sleep modes and are known to only operate above a certain power threshold due to the nature of switching power supply operation. This has the effect of

‘windowing’ availability of renewable energy to between certain times of day in the case of PV and further, creating a demand at night. The amount of energy excluded early and late in the day by the inverter minimum power threshold is not usually deemed significant (< 5%) but nevertheless represents an opportunity missed. Although the energy consumed by these devices in standby modes is only usually a few watts in newer models, this still represents a cost to the owner which can be substantial for smaller systems using low cost or older designs which dissipate much more energy.

One would think that solar PV inverters and DC/DC converters would be sized for peak generation i.e. a 1kW inverter for a 1kWp array. In practice however, it is common to see a 1kW rated inverter matched with a 1.2-1.3kWp array. The intention of this practice is to improve the overall efficiency of the inverter by increasing its utilisation but the downside is that a very high irradiance value might saturate the device for short periods, known as clipping. These high values of irradiance appear as fast transients during dynamic conditions and on clear sunny summer days.

Grid-tie inverters are regulated devices and are rated for efficiency under EU defined operating conditions. Although the EU defined inverter efficiency method results in a close fit with real operational curves at full load, it has been criticised in industry for overstating part load performance during dynamic conditions. Kirschen supports this view in an analysis of device behaviour during high rates of change.

With the emphasis in this work being behaviour during dynamic conditions, rather than the EU standard model or even a more complex model to represent decreased efficiency at certain loadings, an inverter converter or charge controller can be reasonably accurately modelled according to:

$$\eta_{inv} = e^{\frac{-(100-\eta_{\max})}{pL}} \qquad \text{Equation 2-23}$$

This model results in an efficiency curve shape for a 90% rated device as given in Figure 2-17.

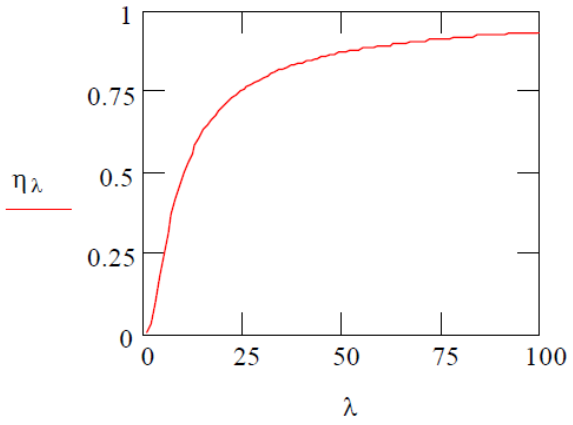

Figure 2-17 Inverter/ Converter Characteristic Efficiency Curve

It is also common in PV modelling to simply use a constant to represent power conversion efficiency [Jones].

2.6.1. Optimisation

A maximum power point tracking (MPPT) algorithm is a form of control often incorporated into the power conditioning stage of photovoltaic systems which aims to optimise the output power of the array irrespective of unknown climatic input conditions and plant behaviour. In all cases, the assumption is that the electrical characteristics of the load do not impede this process. This assumption is taken as true for grid connected systems as these use the AC network as an infinite capacity storage element. The assumption is less true for off-grid battery charging systems as batteries can saturate and currents are limited.

In control terms, the goal of a maximum power point tracking device is to find the array voltage set-point which transfers the most power through the conditioning device given a limited rate of supply. This is illustrated in Figure 2-18 for a single 36-cell module.

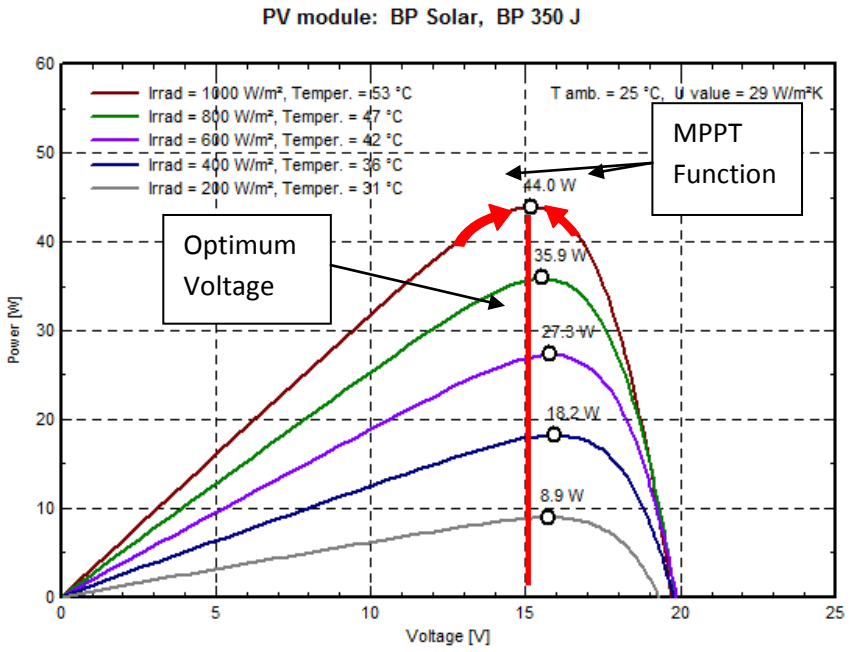

Figure 2-18 Illustration of MPPT Function

Historically, the most common method of tracking maximum power point is to compare the PV array voltage or current with a constant reference corresponding to a pre-calculated optimum value under certain environmental conditions. As is shown in Figure 2-19, implementation of this method is relatively simple but is least accurate since the reference value does not change with irradiance or cell temperature.

Presently, the most common and cost effective method of implementing MPPT uses a perturb and observe (P&O) type algorithm. In this method, the optimum voltage is calculated by noting that at optimum power transfer $(di/dv) = -i/v$

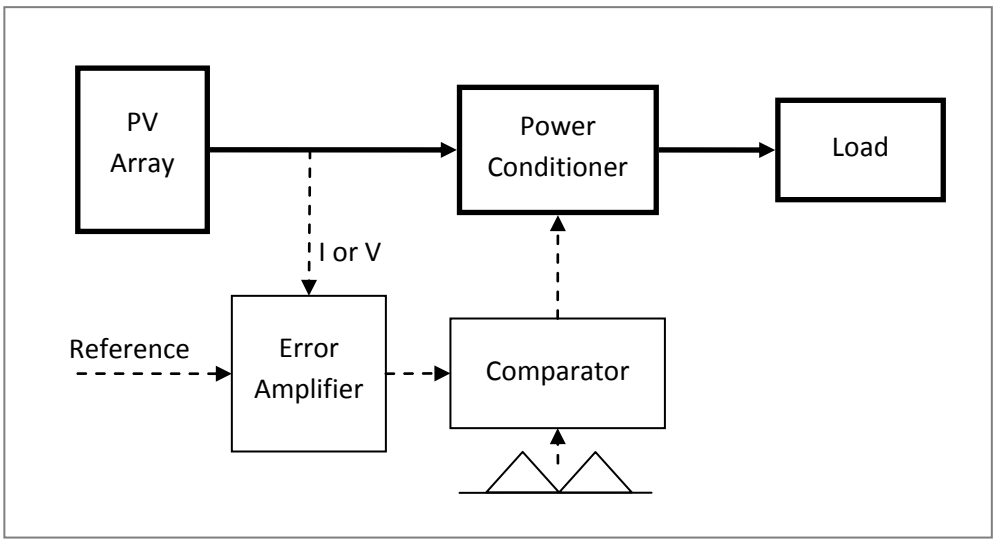

Figure 2-19 Illustration of Constant Reference MPPT

This form of algorithm is well documented in literature and has been shown to track reasonably well under steady state conditions. However, a known issue is that even after maximum power point is achieved, the control continues to modulate the voltage across the optimum point, leading to a small loss in overall performance during steady state. This is shown in Figure 2-20 for data gathered at Strathclyde from a parallel arrangement of 4 BP350J modules connected to a MPPT/ inverter in almost steady conditions. With the sampling period set at 1Hz, a continuous 5V oscillation in array voltage can clearly be seen between 14V and 9V. Also noted was an open circuit voltage of 16.5V and almost steady MPP voltage of 11.5V. The datasheet rated voltage of the array was 18V.

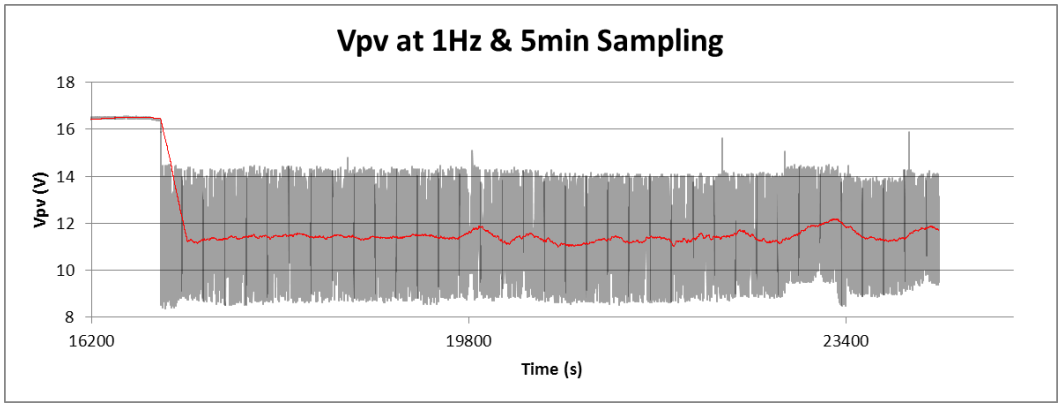

Figure 2-20 P&O MPPT Effect on PV Voltage during Steady Conditions

Several authors have tested models which aim to better model the dynamics of P&O controlled PV arrays in operation. Kirschen reports that P&O algorithms have problems tracking under varying conditions (and have been known to track the wrong way) since its method of deriving its set point relies on the previously calculated values and so is sensitive to rates of change, leading to overshoot and oscillatory behaviour which detracts from its overall efficiency and therefore generating capacity.

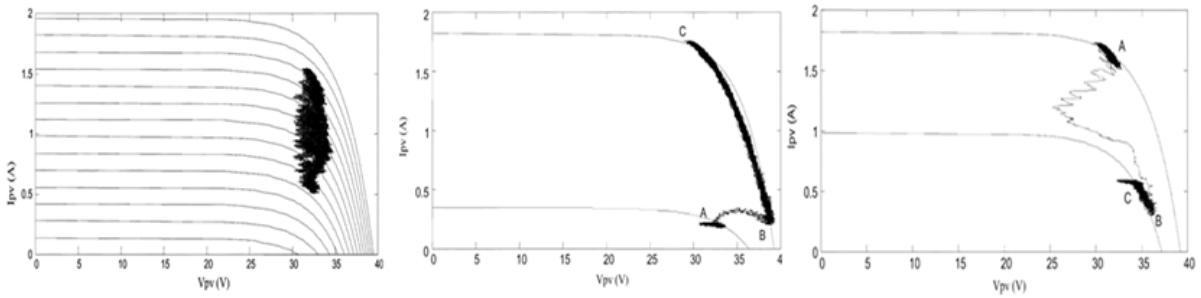

Figure 2-21 P&O MPPT Performance under Variable Conditions [Source: Kirschen]

Figure 2-21 shows the effect of a P&O type MPPT control as plotted against an I-V curve for three different conditions at 1s sample rate from Kirschen.

In the first case, a slow rise in irradiance results in a slow rise in maximum power point with small loss in performance due to the oscillatory MPPT function. The range of operating points is clearly defined and shows a 5V oscillation about a nominal 32V. The second case illustrates the effect for a sudden increase in irradiance and shows typical behaviour when tracking is lost. From A to B in the 2nd plot, the system voltage is initially forced towards open circuit voltage before drifting towards maximum power point at point C as the load is increased. The third plot illustrates a sudden decrease in irradiance. From a near optimal operating point at A, the trace is seen to deviate towards a very low performance ratio before overshooting at B and finally settling at the new operating point C. This behaviour is typical of output regulated PV systems using this algorithm.

Improvements on the P&O algorithm such as an Incremental Conductance (INC) method do not exhibit the same rate or magnitude of oscillation since it uses the array incremental conductance value (di/dv) to calculate the sign of the power increment (dP/dV). This is achieved using an expression derived from the known condition that at MPP $(dP/dV) = 0$. It therefore follows that at MPP $(di/dv) = -i/v$ and so the algorithm can determine when it has reached MPP and stop oscillating the operating point, hence preventing some of the unwanted behaviour seen in P&O type controls. The INC approach is seeing increasing usage in newer inverters.

Other methods of deriving a set-point include neural networks [Gomez et al 2006] and fuzzy logic [Bahgat et al 2005]. However these rather complex methods fair little better under dynamic conditions given the fundamental uncertainty in generation.

2.6.2. BIPV Integration Topologies

The fundamental disconnect between longer timestep model based prediction and real-time power optimisation has shaped use of the technology to a high degree in terms of system topology and also therefore control. This is evident in the much preferred method of grid-connection and no active integration of this source with control of local demand. This simply shunts all uncertainty in renewable generation onto the network operator at all times. The owner is therefore isolated from this risk but is also penalised through grid-connection policy mechanisms mentioned earlier. Further, for large arrays, the local DNO has the right to insist on network reinforcement if necessary to maintain capacity factor and security of supply to other local customers. A portion of this extra cost is borne by the prospective array owner and may be significant.

In an effort to redress these issues, other deployment solutions may be completely off-grid or may involve some hybrid solution combining battery storage with a grid-connection. Off-grid systems tend to be smaller mobile or ‘last mile’ applications where a PV and battery combination is the cost effective solution.

The value of MPPT and optimisation in applications which feature battery storage is a little more subjective in these cases. For a completely off-grid battery charging application with a DC load, the most cost effective solution to integrating a PV array is to size the array, battery and the load for energy and simply connect all three components in parallel. The array voltage is therefore determined by the state and state of charge of the battery and the battery state is determined by the load. Manufacturers of MPPT and charge controller devices usually state a loss in performance of 'up to 30%' if a MPPT/charging device is not employed in a battery backed system (Figure 2-22) but in reality the loss is nearer 10-15% average if the components are sized correctly from first principles and best practise or a sizing utility such as MERIT [Born 2001].

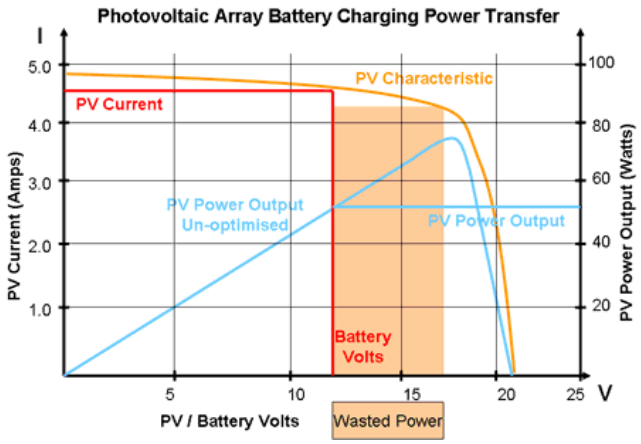

Figure 2-22 MPPT vs Fixed Voltage

In addition to MPPT between array and battery, a regulation DC/DC or DC/AC converter between load and battery can stabilise voltage output to the load network regardless of PV and battery behaviour and although necessary for grid-connected systems, is also common in off-grid systems. Despite addition of these components at significant investment, there is still a danger that such a closed system will fail due to lack of a back-up source and so off-grid systems although utilising 100% of the renewable supply are only used in non-essential or bespoke applications.

A feature of most electrical systems including off-grid PV systems is that of voltage control. The nature of a resistive load is such that current delivery is sustained within a

voltage range therefore a regulation device usually provides a variable current output at constant voltage. This also applies to MPPT inverters, converters or other intermediate conversion devices and is important in considering the implications for further integration.

A hybrid topology includes a second source as back-up should the primary fail. Internally, these hybrid systems are often nothing more than off-grid systems with the value add option of switching to an alternative source should the off-grid topology fail through battery depletion. However, given that the internal system is voltage controlled, connection of an additional component in parallel creates a significant control problem in that both the battery and the back-up source will try to support the load at the same time but since the battery typically has lower output impedance than any conversion device, its energy is always depleted first. Attempting both current and voltage control in the same circuit is not advised.

The usual result is a control strategy where only one source at a time is permitted and once activated (via a low voltage trigger for example), the single dominant source supplies the entire load circuit either indefinitely or until some reset condition is met such as a defined state of charge. Present PV system topologies are therefore limited in effectiveness by the uncertain and unpredictable nature of the renewable and consequent on/off implementation of control.

2.7. SUMMARY

This chapter introduced photovoltaics as the preferred low carbon renewable power generating technology for deployment on buildings. Both conventional steady state and state of the art dynamic PV models were detailed and highlighted areas where plant and system modelling errors originate. General values for various loss factors in steady state performance of PV systems were presented with particular emphasis on the highly dynamic nature of incident radiation and uncertainty in climatic parameters. The conclusion from this section is that although the generator itself can be modelled and

performance predicted to a reasonable degree of accuracy at longer timescales, dynamic performance prediction is not yet fully developed. Both methods were seen to lack a reference parameter.

The further suggestion is that a sampling period of around 1min is required to retain some degree of accuracy and stability in dynamic modelling. It is also clear from the above summary that inferring sub-hourly values of clearness index from hourly data from any source involves risk as does inferring cloud cover from any distance.

Being able to predict future insolation would be beneficial to a control regime which matches generation with demand. However, the dynamics of solar availability as discussed would also add weight to the statement that solar input to a PV system is, essentially, unknown and neither predictive modelling nor using historical data is sufficient to accurately model weather conditions at 1min intervals with more than a nominal certainty. The key implication for control is therefore that for shorter timescales of less than hourly, conventional predictive modelling is not particularly accurate.

The system topologies resulting from this fundamental generating uncertainty either tend towards conventional grid-connection or similarly conventional off-grid. Neither of these solutions makes best use of resources due to a lack of integrated control.

The conclusion arising from this review would suggest that a control aiming to utilise a PV source cannot rely solely on predictive modelling at short timesteps without significant improvements in the models and methods used. This is a key assumption in proposing a novel form of controller as detailed in Chapter 3.

2.8. REFERENCES

Anderson B, *SAP 2009*, www.decc.gov.uk, online resource retrieved 2010

ASHRAE, *ASHRAE Handbook: Fundamentals*, 1989

Buresch M, *Photovoltaic Energy Systems – Design and Installation*, McGraw-Hill, 1983

Clarke J, Johnstone C, Kelly N, Strachan P. *The simulation of Photovoltaic Facades*, Building Simulation Conference, 2005

Cooper P., Christie E., Dunkle R. *A method of measuring sky temperature.* Solar Energy, 26 Vol 2, (1981), pp. 153-159.

De Soto W, Klein S, Beckman W. *Improvement and Validation of a Model for Photovoltaic Array Performance,* Solar Energy, Vol 80, 2006, pp 78-88

Einstein A, *de l'éther aux quanta*, Presses universitaires de France, 1905

Holman J, *Heat Transfer*, McGraw Hill 1992

Jones A, Underwood C, *A Modelling Method for Building Integrated Photovoltaic Power Supply*, Journal of Building Services Engineering, pp167-177, 2002

King D, Boysen W, Kratochvil J, *Analysis of Factors Influencing the Annual Energy Production of Photovoltaic Systems*, Proceedings of 29th IEEE PVSC, 2002

Kirschen et al, *A Model of PV Generation Suitable for Stability Analysis*, IEEE Transactions on Energy Conversion, Vol 19, No.4, 2004

Klise G, Stein J, *Models Used to Assess the Performance of Photovoltaic Systems*, Sandia National Laboratories, online publication retrieved 2010

Koutroulis E, Kalaitzakis K, *Development of an Integrated Data Acquisition System for Renewable Energy Sources Systems Monitoring*, Renewable Energy Vol. 28, pp139-152, 2001

Lui B, Jordan R, *The Long Term Average Performance of Flat Plate Solar Energy Collectors*, Journal of Solar Energy No 7, Vol 2, pp52-73, 1963

Lunt R, Bulovic V, *Transparent, Near-infrared Organic Photovoltaic Solar Cells for Window and Energy Scavenging Applications*, Journal of Applied Physics Letters, Vol. 98, 2011

Mottillo et al, *A Comparison and Validation of Two Photovoltaic Models*, Canadian Solar Buildings Conference, Montreal, 2006.

Mullejans H, Hyvarinen J, Karila J, Dunlop E, *Reliability of Routine 2-Diode Model Fitting of PV Modules*, Proc. 19th EU PV Solar energy Conference, 2004

Perez et al, *A New Simplified Version of the Perez Anisotropic Diffuse Irradiance Model for Tilted Surfaces*, Solar Energy, Vol 39, No 3, pp221-231, 2001

Pratt A, *Heat Transmission in Buildings*, Wiley, 1981

Ransome S, Funtan P, *Why hourly averaged measurement data is insufficient to model pv system performance accurately*, 20th European PVSEC, 2005

Schott T, *Operational Temperatures of PV Modules*, Proceedings of 6th PV Solar Energy Conference, pp 392-396, 1985

Shockley W, Read W, *Statistics on the Recombinations of Holes and Electrons*, The American Physical Society Vol. 87, Issue 5, 1952

Thevenard D, *Review and Recommendations for Improving the Modelling of Building Integrated Photovoltaic Systems*, 9th International IBPSA Conference, 2005

Villalva et al, *A Compreshensive Approach to Modelling and Simulation of Photovoltaic Arrays*, IEEE Transactions on Power Electronics, Vol. 24, No. 5, 2009

Xantrex, *How Well Do PV Models Predict Performance*, Public Document, www.xantrex.com/web/id/227/docserve.asp, Retrieved 2009

CHAPTER 3 – ACTIVE DEMAND SUPPLY MATCHING

This chapter introduces the main problem in actively utilising a building integrated renewable source within the building as one of uncertainty in both supply and demand. A review of past and present solutions in demand management activities is given with a focus on the controller attributes and limitations. Development of a novel controller structure is proposed which aims to reliably match this renewable supply with local demand.

3.1. INTRODUCTION

The rising trend in electricity consumption due to saturation of information and communications technologies (ICT) and consumer electronics equipment in office buildings is of major concern worldwide. For the building owner, this increasing demand intensity not only results in increased operational overheads but also results in elevated CO2 emissions attributed to the building through unavoidable use of poor quality utility produced electrical energy. The total impact for ICT intensive enterprises in terms of direct operational costs and indirect emissions penalties can be significant with BERR attributing 20% of a building's energy consumption solely due to ICT appliances and ICT network management [BERR 2008]. Several operational demand management methods and systems are available to building operators to reduce this impact such as raising user awareness to the typically high ratio of operational energy waste in buildings and adoption of building and appliance level automatic controls to reduce this waste.

The total impact of electrical energy use can also be mitigated by improving the quality of the supply with investment in a building integrated renewable generation technology such as photovoltaics. Despite investment in a building integrated low carbon electricity generator however, the potential value of this expensive asset in reducing the total

impact of electricity consumption is significantly reduced since building demand is not actively shaped to coincide with energy supply from this source.

Active demand shaping is necessary given that photovoltaic generators are, by nature intermittent and so poses significant difficulties to classical demand management control theory. The challenge is therefore to design an extended appliance and building level control to include the renewable such that demand matches with this valuable supply in a reliable manner without compromising conventional electrical supply or quality of service to the building or its existing systems.

3.1.1. Load Characteristics

The particular loads considered in this work consist of networked groups of common ICT and consumer electronics equipment commonly found on the office desk within commercial buildings. These appliances include computer monitors, desktop multi-function printers and a range of other small power devices but focuses specifically on the mobile class of desktop computing devices since utilisation of the ancillary appliances is largely driven by usage of the computer itself.

A mobile computing device is an integrated system containing two main distinct components; the computing hardware and a battery. Built-in energy storage capacity is a highly valuable attribute and target for many prospective demand management systems as extra investment in energy storage is minimised. The present focus is therefore on the potential management capabilities and limits of individual and fleets of batteries embedded in ICT networks.

Besides the battery, energy requirement for the computing hardware can vary significantly and depends not only on the specific usage pattern of individual users but also very much on the particular tasks being performed. This variation can be ±50% against a nominal consumption figure for a modern mid-range business class laptop with the battery typically sized to around 300% or more of this nominal figure in terms of charging power draw.

A rough analysis of the laptop devices tested during the course of this work would suggest the following ratios of internal consumption based on an external measurement:

- Rated Device Consumption 1.25C
- Rated Battery Consumption 0.9C
- High Hardware Consumption 0.5C
- Nominal Hardware Consumption 0.33C
- Low Hardware Consumption 0.25C

The operator C in the above is the capacity of the battery in Wh units, hence a 48Wh battery results in a rated battery consumption of 43W, rated device consumption of 60W and nominal power draw of the computing hardware of around 16W. These figures are modified slightly by scale and by considering a battery charging circuit consuming around 5W when active. However, the above figures only represent this moment in time of the ICT industry; future machines will have different ratios of demand to capacity and so the long term value of the above small sample is doubtful.

In terms of behaviour from an external viewpoint, a laptop device can therefore draw anywhere between zero watts when off or when powered via its own energy storage, its operational range with the battery quiescent and rated value when charging.

There are therefore two semi-coupled loads to consider in the proposed network; the embedded battery as the target for control and the computing hardware itself which is deemed uncontrollable.

3.1.2. Supply Characteristics

As discussed in chapter 2, the preferred supply to the selected network of loads is a building integrated photovoltaic array. BIPV systems are presently the best rewarded

under the Clean Energy Cashback FiT scheme in the UK as well as also being well rewarded through various other schemes worldwide, providing a financial incentive and certainty in long term investment. However, it is noted that a business model based solely on continuing levels of artificial subsidy is fundamentally flawed and that technologies should be able to stand or fall on their own merits. In this respect, future photovoltaic technologies are expected to benefit from falling manufacturing costs as the industry replaces high cost, resource intensive silicon wafer based panels with much lower cost and lower resource organic and thin film technologies. Further, the energy and cost dynamics of utilising PV energy in house depend on how the energy is buffered and subsequently used in loads – none of which is easy to generalise. These 'stand-alone' economics are an area identified for further study.

Generation from solar photovoltaics is characterised by intermittency. Although there is naturally a daily generating characteristic associated with relative position and angle of the sun which also varies more slowly with season, the nature of clouds and cloud behaviour can be highly variable at times and hence the output from PV is dominated in time and magnitude by the largely unknown dynamics of cloud cover.

As a result of intermittency in sunshine, there is uncertainty in generation such that best practice system design would target building integrated networks and control to provide security of energy supply to the system at all times. In addition to there being two loads considered, there are also therefore two supplies considered part of the network; the desired renewable and the conventional network supply.

3.1.3. Matching Supply and Demand

In any contained power system, the supply of energy and the demand for that energy must match. This statement is true for individually powered devices such as laptops and also true for large interconnected networks such as the grid.

However, the definition of 'matching' in past and present classical demand management solutions refers to performance over a period of time hence the often stated aim in

traditional demand management of energy optimisation. Given that energy optimisation translates to cost optimisation, this indicator has been extensively used to quantify the value of a demand management system in operational terms and has largely guided control strategy and implementation of these systems for at least 15 years [Counsell et al 1997].

The energy optimisation control strategy adopted by all classical demand management systems necessarily implies predictive modelling and a demand scheduling approach through some form of load shifting algorithm [Hong 2010] or set of defined rules [Ainsworth 2010] to anticipate or defer load to more favourable conditions.

Prediction of future demand is inferred through detailed modelling of the process coupled to knowledge of past demand and conditions. This is a weakness of classical prediction based systems since the resultant act of scheduling demand places artificial restrictions on user behaviour.

Rather than optimisation of energy by predictive modelling and risky scheduling of demand, the approach taken in this work seeks to reliably match demand with an intermittent renewable supply. This is justified on the supply side by considering the conclusions from Chapter 2 that at short timesteps, renewable generation cannot be predicted with any confidence unless conditions remain steady. The application to networks of mobile computing devices would also strongly suggest that demand cannot be predicted with any certainty.

3.1.4. Potential Benefits

Matching a building integrated renewable electricity supply with local demand at the building level can potentially solve a number of issues simultaneously and bring a number of significant benefits to the owner of a complete and integrated system.

In general terms of costs, import of increasingly expensive grid electricity is off-set by local production, reducing the operational cost of the loads. As a further beneficial

consequence of matching, emissions due to demand are also reduced and therefore also any financial penalty ascribed through the Carbon Reduction Commitment scheme. Although the market price of carbon is presently low, it is anticipated that future carbon values will be significantly higher, raising the value of this aspect.

For example, in-house utilisation of an ideal 100% of the energy generated by a 1kWp PV array in Sheffield (around 800kWh/year) could theoretically offset (at 15p/kWh import) roughly £120/year and reduce emissions by almost a ½ tonne/year. This is against the present artificial FiT scenario (at 41p/kWh) of £60 offset and £340 in subsidy. As these subsidies are gradually withdrawn and the cost per kWh of grid-generated electricity continues to rise, the economics of in-house utilisation improves. Using the 50% 'deeming method enshrined in the FiT and assuming other costs are constant, the price point for viability of in-house utilisation of all PV energy *for the asset owner* is a subsidised generating tariff of less than 7p/kWh. Other benefits to the owner and other stakeholders are less tangible but still high value.

A level of energy independence can be achieved for the building operator and so risk associated with traditional demand management solutions is completely removed since any control is now initiated and managed solely by the asset owner. This is a major consideration for commercial businesses in particular where take-up of utility driven DSR is low due to the perception that these systems may interfere with productivity. In addition to the financial rewards and penalties imposed on building operators, matching demand with a local renewable also raises the profile of the organisation in terms of corporate social responsibility.

Active supply and demand matching from the individual building level also unconsciously benefits other stakeholders. From a utility perspective, stress on the local distribution network is reduced and across a fleet of individual such systems, a net drop in demand could be realised at peak times when conventional electricity production is most expensive. At a strategic level, such a system would be aligned with UK policy on both demand reduction and increased use of low carbon electricity to reduce emissions.

Aiming for reliability in matching is proposed as a first step towards true integration of building integrated renewable generation on the demand side since the goal is to take advantage of local renewable availability when and only when the opportunity arises.

There are therefore a number of potential benefits of using building integrated renewable energy. However, many of these benefits are coupled across several stakeholders, including the utility, and are difficult to fully quantify within the remit of one thesis.

3.2. LITERARY BACKGROUND

The concept of controlling energy demand to fit with a nominal supply profile of some kind is far from new [Gellings 1985] and although most past and proposed systems are utility driven, there are also a number of 3rd party solutions which aim to engage and utilise demand side resources for various end purposes. Past demand management services, products and programmes differ greatly in how they operate in terms of objectives, appliance utilisation and system topology, in terms of the control signal used, the control structure and action and also in risk.

The latest utility proposed collection of initiatives aimed at mass market roll-out in the UK and in other countries is loosely called the ’Smart Grid’ [DECC 2011]. At the building level, the aim is to control (smart) appliances within the building through integration with a communications enabled smart meter, allowing the utility to either completely defer or restrict use of individual or fleets of appliances during peaks or to modulate the supply very short term and take advantage of the energy storage capacity of the appliance itself in an effort to satisfy both stakeholders to a degree.

The purpose of utility driven demand management is to reshape the overall demand profile through one or more defined mechanisms to optimise generating cost and other market conditions or to support network balancing. These two utility purposes differ in the control signals used.

Infield et al proposes that participating loads within the building respond to network frequency target of 50 Hz [Infield et al]. The benefit of this approach is that this is the same feedback signal used by utilities to indicate the real time balance of the grid and is a signal already available at the input to all grid-connected appliances. This method of controlling demand is standard practice by network operators in a number of countries including the UK as a pre-arranged and contracted method of load shedding [ENERNOC 2011]. However, as stated previously, network frequency only indicates overall imbalance and cannot identify whether this imbalance is due to changes in load or scheduled supply or a fault or renewable availability.

Various authors and utilities have in past publications proposed time-of-use pricing, real-time-pricing and other tariff optimisation structures as a control signal to customers and a number of relatively small pilot trials are on-going worldwide with mixed results thus far. This concept is hugely attractive to utilities since the cost of generating electricity varies throughout the day and season by season, being more expensive at peak times. By passing this cost on to consumers throughout the day, the intention is to discourage use during this period [Roscoe et al, Counsell et al]. Importantly, risk associated with the decision to control is borne by the user. However, there are technical challenges to overcome before this signal can be used extensively in automatic control systems. For example, in a study which characterised communication delays in a load following application, Bhowmik et al suggests that random delays, to which all data networks are subject, could result in failure to meet demand and may even result in system instability [Bhowmik et al 2008]. This is supported by others such as Nutaro who reports on this effect on present rule based market controls, suggesting incompatibility of a variable pricing structure with proposed smart grid controls [Nutaro et al 2009]. Grid based implementation of demand control is therefore highly limited which may go some way to explaining the relatively low take-up of potential solutions over the last 2 decades.

The CELECT control system as applied to electric storage heating can operate within a utility driven static TOU or real time pricing regime broadcast over radio teleswitch [Counsell et al 1997]. The system features a sophisticated robust control method with

predictive modelling techniques to anticipate demand and optimises based on cost to the consumer in an attempt to bridge the gap between utility and 3rd party stakeholders.

By comparison to demand management systems which use an energy or cost optimisation approach, controlled integration of a renewable source of energy by demand led measures in a reliable manner is a relatively new field and few published papers are available.

A solution proposed by Hong aims to integrate a renewable supply within the demand control structure by manipulating appliance energy storage such as to coincide with either a modelled or measured renewable supply [Hong 2009]. However, the load shifting algorithms developed by Hong are complex and in common with most proposed solutions are heavily dependent on detailed demand modelling and prediction for control function. As a result, it is rather inflexible and scalability of the solution is limited by exponentially increasing calculation times necessary for additional controlled loads in a limited supply situation since calculation of each load 's capacity state and potential involves an iterative process between all networked components.

If the conclusions reached by Bhowmik and Nutaro are corroborated by additional research, it would support the view that perhaps smaller independent solutions may provide the best option to increase saturation of renewable technologies in urban settings.

Although several 3rd party independent demand management systems exist such as Moixa, these systems tend to focus on optimisation and user based control rather than providing an automatic control regime [Moixa]. An interesting solution from Coolwater Products purports to integrate a range of alternative fuel sources but focuses on powering inflexible loads which do not feature energy storage instead of to dedicated energy storage devices. The storage element in this case is not actively integrated as part of the controlled system [Coolwater].

A final state of the art solution is seen in a recent patent by Apple. However, the focus of Apple's approach is integrating the renewable with a single device and not to a network of controlled devices and so the scope and objective of the control is likely to be more similar to that of Coolwater [Sander et al, Apple 2010].

All of the systems noted above are characterised by complexity either in function or in control or both since they rely on model based prediction. For example, non-linear models of nonlinear demands controlled by nonlinear actuators operating on nonlinear signals are common in part or in whole to all past solutions with the result that the system control structure is highly complex, hard to validate and it is therefore difficult to guarantee robust performance. All of the solutions presented previously assume control is of a mostly deterministic system i.e. that the models accurately describe the processes involved and that significant deviation from these models will not occur. This has the effect of severely limiting stable control to a narrow band of conditions outside of which, the control objectives will not be met.

3.2.1. Uncertainty

In design of critical energy networks such as the proposed integrated system, the 'three R's' of robustness, reliability and resilience must take precedence over all other aspects. These are familiar concepts to system design engineers and give confidence to qualitative validation of performance in a recognisable and comparable way.

The natural characteristic of a mobile computing demand including user interaction at the individual appliance or building level is anticipated to be highly random and so the usefulness of classical predictive modelling approaches is limited in its potential effect.

The generating profile of a photovoltaic array can also be highly random during erratic weather conditions and so the future array response based on modelling is also uncertain during these periods. Unless control is restricted to steady, more predictable conditions or designed to be immune to generating uncertainty, the availability of the renewable at time t+1 is largely unknown at short time steps.

A novel approach in demand management taken in this work is to consider the problem in functional terms of reliability in matching controlled demand with renewable supply rather than the conventional system optimisation approach. With high levels of uncertainty in both demand, supply and plant dynamics, the strategy adopted in

designing a controller for the proposed system is based on governor theory [Dickinson H W, 1935].

3.2.2. Governor Analogy

As far back as 1698, Savery's steam engine demonstrated a useful mechanical output from a thermal energy source by alternating a simple pipe and valve system above and below atmospheric pressure to pump water from mines. The Newcomen engine overcame a high pressure issue in Savery's design but the engine itself still used external atmospheric pressure in part of its cycle as a crude regulator. Watt made several significant advances to Newcomen's steam engine technology. A first key design improvement replaced atmospheric pressure with low pressure steam, hence isolating the system. Such was the step improvement that Watt in partnership with Boulton commercialised on their opportunity by charging mine owners a license fee based on the displaced cost of fuel rather than for the machine itself.

By completely closing the system, Watt introduced a problem in that the system might not now be stable since regulation by exposure to atmospheric pressure was now lost. This was a major obstacle given that the engine speed was to remain constant (balanced) at all times and under all conditions.

Watt's solution linked a steam regulator to a modified centrifugal governor similar to those already used to regulate the speed of water and wind driven millstones to give constant speed output to the steam engine and importantly, allowed factories to be sited away from rivers and waterwheels, providing a key enabling technology for the industrial revolution.

An illustration of Watt's fly ball governor mechanism is shown in Figure 3-1. At rest, the fly balls are at their lowest position and held by gravity. In this state, the butterfly valve controlling steam input to the engine is open. Should a drop in load occur, the engine speed increases and the masses rotate faster through the pulley mechanism until their centrifugal force exceeds the gravitational force and they rise outwards and

upwards. This motion through the linkages shown results in proportional closing of the valve until the engine speed balances with demand at which point the vertical height of the masses becomes steady and the system is in equilibrium. An increase in demand reduces the speed of the engine, slowing the rotation of the governor, allowing the fly balls to drop and opening the valve to allow more steam through again until a state of equilibrium is achieved.

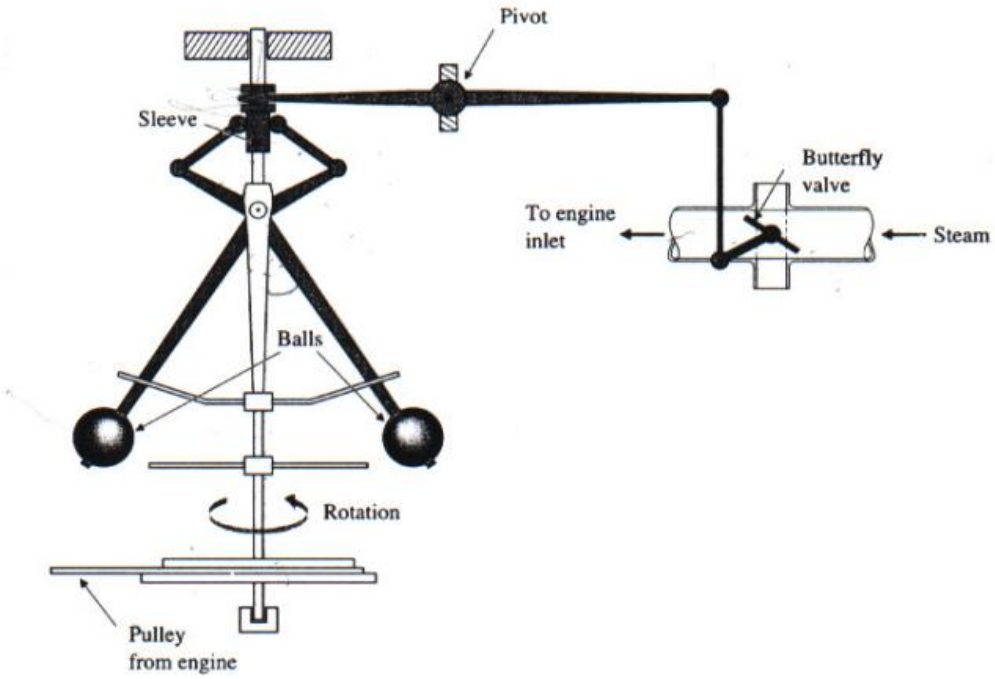

Figure 3-1 Watt's Flyball Steam Governor

Mathematical analysis of the dynamics of the governor as separate from its steady state operation is not a trivial exercise however and it was almost 100 years before Maxwell detailed the function of a governor as fundamentally different to that of a moderator [Maxwell 1868].

A concise definition of a governor is a device which controls the supply of energy to a system without prior knowledge of the supply or demand.

In the present context, the steam engine represents both the known demand of the battery in the proposed network and the unknown demand of the computer hardware and any other unconsidered demands whereas the steam boiler represents both the certain (but unwanted) grid supply and the uncertain renewable supply. The governor represents the control action on the system, removing fluctuations in demand and/or supply to maintain a steady and balanced output to the load.

Watt's Governor is by no means a perfect solution but provides a simple and reasonably accurate analogy to the present problem of reliably matching demand with supply in an uncertain system with uncertain dynamics, subject to uncertain disturbances.

3.2.3. Feedback Control

The structure of a feedback controller is illustrated in Figure 3-2. Basic operation of feedback control is detailed in Appendix A1.

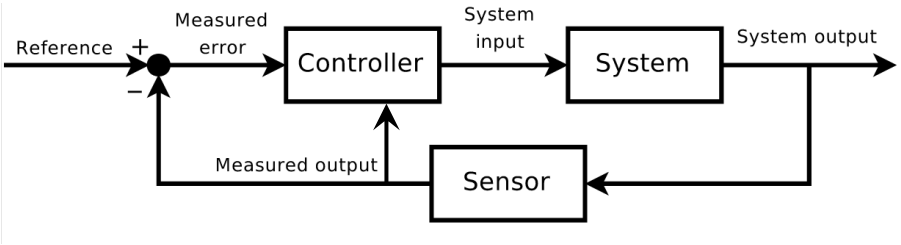

Figure 3-2 Feedback Control Structure

Watt's governor is a form of proportional feedback control. Feedback control relies on generating an error signal between a desired set-point and response feedback from the system. The feedback signal must therefore represent a measureable response from the plant. For example, given its construction, the error signal in Watts's steam engine governor is inversely proportional to the square of the feedback signal - engine speed.

However, this is a non-linear relationship and as such, the control loses sensitivity as speed increases.

The relation coupling the error to the controlled parameter is therefore critical in determining the sensitivity of the system over its operating bandwidth range and can also impact on the stability of the closed loop system. The best error signal is therefore the simplest one which represents observed changes in the controlled plant in a linear manner.

Design of feedback control systems involves employing one of a number of controller types in the loop. The controller type is usually selected based on the complexity of the system and its closed loop relative degree. The relative degree of a feedback control system is derived from its closed loop transfer function and the order of its denominator subtracted from the order of its numerator, indicating the number of finite zeros in the system. Further, tracking a set point raises the relative degree of the system by 1. Although this increased complexity can be countered by model order reduction techniques, the choice of controller type is still dependent on whether or not the system is linear. The present application requires a nonlinear control due to energy rate limits and battery saturation conditions.

3.3. ERROR SIGNAL

Choice of error signal in feedback control is critical in determining the sensitivity of the control system to change over a range of operating conditions as indicated above. However, the proposed building integrated system has two continuous inputs inversely proportional to each other within limits and therefore the choice of error signal must be equally and proportionally representative of both sources in such a way as to correctly indicate the error magnitude and sign on which the controller operates.

As was stated in chapter 1, the fuel mix of the grid determines its carbon emissions. Since network demand changes second by second, the generating mix also changes second by second and also therefore the carbon emissions due to this generation. This

situation also describes generation from a renewable but intermittent supply such as a building integrated PV array.

Until fairly recently, reporting on carbon emissions due to generation, transmission and distribution of electricity was limited to an annual value issued by the system operator. At present, this value is 0.537kgCO2/kWh delivered and includes a nominal transmission and distribution loss of 9% [DECC 2010].

However, ELEXON (the UK's Balancing and Settlement Code Company), gathers data on present generators attached to the grid to make it possible to view a great many operational parameters at traditional half hourly and up to 5min resolution. This information is available from the Balancing Mechanism Reporting System website and can be licensed to a third party to offer a carbon intensity based signalling service [AMEE 2009]. The modelling method used to arrive at carbon intensity (CI) values uses a simplified utility network model since emissions from even a single generator vary significantly with loading but is accurate enough to represent the state of carbon attached to electrical energy at 5 minute intervals although it is also noted that improvement could be made for example in determining the true CO2 intensity of pumped storage and the effect on UK grid carbon intensity of export to other countries.

An example of this data is shown as Figure 3-3 and is overlaid with half hourly demand for a 24 hour period also from ELEXON. The various colours on the graph indicate the different generators contributing to the mix as given by the legend.

As is shown in the graph, carbon intensity is higher during peak times and lower at night as would be expected. As can also be seen, carbon intensity is almost totally dominated by emissions from conventional generation. Although the UK has around 5GW wind capacity installed at present, the overall carbon intensity value is not very sensitive to wind given its operational capacity factor and also since there are also other sources of low carbon electricity on the network usually, but not always, used in conjunction with wind as part of the balancing mechanism such as pumped and non-pumped hydro. These sources often contribute more to the mix than wind, including on the day illustrated above and so also therefore affect carbon intensity to a greater

degree. At present rates of wind and other low carbon generating plant deployment, the carbon intensity of the grid is expected to drop around 10g/kWh per year [PWC 2010].

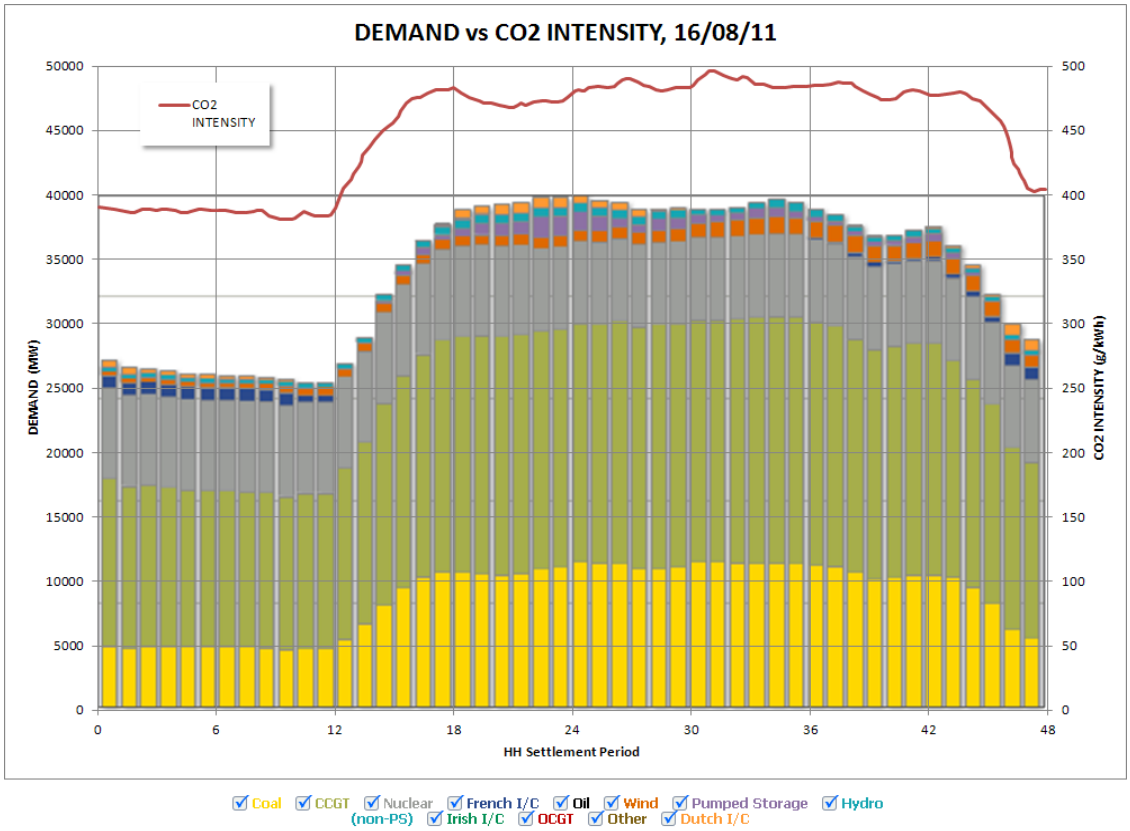

Figure 3-3 Grid Daily Demand and Network Carbon Intensity [Source: ELEXON 2011]

The carbon intensity of output from a building integrated PV renewable energy source is as contentious an area as embodied carbon in all aspects of energy supply and there is little real agreement between researchers regarding embodied and even true operational carbon emissions from generation, transmission and delivery of electricity. Further, reporting on this issue often does not include the methodology used or relies on out of date data.

Although operational emissions from BIPV is arguably zero if the embodied carbon of the system components is not considered (as is usually the case), technically, there will be some degradation in power quality due to use of the grid in transferring energy to a load. This is also a contentious area and no hard figures are available. The UK's grid

operator only states a nominal figure of around 9% losses in transmission and distribution but this could be much higher at lower levels in the network.

A paper by Sovacool et al proposes a nominal carbon emissions figure for PV of 0.032kgCO2e/kWh to include embodied carbon over the PV generator lifespan and compares this to other calculated values, recopied in Figure 3-4 [Sovacool et al 2008]

However, any demand control which responds to relative carbon intensities of the grid versus that of a local low carbon renewable source, the renewable will always be seen as the preferred source of the two. Presently, this difference is at least two orders of magnitude.

Technology	Capacity/configuration/fuel	Estimate (gCO_2e/kWh)
Wind	2.5 MW, offshore	9
Hydroelectric	3.1 MW, reservoir	10
Wind	1.5 MW, onshore	10
Biogas	Anaerobic digestion	11
Hydroelectric	300 kW, run-of-river	13
Solar thermal	80 MW, parabolic trough	13
Biomass	Forest wood Co-combustion with hard coal	14
Biomass	Forest wood steam turbine	22
Biomass	Short rotation forestry Co-combustion with hard coal	23
Biomass	FOREST WOOD reciprocating engine	27
Biomass	Waste wood steam turbine	31
Solar PV	Polycrystalline silicone	32
Biomass	Short rotation forestry steam turbine	35
Geothermal	80 MW, hot dry rock	38
Biomass	Short rotation forestry reciprocating engine	41
Nuclear	Various reactor types	66
Natural gas	Various combined cycle turbines	443
Fuel cell	Hydrogen from gas reforming	664
Diesel	Various generator and turbine types	778
Heavy oil	Various generator and turbine types	778
Coal	Various generator types with scrubbing	960
Coal	Various generator types without scrubbing	1050

Figure 3-4 **Lifecycle Estimates of Specific Emissions for Electricity Generators [Source: Sovacool]**

3.3.1. Control Objectives

From an ownership perspective, the intention is to define the building or electricity network within the building as the bounded system.

The deliberate intention in feedback control design is to keep models and control functions as simple as possible without being simpler than is possible. Rather than specify some unattainable or unrealistic goal, the function of the control algorithm can be simply stated as making the best use of the resources available. To this end, the controller design objectives are:

- Minimise transfer of energy across the system boundary
- Minimise the environmental impact of the integrated system

In the first case, minimising energy transfer across the system boundary effectively means minimising import and export of electricity to and from the system. By specifying a building integrated photovoltaic source of energy as within this boundary, the control implication is that all renewable generation is to be offered for use within the building. This objective therefore intends to replicate the independence of an off-grid system but without actually being off-grid and hence conventional security of supply is maintained. Choosing zero energy import or export as the ideal system state is further justified by realisation that this represents best use of resources in owned assets and that there is presently little financial gain in export to the network and an increasing severe penalty for import.

The second control objective is to minimise environmental impact of the integrated system for the asset owner. Minimising operational CO2 emissions from the building is highly desired both from an ethical viewpoint and also from a financial viewpoint with the UK's CRC policy imposing penalties on emissions. This is an important feature

since other countries such as Japan are also implementing a ‘cap and trade’ type mechanism at the individual building level and other countries are likely to follow.

However, energy and carbon are strongly coupled in power supply systems. This coupling is exploited in achieving the above objectives in the control strategy for the system.

3.3.2. Control Strategy

The simple strategy adopted intends to achieve the defined objectives by driving the carbon intensity of the electrical supply to zero as shown below.

Carbon emissions as a function of time due to electricity use can be given by carbon intensity of the fuel being used multiplied by the energy supplied:

$$CE(t) = CI(t) \cdot E(t)$$

Equation 3-1

Where: CE is carbon emissions in $kgCO2$

E is energy consumed in J

CI is carbon intensity in $gCO2/J$

t is time in s

By inspection of the above simple equation, and considering the assertion that both supply and demand energy is unknown, it is clear that instantaneous carbon intensity (the rate of carbon emission) is the desired feedback parameter and that driving this parameter to zero results in minimum carbon emissions for the energy system.

3.4. CONTROL ALGORITHM DESIGN

3.4.1. Topology and Descriptive Model

As indicated previously, the supply to the network consists of two inputs. This energy supply enters the closed network at a single point and can therefore be analysed using standard nodal techniques. Figure 3-5 illustrates this simple supply topology.

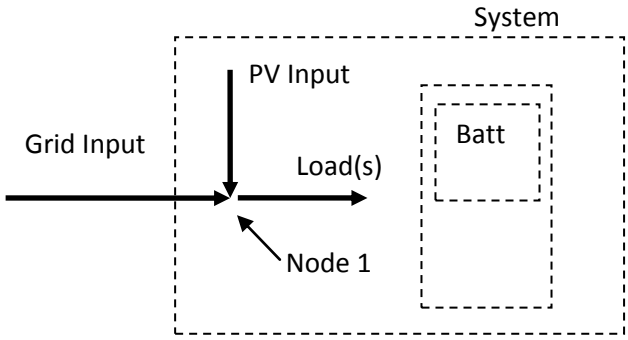

Figure 3-5 Network Input Node

From the figure, demand power to the load (including uncontrolled load) is simply the sum of both the PV generation and the grid input.

$$P_G + P_{PV} = P_D$$

Equation 3-2

The carbon intensity of the total demand is therefore given by:

$$CI_D = \frac{CI_G \cdot P_G}{P_D} + \frac{CI_{PV} \cdot P_{PV}}{P_D}$$

Equation 3-3

Assuming zero emissions from the renewable reduces the above function to

$$CI_D = CI_G \cdot \frac{P_G}{P_D} \ .$$

Function of a typical laptop, and other devices with embedded energy storage, can be ideally summarised by considering the system as a capacitance representing the battery in parallel with a load representing a real demand. At the system boundaries, an effort or tension is maintained so that the variable parameter is flow; in DC electrical terms, constant voltage with variable current. This is valid since an end-device typically includes dedicated regulation and charging circuits in addition to an input power stage which automatically adjusts output current to maintain a constant voltage to the device. This is also consistent with the rest of the system for the same reasons and so all that is required is knowledge of the particular fixed voltage level and measurement of current.

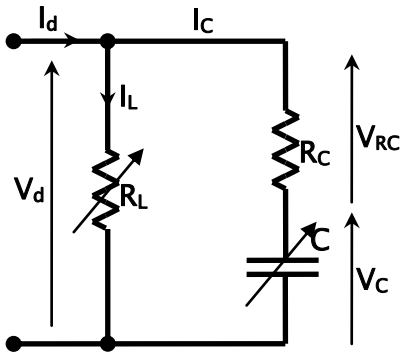

Figure 3-6 1st Order Electrical Equivalent of a Mobile Computing Device

In the charging circuit shown in Figure 3-6, the battery resistance is approximated as constant while the remaining two elements are variable. The charging or discharging current is therefore dependant on the applied voltage, fractional ohmic resistance of each leg, battery time-constant and state of charge. The total demand current for the circuit shown is given by a simple 1st order response:

$$I_d = \frac{V_d}{R_c} \cdot e^{\left(-t/R_c \cdot C\right)} + I_l$$

Equation 3-4

And for multiple devices is simply given by

$$I = \sum I_d = \sum I_l + \sum I_C$$

Equation 3-5

The model above allows simple calculation of the charge stored and extracted from the battery, allowing condition assessment of the device and calculation of control parameters.

Modelling of electro-chemical batteries usually starts with the above circuit and adapts it to represent real behaviour typically using Peukert's equation in conjunction with other adaptations but for present purposes, a simple 1st order energy storage representation is sufficient.

3.4.2. Control Loop

According to the theory presented in the Appendix A1, the order of the closed loop system is 2 with a relative degree of 1. Feedback controller options therefore include on/off or bang-bang types, traditional proportional/Integral (PI), integral variable structure controllers (IVSC) and pseudo-derivative feedback (PDF) types. The relative merits and demerits of these controllers are better discussed elsewhere [Young et al 1977, Wu et al 1992, Phelan 1977].

Phelan describes control of a system with relative degree of 1by introducing a controller type with superior performance than alternative controls. The controller, also adopted in this work is known as a pseudo-derivative feedback (PDF) controller. A PDF type

controller is an improvement in alternative forms due to position in the control loop of the proportional and derivative elements which results in a zeroth order system with linearised output [Phelan 1977].

A difficulty in casting the control for dynamic systems is how to remove unwanted influences in the system from appearing at the controller input. In present context, these unwanted influences are the uncontrolled loads and the energy input from the grid to supply these loads. However, the system topology from Figure 3-5 dictates that this energy stream is simply the difference between the total and the renewable streams. The real load and the renewable are therefore both cast as disturbances in the system and rejected using Phelan's treatment of such load elements up to the closed loop bandwidth of the system.

Ohm's law describes the behaviour of the computing load and also the renewable input as first order but by considering these as reduced linear equivalents, high gain theory states that in the closed loop analysis, the influences of both the real load and the renewable supply are rejected and do not appear in the error signal to the controller as the system is driven at higher gain. A schematic of the complete control loop is shown in Figure 3-7 and detail of how, mathematically, disturbances are rejected in feedback control systems is included in Appendix A1.

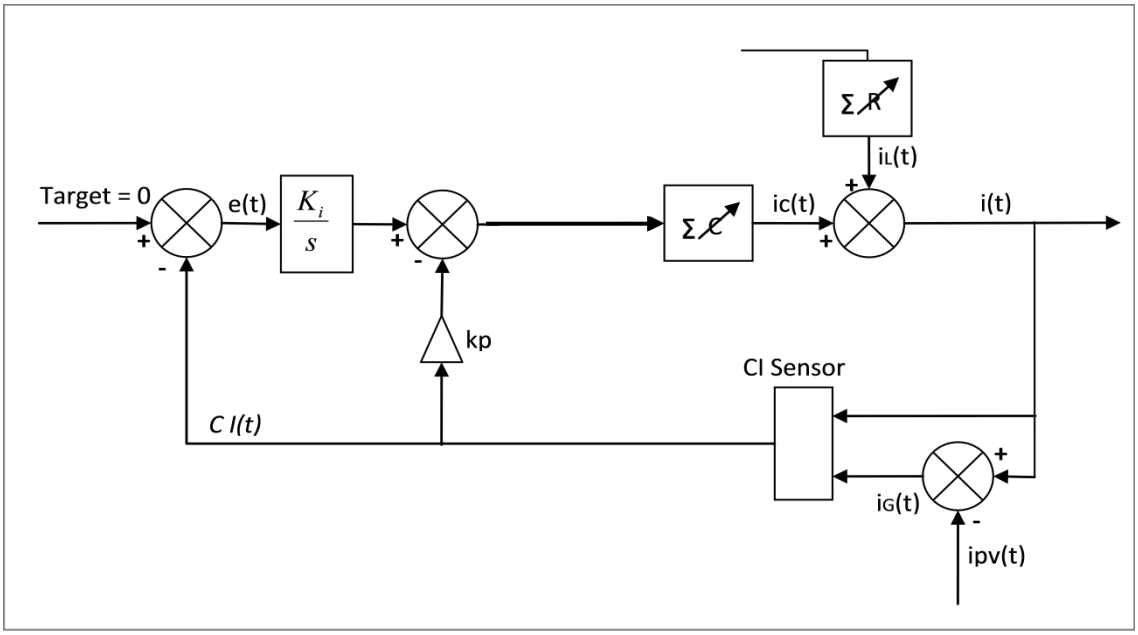

Figure 3-7 Closed Loop Control Structure of the Integrated System

The figure shows a pseudo derivative feedback (PDF) type controller in situ within the control loop for a system of relative degree of 1. As can be seen, control action is on the energy storage element whose current demand response is added to that of the real load to give a total response. The total network current demand is then passed to the feedback sensor which calculates carbon intensity in the manner already discussed. The system response in terms of carbon intensity is then fed back to the controller via the error signal summing junction. The controller is highly accurate in tracking, proportional in response, linear and equally sensitive across its bandwidth and also intermittent in operation since corrective action is only required when there is deviation from the set-point. It is perhaps a little ironic that the chosen solution to matching an intermittent demand with an intermittent supply is to use an intermittent controller.

3.4.3. Nonlinearities

Tackling nonlinearities in feedback control systems can be a challenge. The main nonlinearity in this system is battery saturation. Given that the function of the control and integrated network is to fill the batteries with sunshine, instances of full batteries are intended to be a common feature of the system and so the controller must consistently do the right thing when these events occur.

From a controller performance perspective, hitting a limit such as battery saturation can cause instability and lock up of the controller, known as integral wind-up. Therefore, within the controller structure, the need is for the control to stop driving the system until response is back within this limit.

Integral wind-up can be dealt with using an algorithm which calculates and negates the integrator effect when a limit is reached [Hanus et al 1987]. However, Phelan deals with the integral wind-up problem by introducing a switch into the loop which detects when a limit has been reached and sends a signal switching off the tracking integrator element. Often combined with a damping term, this provides an effective and relatively

simple method of coping with nonlinearities in the closed loop control and provides a measure of system safety.

3.4.4. Stability

Stability is obviously of critical importance in feedback control. Although several methods exist such as Routh-Hurwitz, Nyquist and Lyaponov methods which give the stability criteria for control, the present system benefits from being of low order in that stability is predominantly sensitive to sampling rate and rates of change of load against time constants. This is shown in Appendix A.

3.5. IMPLEMENTATION OF SISO CONTROL FOR DISTRIBUTED ENERGY STORAGE SYSTEMS

Across a fleet of discrete storage elements, implementation of the single input single output (SISO) control can take several forms.

The control could simply act on the total demand of the system and issue a command to all devices to increase or decrease consumption simultaneously and to the same degree. This is, at first glance, the easiest option to implement since no additional knowledge is required of the plant such as state feedback. However, without any knowledge of present capacity in a fleet of embedded batteries, there is a large degree of uncertainty in how the plant will respond to any command. Even if present capacity is known, the magnitude response of the plant is not controlled and may or may not be sufficient to completely utilise a renewable stream and follow a supply profile. Further, 2-way negotiation between prospective demands and a central control may result in long computation times. This is a highly restrictive solution and would limit robustness to certain demand conditions or particular times of year to a large degree.

The preferred alternative is to select a number of storage elements from a pool as priorities for control. With the present focus on matching renewable generation in time and magnitude, this approach to implementation is far superior in a number of ways.

Prioritisation of devices is a common feature in a number of networks including ICT data networks and the grid and is usually done through some justifiable methodology. In conventional domestic demand management where a number of appliances may be controlled, the preferred rank of each device is usually input by the user but several authors propose different rankings for different appliances e.g. Hong, Infield, based on market research, penalties for use or perceived needs or other sometimes more subjective criteria. In this particular respect, the present approach is simpler since the network will likely consist of numbers of similar if not identical devices where state of charge is only based on the balance between low carbon availability and user's needs and therefore directly indicates utilisation of renewable energy. Ranking mobile devices by their utilisation of the low carbon resource seems the fairest and most useful approach and is actually very similar to the analogy of utilities ranking generators by capacity and response.

The output signal of the closed loop system is total demand current. Given that regulated voltage output is a feature of all intermediate power conditioning devices upstream to the PV array, the demand current magnitude can be tuned to match the generated solar current in a similar manner to a maximum power point tracker (MPPT) but with an extended and distributed storage element. This method also overlays the MPPT function of the grid-tie inverter without compromising function.

Figure 3-8 illustrates an example of filling the capacity of the array to maximum power point by matching a number of laptop load currents to the generating maximum current. As is shown, the batteries demands are stacked until maximum power point conditions are met. This simple method is valid since maximum power point voltage is already maintained by the inverter device.

A significant advantage of this method over those usually employed is that of scalability. Since the system is single input single output, cumulative demand, supply

and capacity are inherently scalable within a range, allowing a much higher degree of flexibility.

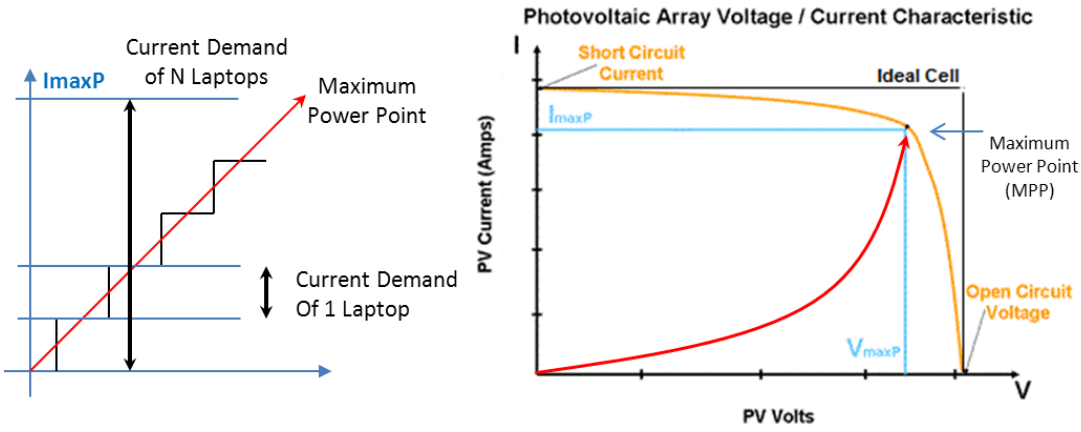

Figure 3-8 Illustration of Cumulative Current Matching of Supply and Demand

3.6. MATLAB MODELS

The closed-loop control was implemented in Matlab/ Simulink modelling environment deliberately only using basic control building blocks.

The model itself features a scalable PV input, scalable demand and scalable storage elements as well as several other tuning parameters to allow a full ‘what-if’ analysis of the control in simulation.

There are several additional internal functions included in the model. Some of these deal with nonlinearities and limits; others are to remove unwanted data from measurements and to convert units to those desired. Inputs are from a PV profile and from a demand profile and the output control reporting structure is via a multiplexed current vector to an exportable Matlab ASCII format .mat file.

The complete controller including these ancillary components is shown in Figure 3-9.

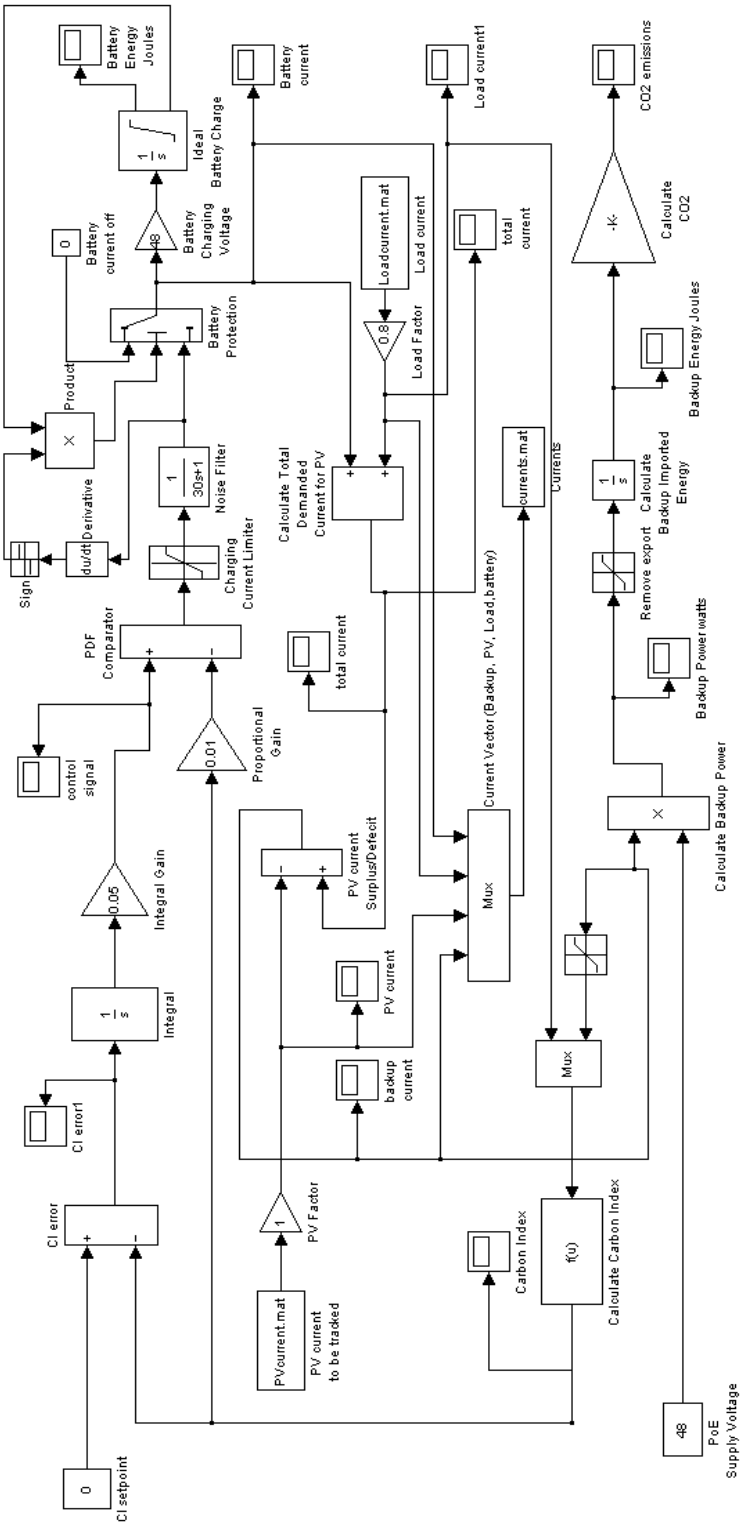

Figure 3-9 - Carbon Governor Control in Simulink

3.7. RESULTS & DISCUSSION

For the simulation, a sampling rate of 15min was used and input PV and demand current profiles constructed to represent a full day.

The PV profile generated for the simulation is semi-realistic in occurring at the correct time of day and in a shape (and frequency content) reasonably similar to that of a real profile [Jones]. After a clear sky in the morning, several oscillatory steps were also included to mimic transient cloud events before becoming totally overcast later in the afternoon. This nominal profile is shown in Figure 3-10.

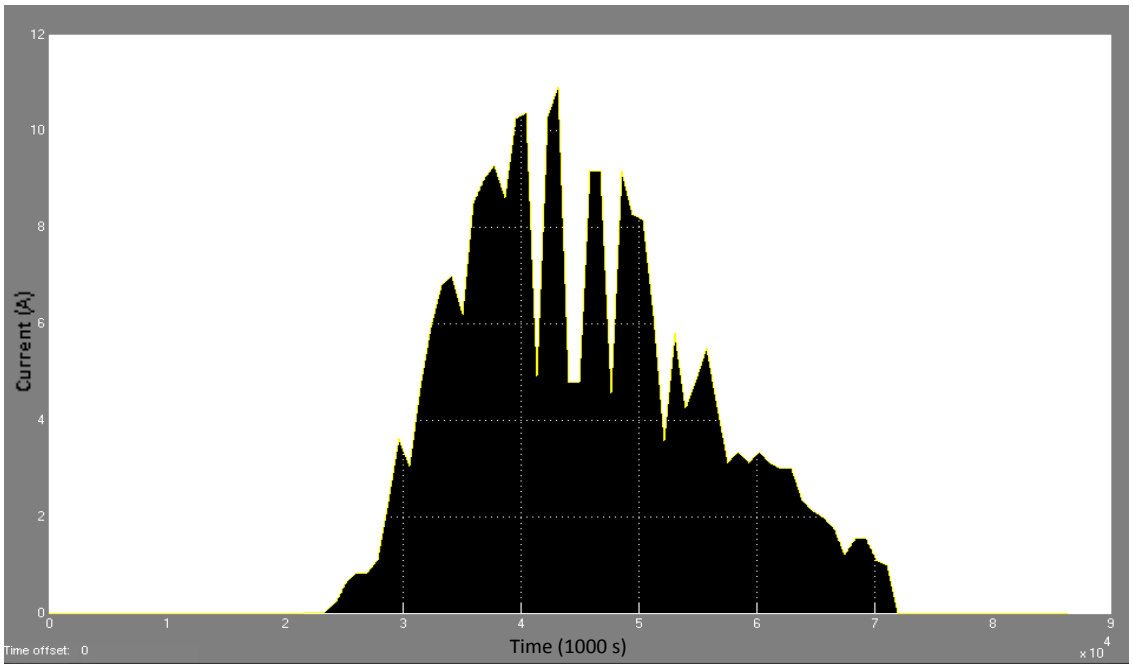

Figure 3-10 Nominal Daily PV Generation Profile

Similarly, the demand profile generated is only nominally representative of any particular profile. The choice of a subjectively generated profile is justified by recalling that the application is mobile devices and therefore the defining feature is mobility and not always being connected to a power network. Figure 3-11 illustrates the demand profile generated and includes a drop in consumption around lunchtime as might be

expected but also includes a small portion of energy used after working hours. This arbitrary inclusion could represent applying computer updates or other routine network management functions. Also note a small baseload at night. This is deemed typical of the chosen application but in reality may or may not be present depending on implementation of Wake-on-LAN (WOL) or other demand reduction measure [Energy Star].

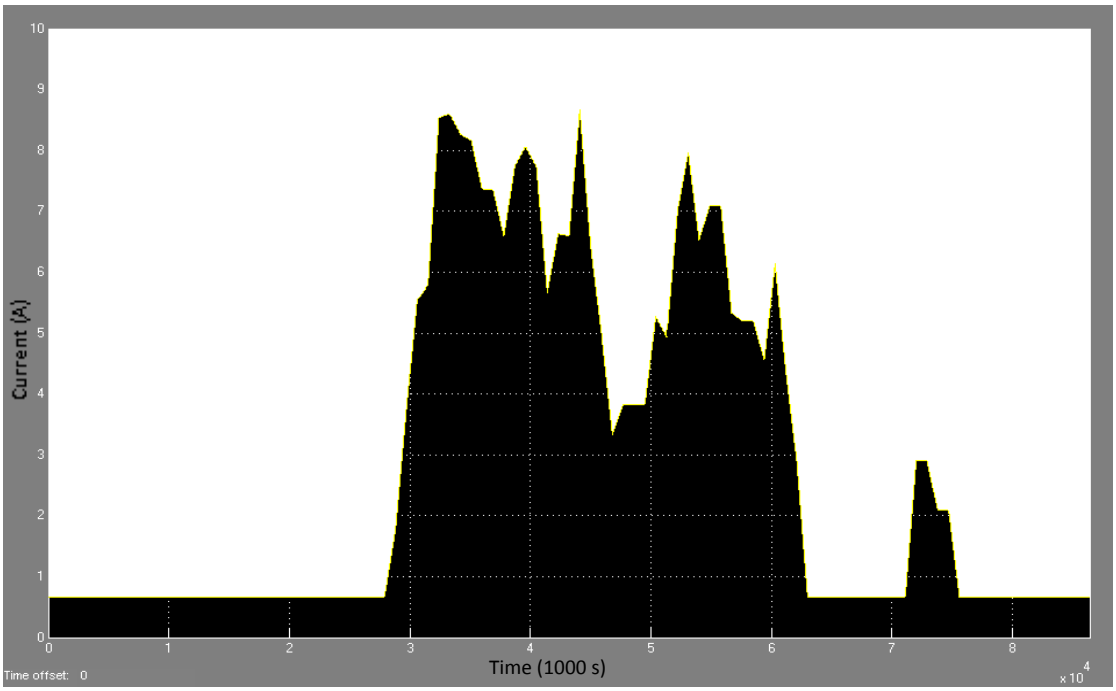

Figure 3-11 Nominal Daily Demand Profile

The relative scale of peaks and troughs in the demand profile are presumed to be very specific to particular working practices and could, in theory, be a simple almost flat demand if workers breaks are staggered.

The first simulation scenario scaled the above PV and demand profiles to 1 and set the battery storage capacity and limits as shown in Figure 3-12. This simulation assumes a summer day in the UK.

In this case, the initial condition of the cumulative battery capacity was 50% SOC and with a lower limit of 33% SOC, below which the control would ‘let go’ i.e. revert to open loop and a conventional grid-connected installation. This avoided over discharge of the battery. The total capacity of 1200Wh is roughly equivalent to 24 laptop batteries of 50Wh each against a nominal PV supply equivalent to an array of around 800Wp.

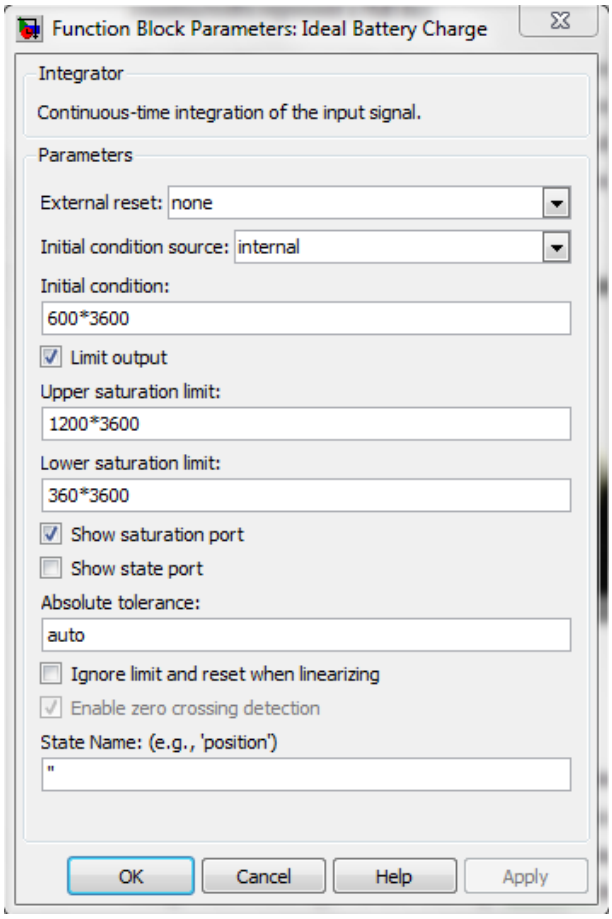

Figure 3-12 Simulink Battery Block Parameters

In terms of control robustness, the most important parameter result to study is the ideal battery state of charge. For the simulation as described, this is given below in Figure 3-13 and shows that for this set of sizing parameters, the cumulative capacity peaked at around 75% SOC.

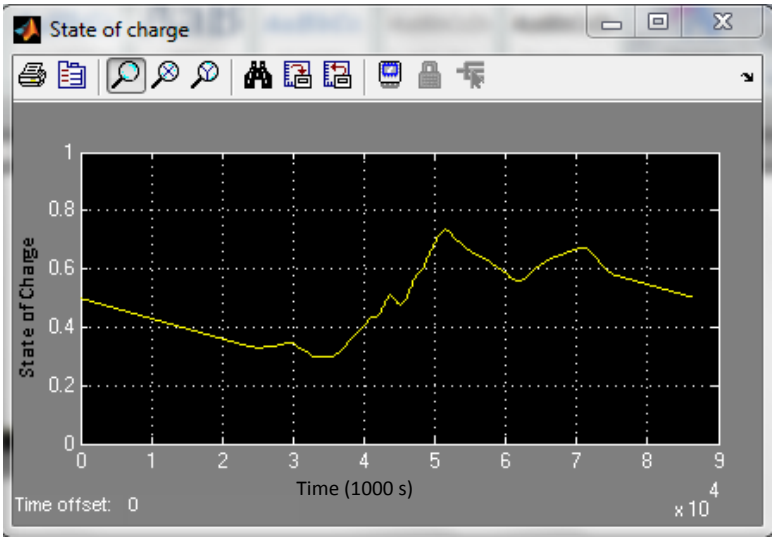

Figure 3-13 Simulated State of Charge 1

A small portion of the SOC figure also shows the battery capacity depleted and unable to provide any more power thus during this time, the back-up source (grid electricity in this case) was utilised. This is shown in Figure 3-14 which also shows that except for the time when the battery capacity was unavailable, there was no input at all from the grid.

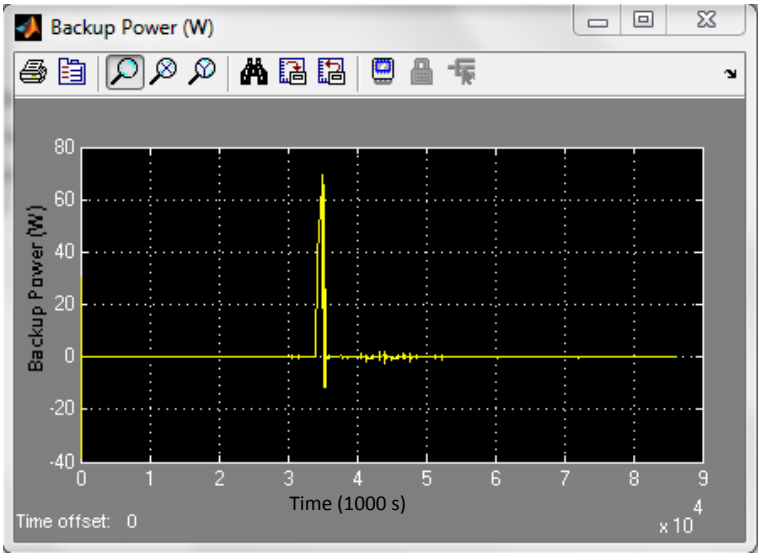

Figure 3-14 Simulated Back-up Power 1

The scenario simulated above would be considered an almost ideal case since very little energy was imported and none exported. However, there will be many days per year when this ratio of input to capacity to load does not hold and either the PV supply will be very much lower or higher than demand.

A second simulation was set up to illustrate these effects on robustness by deliberately sizing the battery element to be smaller compared to the PV scale. In this simulation, the ideal battery element was halved in capacity while retaining the 33% cushion below which the control does not operate. The battery initial condition was set to 100% and the PV scalar set at 1.

As can be seen in Figure 3-15, the battery capacity initially drops to just over 50% before climbing and saturating at full for a period during the early afternoon.

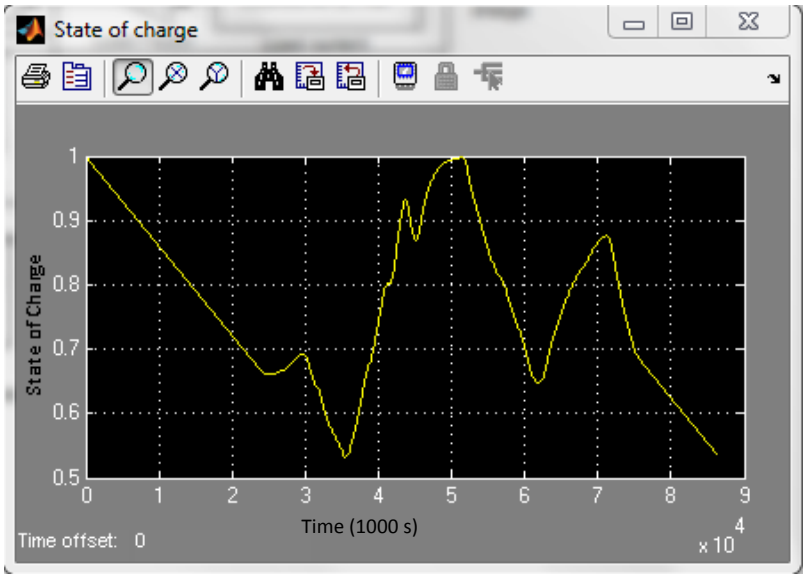

Figure 3-15 Simulated State of Charge 2

The 1st order response curve can clearly be seen in the figure just before the capacity saturates. However, what is not shown in this figure is that as the battery saturates, the rate at which it accepts charge drops and may exceed a defined limit imposed on the

system. This behaviour is evident by comparing Figure 3-14 above with Figure 3-16 below which again shows backup power from the grid source.

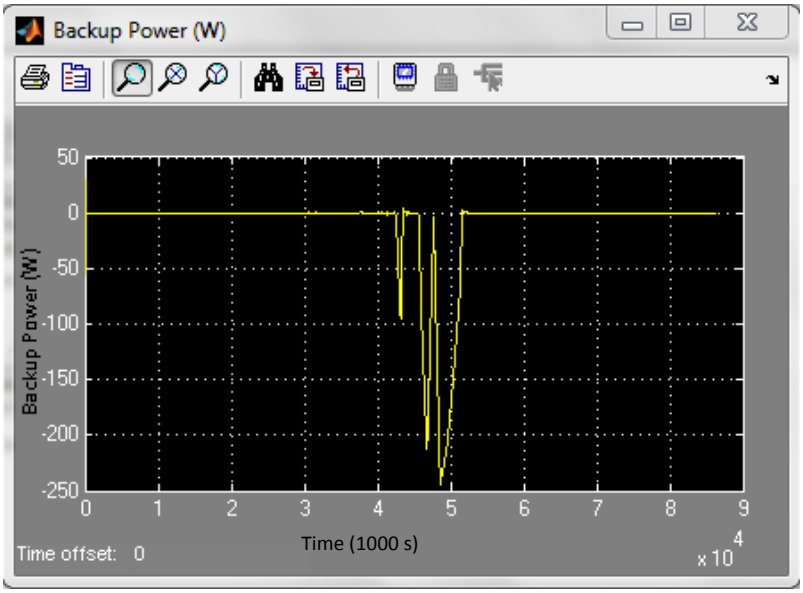

Figure 3-16 Simulated Back-up Power 2

There is in this case a period where there is nowhere within the closed loop system for the renewable power to go and so the control reverts to open loop, resulting in conventional export onto the grid until such times as there is spare capacity again.

There is little else that can be asked of the control; it behaves in the manner intended to make best use of available resources without compromising supply to the real load.

The results indicate that robustness of the control is sensitive to component sizing ratios between the available capacity for storage, the renewable supply and the network load as well as integral and derivative tuning constants. This also parallels the steam engine analogy where many designs, including the Newcomen steam engine using Watt's governor, were seen to waste fuel due to incorrect sizing between components [Dickinson]. Since robustness is a major feature in justification for a particular control

design, this issue is also highlighted as perhaps requiring further work. As a consequence, capital costs are also difficult to ascertain.

3.8. CONCLUSIONS

Demand side utilisation of a valuable building integrated renewable energy supply has the problem of mismatch between intermittent generation and local demand. Utilising embedded energy storage, a novel control has been developed and proposed which aims to reliably solve this problem. Simulation of this novel control indicates that if components are sized correctly, the control can optimise CO2 emissions of the building integrated network without prior knowledge of either supply or load and over a wide range of operating conditions.

A guiding rule of thumb in systems design using feedback control is that if the design works well in an ideal simulation environment, then it is likely that it will also work in a real world environment hence application for patent protection of the control process and design as described above [Counsell et al 2011].

The control solution proposed in this chapter is not the finished article in a number of respects. However, the novelty in the proposed closed loop controller design as a solution to reliably matching flexible building demand with building integrated low carbon resource independently of the utility while remaining fully grid-connected at all times represents a step in a wholly new direction for demand management.

3.9. REFERENCES

BERR, *Energy consumption in the United Kingdom, 2008 Update Pub URN 08/456 – Department for Business Enterprise & Regulatory Reform*, 2008

Bhowmik S., Tomsovic K., Bose A., *Communication Models for Third Party Load Frequency Control*, IEEE Transactions in Power Systems, Vol. 19, No. 1, pp 543-548, 2004

Born F. J., *Aiding Renewable Energy Integration Through Complementary Demand Supply Matching*, PhD Thesis, University of Strathclyde, 2001

Counsell J, Reeves J, *Heating Apparatus Controlled to Utilize Lower Cost Energy*, Patent Publication: US5700993 (A), EC: G05D23/20G4C2, 1997

Counsell J M, Stewart M J, Williams A, *Powering of Devices*, US Patent Application: WO/2011/101687, 2011

DECC, *The UK's Clean Energy Cashback Scheme*, http://www.decc.gov.uk , 2011

DECC, *Smart Grid Policy in the UK*,

http://www.decc.gov.uk/en/content/cms/meeting_energy/network/strategy/strategy.aspx , Retrieved 2011

Dickenson, H W, *James Watt: Craftsman and Engineer*. Cambridge University Press, ISBN: 978-1108012232,1935

EA Technology, *Task XI – Time of Use Pricing and Energy Use for Demand Management Delivery*, Public Document, 2007

Energy Star, *Energy Star Programme Requirements for Computers Version 5*, Retrieved 2010

ENERNOC, *Demand Response*, http://www.enernoc.com/, Press Release, 2011

Gellings C. W., *The Concept of Demand Side Management for Electric Utilities*, Proceedings of the IEEE, vol. 73, no. 10, pp 1468-1470, 1985

Hanus R, Kinnaert M, Henrotte J L, *Conditioning Technique, A General Anti-Windup and Bumpless Transfer Method*, Automatica Vol. 23, issue 6, pp729-739, 1987

Hong J., *The Development Implementation and Application of Demand Side Management and Control (DSM+c) Algorithm for Integrating Micro-generation Within Built Environment*, PhD Thesis, University of Strathclyde, 2009

Infield, D, Short, J, Home, C, Ferris, L, *Potential for Dynamic Demand Side Management in the UK*, Power Engineering General Meeting, 2007

Jones A, Underwood C, *A Modelling Method for Building Integrated Photovoltaic Power Supply*, Journal of Building Services Engineering, pp167-177, 2002

Maxwell J. C., *On Governors*, Proceedings of the Royal Society of London, pp270-283, 1868

Nutaro J. Protopoescu V. *The Impact of Market Clearing Time and Price Signal Delay on the Stability of Electric Power Markets*. IEEE Transactions on Power Systems, pp1337-1345, 2009

Phelan R., *Automatic Control Systems*, Cornell University Press, ISBN: 0-8014-1033-9, 1977

Sander et al, Apple INC, *Portable Devices Having Multiple Power Interfaces*, US Patent 7,868,582, 2011

Young K K D, Kokotovic P V, Utkin V, *A Singular Perturbation Analysis of High Gain Feedback Systems*, IEEE Transactions on Automatic Control, Vol. 22, pp931-938, 1977

CHAPTER 4 – SUPPORTING AND DEPLOYMENT TECHNOLOGIES

This chapter describes the rationale behind the choice of supporting technologies for the control as described in the previous chapter. The review discusses ICT appliances and networks in office buildings before addressing additional and desired elements in the monitoring and control system. The extended Ethernet suite of protocols is proposed as a unified data and power infrastructure to facilitate deployment of the control and features of this infrastructure are detailed. Additional potential building integrated resources are identified and the potential benefits of RE integration in or near the switch room highlighted. A brief cost benefit analysis of the proposed system is given against the present mechanism of separate controls for supply and demand.

4.1. INTRODUCTION

Structure of monitoring and control systems is based on 2-way communication between components; sensory feedback from the controlled plant is passed via some physical medium to hardware hosting the controller which then calculates and issues a command via some physical medium to an actuator which modulates energy supply to the plant being controlled. There are therefore a number of physical and infrastructural design elements to consider in controlling a system; communications protocols and physical data mediums, bulk power supply to the controlled plant, sensors, actuators and other hardware in the form of signal interfaces and data processing units. Further, many of these hardware items require power to operate and so design of a supervisory and control system involves design of a small dedicated data and power network in its own right.

The deployment and maintenance costs associated with monitoring and control are critical and the sensible strategy adopted here is to utilise resources already available wherever possible in reducing these costs and enhancing the value of ownership of building integrated assets.

The controller design described in Chapter 3 is novel in that it allows closed loop control over the entire integrated low carbon electricity supply chain within the building. A guiding rule of thumb in systems design using feedback control is that if the design works well in an ideal simulation environment, then it is likely that it will also work in a real world environment hence application for patent protection of the control process and design [Counsell, Stewart 2011]. As a consequence of this move and the perceived potential of the control in its chosen application, this chapter is therefore geared towards development of the technical characteristics and deployment topology of the fully integrated system within the chosen application of commercial office and other information and communications technology (ICT) dense buildings.

4.2. ICT DEVICES IN OFFICE BUILDINGS

The Law of Miniaturisation, better known as Moore's Law, is often used to describe the long term trend in the pace of evolution of digital hardware in general [Moore 1965]. This trend, fairly consistent for the last 50 years, is expected to continue at least until 2020 when processor ratings are predicted to be well into the tera-Hz range (although not using silicon technology). By extension, the access and processing speeds of auxiliary computing components; hard drives, data storage technologies such as RAM and Flash, sound and graphics engines are also continuing to evolve at pace. With miniaturisation comes lower cost, greater functionality and lower power consumption per task [Feynman].

There are two general categories of desktop computing device found in modern offices; fixed and mobile. Although preference for mobile devices is increasing and predicted to sustain this increase, fixed thin client architectures are also presently popular.

A thin client is a light desktop PC which shares its processing tasks (virtualisation) with a central mainframe machine elsewhere in the building (cloud computing). By shunting processor intensive tasks off-machine, the power draw of the device on the desk can be very low and typically around the 15W mark e.g. HPt3630w. A zero client takes this

logic to its conclusion by only providing the bare minimum computing power necessary to run a mouse, keyboard, display and interface with the network; all processing tasks are shunted to the mainframe. These devices draw as little as 5W in operation e.g. Arcus Z. Given the lack of on-board functionality, these devices are popular due to their relatively lower price.

It is noted however, that power consumption of the mainframe and data switches must increase and the argument for a thin client based network configuration is that this is done more efficiently at the mainframe than individually at the desk [IBM 2011]. It is also likely that any cost benefits are also linked to the relative product refresh rates of switch room equipment versus that of desktop ICT appliances.

Although these devices and networks are not the primary target of this work as they do not normally feature any embedded energy storage, the intention is to highlight some additional opportunities in other common ICT topologies which may also be relevant to the proposed SISO control. Thin clients and virtual desktops fall into this category.

Mobile class devices include laptops, notebooks and tablets. In addition to higher computing power and processing autonomy than thin clients, mobile devices obviously feature a built-in screen, wired and wireless connectivity options and its defining feature; a battery.

The typical scale of a modern business class mobile PC battery is presently around 50Wh, of Li-ion chemistry and sized such to give a few hours mobility, hence typical PC operational consumption of between 10-25W depending on tasks. Power consumption of a typical modern medium specification business class notebook including the 40W rated AC/DC external adapter is shown in Figure 4-1 below from data measured during this study.

The 1min sampling rate trace measured at the AC socket shows power while in use and charging from around 70% state of charge (SOC) to full. The normal variability in power consumption between intensive tasks and idling is shown at around 10W for this device. The second superimposed trace shows the power consumption of the battery only peaking at 23W at the point where the charging cycle switches from constant

current bulk charging to constant voltage, usually between 80-90% SOC, before decaying in an obvious 1st order manner.

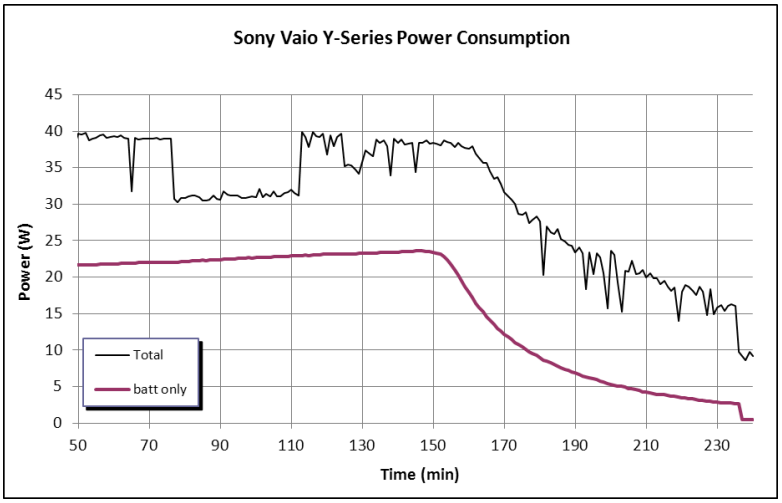

Figure 4-1 Notebook Class Device Power Consumption (2009)

A laptop class device of slightly higher specification and larger battery is shown in Figure 4-2for comparison, showing a peak consumption of 60W with almost 20W PC power variability. The adapter rating in this case was 62W.

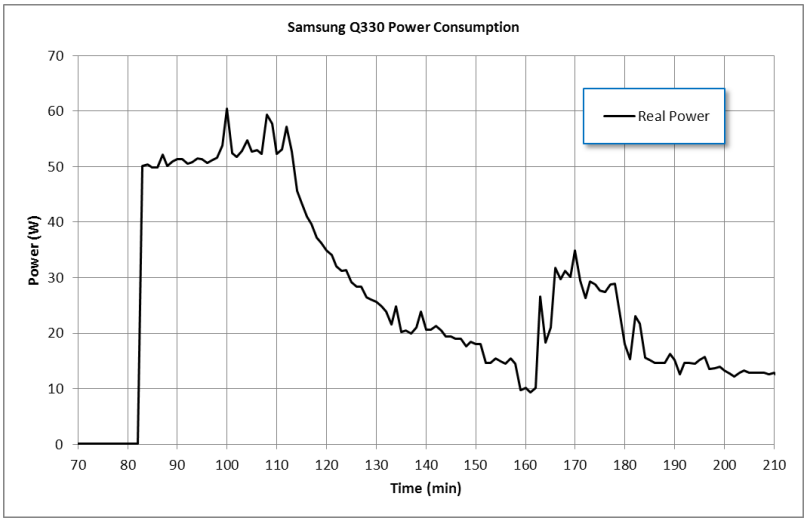

Figure 4-2 Laptop Class Device Power Consumption (2010)

In both cases, further tests concluded that the 13” built-in LED back-lit LCD screens of both machines consumed around 4W maximum.

Tablet devices are a combination of battery and low specification or thin hardware suited to portable document viewing and a simpler range of tasks. These devices are seeing increasing market share and popularity due to being convenient to use in many applications including offices. By comparison, a tablet battery is smaller but still gives more mobility than laptops due to very limited processing power. Although the primary mode of operation is intended to be untethered and using wireless communications, these devices still need to recharge and so still may offer an opportunity for demand control.

Mobile device batteries are managed components and the PC will actively monitor the battery, translating signal data into state of charge (SOC). A typical control regime will include current, voltage, thermal and timed cut-off limits to protect the device and users.

Although these set-points are coded in root software at the BIOS level and could theoretically be manipulated, this strategy is to be avoided since this action would immediately invalidate any warranty. Other than manipulating stored charge via external means, the mobile devices are not to be modified in any way which would compromise safety or liability. These devices illustrate modern low power desktop ICT appliances available and summarises the expected power consumption of these used as the network loads.

The other main power user on the office desk is a second screen. The recommended size of a viewing monitor is 19” [Energy Star] but a larger area allows users to compare documents more effectively. Energy Star stated a power consumption of an average monitor at around 40W for a 19” screen only a few short years ago. By comparison, the power consumption of a modern LED back-lit 23” screen is shown in Figure 4-3 at less than 25W.

Although not strictly an ICT device, the viewing screen is mentioned since operation depends entirely on the computing element and so if the PC goes into sleep or off mode, best practice would manage the screen in the same way as recommended by Energy Star using Wake-on-LAN (WOL) functionality almost universally included in new computing hardware.

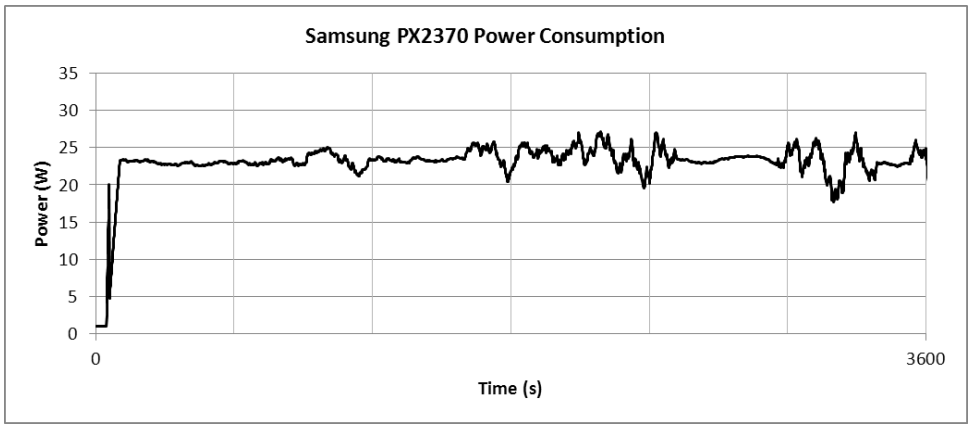

Figure 4-3 Example of 23" PC Monitor Power Consumption (2010)

Power requirement for an active office desk with large 23" screen and a notebook class mobile device can be 65W peak and less than 50W nominal. For an assumed nominal 9-hour working day, this equates to 400-600Wh energy requirement per desk per day. By comparison, a single charge of the embedded battery capacity therefore represents between 12.5-25% of the nominal daily consumption of the mobile device and between 8-12.5% of daily desk energy requirement.

Additional small power ICT appliances in offices include wireless access points, desktop printers and multi-function devices and security cameras. These and a huge number of other devices are typically supplied power via an external AC/DC adapter which plugs into a standard AC wall outlet.

Recent voluntary labelling initiatives such as Energy Star have identified the AC adapter as a target for evolution since the technologies used in manufacture were, until very recently, highly inefficient. The use of linear circuits in power supply is declining

and being replaced by much more efficient switched mode designs. However, the fundamental requirement for a transformer is now limiting efficiency of these devices to around 85-90% peak. Transformerless designs are available for higher power devices (and some grid-tie inverters) but require sophisticated very high frequency switching circuitry and are unlikely to be available at a cost or scale suited to sub-100W devices anytime soon despite a potentially valuable increase in peak efficiency to around 94%.

The above summary gives typical power consumption for a range of low power ICT appliances in an office supporting use of the computer on the desk. Strictly speaking however, Ethernet switches located in switch rooms also consume energy as a result of the PC on the desk. Although this is not a huge amount in absolute terms, at very low load, ancillary switch consumption can be 5-20% on top of end device consumption according to MicroSemi [MicroSemi 2011].

This level of power consumption in data processing at the switch level is already being addressed by IEEE in ratification in 2010 of a 5th amendment to the 802.3-2008 Ethernet Standard, termed Energy Efficient Ethernet [IEEE 2010]. Also known as 802.3az, Energy Efficient Ethernet provides guidance and a management structure to allow powering down or bandwidth throttling of unused ports, increasing switch energy efficiency and reducing consumption by a massive 80% [CISCO 2010]. Despite its relatively recent introduction, major switch manufacturers are already adopting this standard in their products e.g. CISCO Catalyst 45XX Series.

4.3. ICT DATA NETWORKS IN OFFICE BUILDINGS

Data switches are an essential asset in ICT networks. Products from major vendors can easily cost several thousands of pounds for a high bandwidth 48-port machine, equating to investment of over £100 per port including the required power supply to the device e.g. CISCO 3750 Series.

For ICT enabled appliances, data communications networks in offices are as essential as power networks in offices. The typical layout for a modern high bandwidth wired data

network is radial from Ethernet switches in a switch room, along twisted pair CAT cabling through floor and ceiling voids and conduits into the office space, finally terminating at an Ethernet socket. There may be hundreds or even thousands of these cables in a building, representing total lengths measured in the tens or even hundreds of kilometres.

The cable type used in ICT networks consists mainly of shielded (STP) or unshielded (UTP) twisted pairs of conductors. UTP is most common and sufficient for most tasks and consists of 4-pairs of solid or stranded 24AWG conductors. Different twisted pair cables are defined by their category or CAT number. Historically, CAT3 cable was used for older 10BASE-T (10Mbit/s) data networks using a low bandwidth of 16MHz and is still common and sufficient for a great many applications such as telephony and Voice over IP (VoIP). However, CAT5e cabling is required for 100BASE-T (100Mbit/s) and 1000BASE-T (1Gbit/s) Gigabit networks providing up to 100MHz bandwidth and would be the minimum recommendation in a new network installation. CAT6 and 6a cabling standards represent a further improvement in bandwidth and thermal management as does CAT7 and 7a. Although much more common than a few years ago, these last two are not yet formally recognised by the TIA/EIA but are defined in ISO/IEC 11801 as Class F and FA cables respectively. Cabling solutions for application in ICT networks is therefore an on-going development area, driven by the need for better cable performance and higher bandwidth requirements of the ICT devices.

Given the prominence of these networks and the sensitivity of data signals to cable damage or noise, best practice installation follows guidelines and standards for communications networks in commercial buildings for telecom products and services as defined by the Electronics Industries Alliance (EIA), Telecommunications Industry Association (TIA), ISO/IEC and CENELEC. The bulk of these standards define cabling types, distances, connectors, cable system architectures, cable termination standards and performance characteristics, cable installation requirements and methods of testing installed cable. The main standard, TIA/EIA-568-B.1 defines general requirements, while -568-B.2 focuses on components of balanced twisted-pair cable systems. All these documents accompany related standards that define installation quality in commercial pathways and spaces (569-A), administration standards (606), grounding and bonding

(607) and outside plant cabling (758). All key aspects of cabling a building are therefore covered by standards, giving verifiable quality assurance to owners.

4.4. POWER DISTRIBUTION IN OFFICE BUILDINGS

The dominant power distribution network to appliances in a building is single phase mains AC at 230VAC rms in the UK. From metered supply at the consumer unit or busbar, electrical power is distributed to office spaces and outlets throughout the building along fixed embedded ring main circuits. These high power AC cables are routed above, below, around and through office spaces to give convenient access for plug-in electrical appliances at the desk and elsewhere.

Driven by saturation of small power equipment, the high density of these outlets in offices represents a significant portion of capital build costs in cabling and ducting, electrician and commissioning fees. However, in light of the previous evidence that a fast growing number of ICT loads require 60W or much less from a 3kW capacity, AC distribution in offices is an increasingly over specified and expensive solution in terms of power availability versus requirement per outlet.

Although a great many authors have proposed using alternative AC or DC distribution topologies at a wide range of voltages from 350VDC to 24VDC, the first example is well above what would be recommended inside a building for electrical safety reasons and the second incurs high ohmic losses, again likely outside safety limits for thermal reasons. There is also the significant cost issue of installing a second building-wide distribution infrastructure and so an admirable goal of many control systems is to utilise combined data and power topologies or re-utilise existing resources.

4.5. BUILDING INTEGRATED MONITORING AND CONTROL

There are already a great number of controlled systems in office buildings from simple thermostats to security systems to PID controlled zonal HVAC systems to lighting controls to name a few. Many if not most of these will use their own cabling, hardware and communication protocols.

Wireless communication methods have been employed extensively in monitoring and control. Simple radios in the 433/868MHz UHF band allow 2-way communication through a serial protocol interface and many commercial systems utilise this method such as ADAM and Eltek. However, a main drawback is sensitivity to noise in data transfer, particularly within buildings. As a result, this technology level tends to be used only used in non-critical systems. Zigbee is the name given to one of many short range wireless protocols used in automation and intends to be more cost effective than alternative Wide Personal Area Network (WPAN) protocols such as Bluetooth and Z-wave by its relatively low data rate. The Zigbee specification uses IEEE802.15.4 defined access and physical layers and is free to use but requires a license fee for developers [Zigbee Alliance]. Although being pushed for full standardisation in building integrated automation applications, there are more cost effective and ubiquitous alternatives.

Other wireless systems in use in monitoring and control include GSM and GPS protocols which improves data integrity significantly but these solutions remain relatively expensive and use networks not under the control of the building and so represent a risk to dependent systems. The smart grid although not fully developed yet may propose a mixed signal system where the command signal is issued and delivered to a building over broadband internet and then using Wi-Fi to communicate with appliances from a home hub type wireless access point.

Many communications protocols are defined for twisted pair cabling such as LonWorks, SCADA, BACNet, Modbus and TCP/IP Ethernet. Modbus and its variants has long been a popular industry protocol for industrial appliances, battery packs and many other systems but devices suffer from relatively high prices and vendors often adapt the

protocol to their own design making compatibility a problem. The Lon protocol and interoperability standard is in a similar position to that of Zigbee in that although fit for purpose, it lacks the resources necessary to keep pace with other competing standards such as Ethernet.

The perception that using the same network cabling for control packet information as well as routine data increases security risk is not justified in a modern network given the low cost of encryption algorithms and Kim proposes use of existing Ethernet networks in building management applications [Kim 2004]. Hong also uses LAN Ethernet networks in buildings for data communication in an energy management system [Hong 2009]. However, the design focus for both Kim and Hong is on actuating AC connected devices in a domestic application and so power is necessarily supplied to the appliance via a separate medium from the control signal.

Several demand management systems have also been based on wired solutions such as the X10 lighting protocol which uses 2-way power line communications between devices [Moholkar et al 2005]. However, despite strong investment by stakeholders, power line is not an ideal solution since it can degrade AC power quality and cause false positives for utility protection equipment if deployed in numbers. This can be avoided by investment in decoupling transformers although this increase in cost makes adoption more difficult to justify against competitors.

Counsell et al proposes using the existing twisted pair Ethernet networks within the building as a unified data and power infrastructure through industry standard IEEE 802.3 protocols, providing both the data and power requirements for all monitoring and control elements [Counsell et al 2011]. This is an increasingly viable solution since it combines both data and power onto a single cable and also re-utilises the existing infrastructure to do so.

4.6. POWER OVER ETHERNET DISTRIBUTION

The primary objective of Power over Ethernet (PoE) is to increase value of the Ethernet suite of IEEE ratified protocols and ICT appliance asset ownership through unification of data and power infrastructures in a robust and interoperable manner [IEEE 2009].

Derived from existing proprietary protocols developed by CISCO and 3COM, the original standard, now known as Type 1 PoE, was ratified by IEEE in 2005 and provides the means by which many hundreds of millions of IP telephones, security cameras and wireless access points are already powered – traditional markets where both data and power are required but there is either no need or desire for a relatively expensive or potentially hazardous AC supply or one is not available [VDC 2008].

IEEE802.3at Power over Ethernet Plus (PoE+) or Type 2 PoE is the second revision of this industry driven standard, ratified in 2009 and features significantly increased power availability, improved interoperability and advanced power management controls, making the technology a potential solution to powering many low power ICT and consumer electronics devices over and above its presumed use as a method of powering higher power PTZ security cameras.

Deployment of PoE requires three physical components; a source of DC power, standard installation of CAT data cabling and lastly, a hardware interface to the end-device. The PoE standard is designed such that compliance in all three results in extending the features of LAN networks in buildings to include an Ethernet based ‘plug and play’ data and DC power distribution infrastructure implemented in hardware.

4.6.1. Power Source Equipment

A source of power to a data channel, termed Power Source Equipment (PSE) injects power into a CAT data cable. These devices are available as single port versions but are most cost effective at multiples of ports already used for data, usually 24 and 48.

PoE is designed such that injection of power does not significantly increase noise and so interference with data on the same cable remains within regulated limits.

A PSE can be a stand-alone product (midspan) or incorporated within a network Ethernet switch (Endspan). The midspan configuration shown in Figure 4-4 (b) is a cost effective method of retro-fitting PoE to an existing suitable IT cabling network while retaining the client's existing Ethernet switches. Configuration (a) incorporates this power injection within the Ethernet switch itself and therefore choice between these two options is often a question of cost and whether adoption of PoE coincides with the typical switch hardware refresh cycle of (usually) 3-5 years.

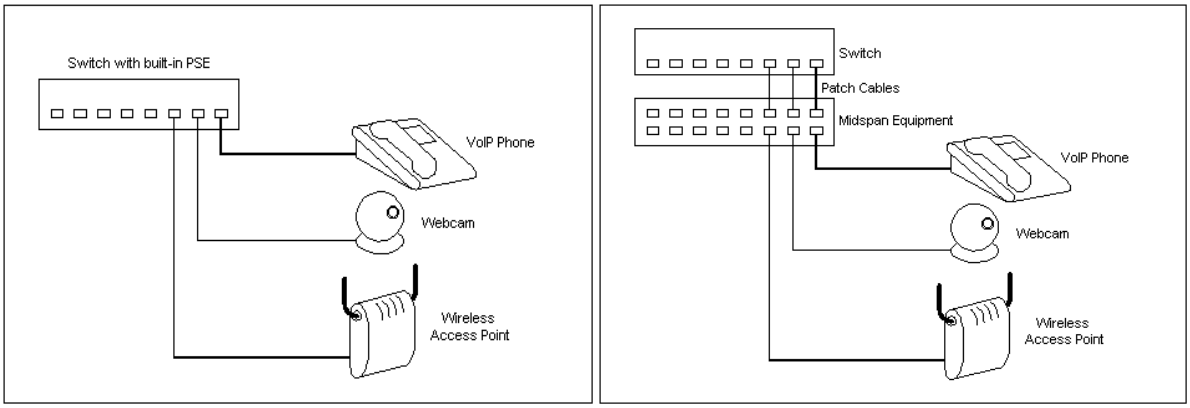

Figure 4-4 (a) Endspan PoE Configuration (b) Midspan PoE Configuration

There are also two types of PSE as defined by power management capabilities; those with an additional software control (managed switches) and those with only hardware control (un-managed switches). Un-managed switches provide basic compliant PoE functionality at low cost where external energy monitoring and control is not required or beneficial.

Managed PSE switches enable active monitoring and a level of control of power supplied via its ports through an IEEE standard Management Information Base (MIB) file for the device, providing the structure for remote monitoring, extended power

management, fault diagnosis and alert services – software functionality over and above that specified in the PoE standard.

4.6.2. Powered Device Interface

The interface between the PoE network and the end appliance being powered is called a powered device interface (PD).

Traditional lower power PoE enabled devices such as IP/VoIP telephony, CCTV and wireless access points are designed such that the powered device interface (analogous to a conventional AC/DC power adapter) is integrated within the device itself. In fact, it is increasingly difficult in 2011 to source an IP telephone or security camera which is not PoE enabled. However, embedding a higher power Type 2 PD interface within a device can be difficult for several reasons and is not yet common; PCB footprint and thermal management being main technical challenges. PoE enabled switch manufacturers have therefore led in this area by also producing a range of ICT device compatible external PD interface products, more commonly known as 'splitters'. In addition to facilitating 2-way power management with a PSE, a PoE splitter simply takes a PoE input from the network and separates data and power onto two distinct output cables, allowing a non-native PoE device to utilise a PoE supply. A splitter does not have a network address and does not interfere with data in any way. Present PoE splitters are fixed voltage output devices and so must be selected based on the specific voltage requirements of the end-device. Typical end-device voltages range from 3.3V to 24V for potential PoE Type 1 and 2 devices and there are splitter designs commercially available which cater for these and the many other device voltages between.

Power over Ethernet can therefore be deployed for a wide range of ICT equipment as a data and power interface and for other consumer electronics devices as a simple power supply of suitably low power consumption as well as those devices identified with embedded battery storage. This level of interoperability between all ICT enabled and potentially all low power DC devices is a key strength of power over Ethernet.

4.6.3. PoE Power Control

In a Power over Ethernet network, many standard ICT devices may be attached which are not PoE enabled and therefore should not be supplied with power. As a consequence, power to cables and PD's cannot be applied continuously as occurs in conventional AC power supply networks and must be applied only after the PSE recognises that a compliant device has been attached and requests power. Sudden connection of a PoE enabled PD to a CAT cable and to a PSE results in a defined multi-stage discovery and classification procedure implemented in hardware in between both the PD and PSE as shown in Figure 4-5. Hardware implementation is much preferred over purely digital signalling since the latter might cause crosstalk or noise on the channel.

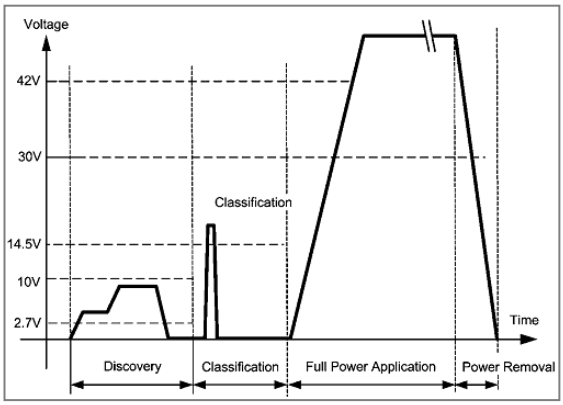

Figure 4-5 PoE Device Discovery and Classification Routine

Device discovery is achieved by the PSE as it probes its ports every few seconds for a valid PD signature of 25kΩ. If this resistance is detected, a second probing of the PD at higher voltage classifies the power limits of the PD in one of six power ranges as shown in Table 4-1. Only once these two steps have been successfully completed does the PSE supply power to the PD at operating voltage. Sudden disconnection of a device is also

certain and the PoE standard gives the PSE 300 milliseconds to shut off supply to that channel.

Class Signature	PD Classification	Power Available to End Devices	Supply Configuration
0	Default, Type 1	0.44W to 12.95W	2-pair
1	Type 1	0.44W to 3.84W	2-pair
2	Type 1	3.84W to 6.49W	2-pair
3	Type 1	6.49W to 12.95W	2-pair
4	Default, Type 2	12.95W to 25.5W	2-pair
4	Extended, Type 2	0.44W to 60W*	4-pair

Table 4-1 Power Over Ethernet Classified Power Levels

Note that the power levels stated in the table represents the maximum power delivered to the end-device *after* losses incurred through a PD interface. These losses are modelled by the assumed constant 85% conversion efficiency of a typical switched-mode buck (step down) converter. As an example, the actual maximum power deliverable through a CAT cable for a Class 4, Type 2 PD signature is 30W per channel with an assumed 25.5W maximum at the PD output. A device which tries to draw more than this power level is seen by the PSE as a fault and so power is removed.

An extended device classification is also available from a growing number of vendors through a deliberate loophole in the ratified Type 2 standard which allows up to 60W to be delivered to a device through a single CAT5e cable. This is possible because the standard specification only states a maximum of 25.5W to devices over any two pairs of conductors in CAT5e and above cables. There are however 4 conductor pairs in standard Ethernet cables and the extended class takes advantage of this by providing power over all 4-pairs, hence providing double the power but remaining standards compliant. This is not by any means an ideal solution to providing more power but given the rates of reduction in power consumption seen in potential PoE ICT equipment, the 4-pair solution may end up a specialist solution or only be applicable to other markets such as domestic applications.

4.6.4. PoE Cabling

Several common categories of Local Area Network (LAN) cable are recognised and ratified by the standards authorities and incorporated into the PoE standard; presently CAT3, 5e, 6 and 6a through TIA/EIA-586-B, 2001. In order that the PoE amendment to IEEE 802.3 remains compatible with present and future industry standard cables, the PoE standard deliberately specifies a minimum cable performance instead of specifying particular cables hence PoE Type 1 requires CAT3 and above and Type 2 requires CAT5e or above cabling.

Although the PoE amendment can accommodate legacy ring topologies in buildings where devices such as IP phones are connected in series, ICT network topologies have naturally shifted towards a radial configuration where higher bandwidth is available per end-device. This trend is also beneficial to PoE since more power is also available per end-device. A radial configuration also allows individual channel power negotiation through simple voltage or current control.

The original Type1 PoE standard defined a nominal 48VDC cable voltage with upper and lower bounds of 57VDC and 44VDC respectively. The upper limit of 57VDC was originally chosen at the safe-for-humans DC limit as defined by standards [BS7671 and BS EN60335] with the range selected to conform to typical 48V uninterruptible power supply (UPS) battery back-up voltage levels. In effect, the Type 1 standard allowed direct and permanent connection of a PSE to both a battery and charger and therefore allowed network voltage to vary. However, this feature of Type 1 PoE was not widely employed due to the then higher prevalence of older sub-standard CAT3 cabling installations in buildings and a concern for thermal safety.

In order that the deliverable power be increased, the new Type 2 standard raised the nominal voltage to 55VDC with new limits of 57VDC to 52VDC – a much tighter range and implemented to manage otherwise significant cable losses at this higher power level.

The Ethernet standard considers a maximum allowable CAT cable length of 100m between an Ethernet switch port output and a PD including provision for 2 ten meter lengths of more flexible stranded UTP cable at either end. This specification is critical to the operation of PoE for thermal management reasons.

4.6.5. Thermal Considerations

PoE necessarily relies on operating within empirically derived cabling thermal limits in unknown operating conditions. The TIA wiring standard TR42.7 defines an absolute maximum of 720mA per conductor pair up to an ambient temperature of 45ºC for single CAT5e, 6 and 6a cables. Above this temperature, current carrying capability is de-rated to 0A at 60ºC as a function of the square of the cable current as shown in Figure 4-6 from TIA.

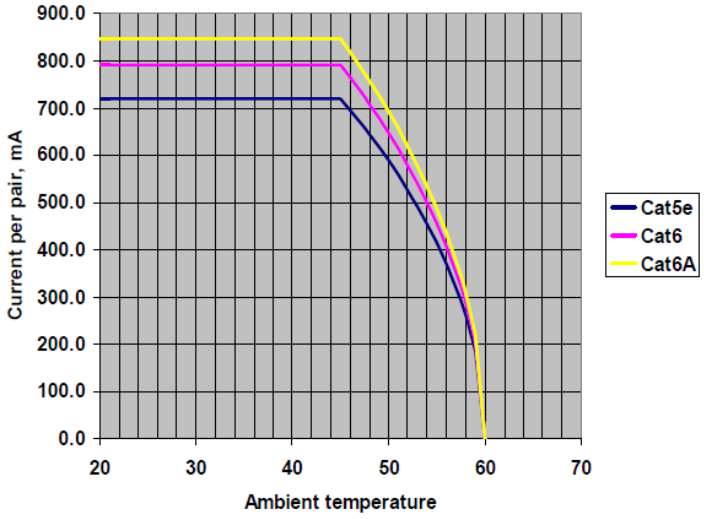

Figure 4-6 Current De-rating for Single UTP Cables Based on TIA

4.6.6. Bundling

A major drawback of the original PoE standard was a lack of specification and guidance on maximum CAT cables in a bundle. This omission was rectified in the Type 2 amendment in 2009 by defining the maximum allowable power transfer in a CAT cable bundle as 5kW. At the upper limit of 36W per cable, this value equates to a theoretical bundle of 138 CAT5e cables in ambient conditions of 45ºC maximum. Allowing for a 30% factor of safety to account for various unknown temperature effects, this figure is reduced to a maximum 96 fully powered Type 2 PoE cables per bundle – two full 48 port switches. This figure is close to a more realistic analysis is specified by TIA 42.7 which gives a maximum of 91 CAT5e cables per bundle at full power and an ambient temperature of 45º. It is unknown whether the TIA analysis considered actual installation characteristics, loom layouts and cable packing density, ventilation and other factors. However, several CAT cabling manufacturers and installers have verified this or similar figures for behaviour of PoE cabling in operation [Darshan 2007].

In this particular respect, the PoE standard has erred very much on the side of caution.

At maximum allowable ambient thermal conditions of 45ºC and delivering maximum power, maximum cable losses are specified as 2.45W and 6W for single instances of 2-pair Type 1 and Type 2 respectively. Cable losses for 4-pair Type 2 should, in theory, be less since the current density against cable cross section is lower however, the maximum loss of 6W per channel should be used until formal de-rating values become available from TIA. The result is that the maximum cable bundle allowable for 4-pair Type 2 extended class is around 48.

In reality, the fact that the PSE can only send 36W along each double pair irrespective of demand makes the system sensitive to cabling and interface efficiencies. For example, a device demand of 25W cannot be met if the device interface is operating at less than 70% efficiency with zero cable losses. This has forced PD manufacturers to produce high efficiency splitter designs right from the start.

4.6.7. Network Level Monitoring and Control

PoE powered channels can be continuously monitored by the switch for faults or other activity using basic IP communications protocols as well as more developed proprietary programs. In addition to safety circuitry implemented in hardware, managed switches and midspans also offer features which allow better power supply management to a device. For example, a class 4 device signature reserves 25.4W of power from the PSE but the device may only actually use 15W, resulting in 10W capacity being reserved but remaining unused and amounting to a significant waste of resource across a fleet of devices on a switch. A software level of control specified in the standard combats this with monitoring at port level at 1Hz sampling frequency and 0.1W resolution, allowing precise scheduling of particular power supplies to the network switches or midspans. Software level control also allows certain ports to be prioritised in the event that there is insufficient power for all ports.

These functions alone put PoE capabilities far above that of any other combined power and data network for the capital cost involved.

4.7. SWITCH ROOM RESOURCES

The switch room is the nodal point of an Ethernet network in a building and contains the main data switches, patch panels, servers and a large number of ancillary systems including chillers, UPS battery systems, redundant power supplies and monitoring equipment. The level of investment in a switch room even at SME scale can be enormous on a per port basis and equipment in the room itself can consume 5-10% of the building's operational electricity or greater if a thin client topology [BERR 2008].

Security of power supply to switch room equipment is therefore of critical importance in offices and substantial capital might be invested in maintaining this continuity on several levels. Backup power supply can be provided through an on-site generator or

battery storage or both while resilience to failure of power conditioning components can be increased by inclusion of redundant PSU's and data switches, known as 1:N redundancy. Such is the requirement for network reliability that several large business ventures offer monitoring and control services, managing fleets of individual data switches and other switch room equipment in real time with the contracted aim of providing a level of system availability often over 99%.

4.7.1. Uninterruptible Power Supplies (UPS)

Given the potential for a computer to corrupt data if power is lost unexpectedly, UPS systems serving both AC and DC networks have become key components in ensuring data continuity to ICT equipment and many other devices including dedicated switch room chiller cabinets. In a switch room environment, the purpose of a UPS is to provide an auxiliary source of electrical energy to the data switches and other ICT equipment should the main supply fail and allow an extended period of network 'uptime' to ride-through a fault or allow for managed and safe shutdown of dependant ICT devices if necessary.

A critical technical feature of any alternative back-up system is transfer time. This is the length of time required for the battery to pick up the load on loss of the primary supply and is very dependent on the topology connecting the battery to a circuit. This feature defines the various main UPS topologies in use. These are:

- Standby (off-line)
- Line Interactive
- Double conversion on-line
- Delta conversion on-line

Each of these topologies has its own characteristics and range of applications. In present context, some topologies may also present the opportunity for control.

In a standby UPS topology, mains AC power is supplied to the load unless a voltage drop occurs and triggers switchover to a battery powered inverter. A rectifier/ charge controller converts mains supply to DC and manages the battery to full capacity and also provides protection against excessive charge or discharge. Most of these systems are square wave or modified sine wave output and are the most common for smaller low cost applications such as individual or small groups of ICT devices. Application to other more sensitive equipment often requires addition of filters.

A line interactive UPS also supplies power directly to the load but incorporates the switch internal to the inverter, allowing limited power conditioning within this device. Line interactive provides faster protection than standby but is sensitive to line disturbances.

Larger loads such as cabinets of data switches require an even faster switchover service should the primary supply fail. This is provided by a double conversion or delta conversion on-line UPS system. An on-line UPS provides complete isolation of the load from the mains thus power supply is continuous with no switchover lag. However, these topologies have the highest capital cost, are complex to control and are of lower operating efficiency since all energy supplied has been regulated twice. Despite these drawbacks, double conversion UPS systems are most common in managed IT switch rooms in offices. The newer delta conversion topology aims to reduce these losses by turning the AC/DC device into a bi-directional machine and reducing strain on the main inverter, so supplying additional energy at high quality to the load through a bypass in the circuit. However, this method is seen as overkill for ICT loads since PCs are generally highly tolerant in terms of power quality. A visual illustration of these UPS topologies is given in Figure 4-7and a summary of the main benefits and drawbacks given in Table 4-2.

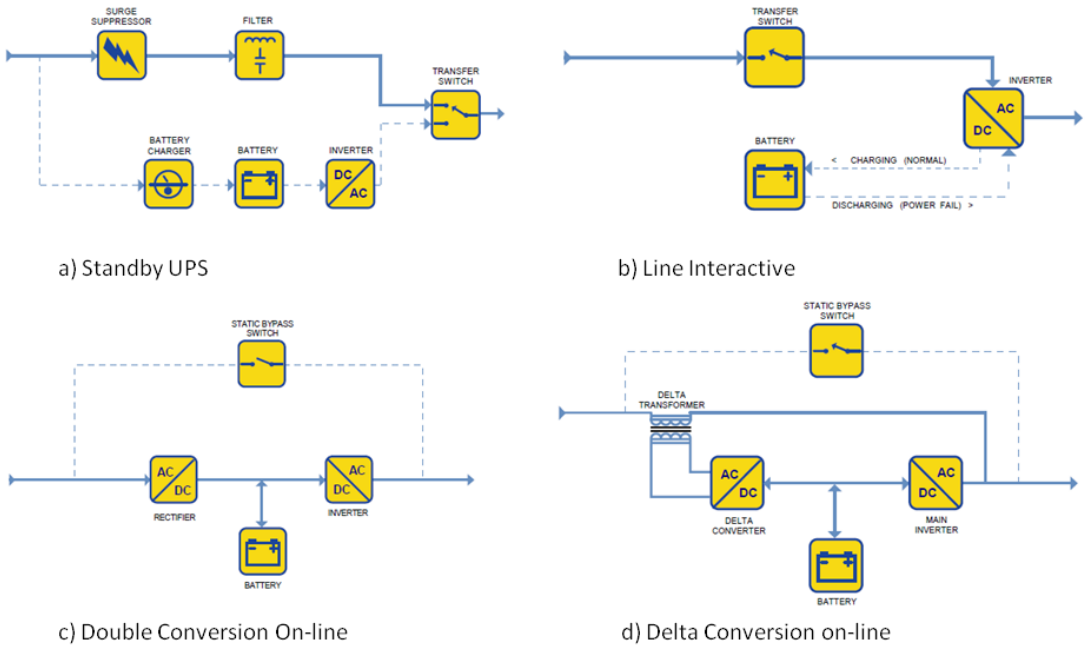

Figure 4-7 Switch Room UPS Topologies

	Practical Power Range (kVA)	Voltage Conditioning	Cost per VA	Efficiency	Inverter always operating
Standby	0 - 0.5	Low	Low	Very High	No
Line Interactive	0.5 - 5	Design Dependent	Medium	Very High	Design Dependent
Standby Ferro	3 - 15	High	High	Low - Medium	No
Double Conversion On-Line	5 - 5000	High	Medium	Low - Medium	Yes
Delta Conversion On-Line	5 - 5000	High	Medium	High	Yes

Table 4-2 UPS Topology Features

Note that in all UPS cases, the norm is to always ensure that battery back-up is maintained at full capacity and in the hope that the device will never be needed or used.

With the integrity of the data network at risk, typical SME scale switch room UPS systems are given regular maintenance and cycling and are usually capable of being polled over the network for status and also capable of sending an alert signal on fault.

UPS systems could potentially be used in conjunction with, or in lieu of, mobile computing batteries if control of the UPS battery management regime was given to the

designed controller. This is possible since the demand supply matching controller only sees the total controllable battery capacity and not any particular device.

4.7.2. Redundancy

Many critical power systems provide a level of redundancy. For example, the typical electrical sub-station consists of two transformers running at half load or less to increase energy security to loads despite the added capital costs and reduced efficiencies. Although the UPS topologies above show output to an AC circuit, it is also common in switch room power supply to adopt a DC topology since the switches themselves are native DC machines, allowing for more efficient 1:N integration of UPS and redundant power supply (RPS) systems and many Ethernet switch vendors manufacture products which can accept either an AC or DC supply or both. The result is that there are often two power networks in a switch room; conventional AC as the primary power bus and a generator/ UPS/ RPS providing a DC source back-up on an isolated bus.

Multiple power supplies in parallel also allows fine tuning and scheduling of power supply capacity to meet a demand in microcosm of a utility AC network, including the ability to prioritise load shedding of devices during an emergency through pre-programmed control action. An example enterprise solution in active redundancy by CISCO pools power supply from PSU's and manages output from each supply to optimise overall supply efficiency against a measured demand. This is illustrated in Figure 4-8 which describes the concept as discussed.

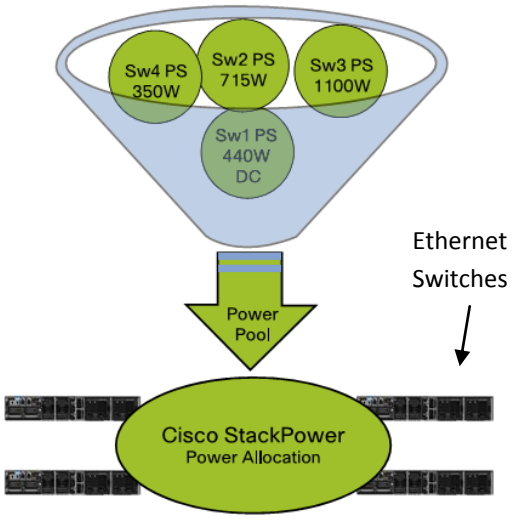

Figure 4-8 Active Redundant Power Supply Schematic

Note that the PSU's are mismatched in capacity and are of mixed domains (AC and DC). This allows different combinations of individual units to meet a load at higher conversion efficiency than would otherwise be the case and CISCO claims 90% efficiency down to 30% load [CISCO]. With relevance to the present control deployment scenario, it is not inconceivable that one of these multiple PSU's could provide a link to a building integrated renewable supply.

4.8. RE INTEGRATION

Although the proposed control is not domain specific, the assumption at present is that of a standard grid-connected system. Technically, all points on the grid at a local level are the same so; does it matter if there is a large distance between the supply point and demand point in the network within a single building? Actually, it might. Although a change in grid frequency can propagate throughout the network in milliseconds, the same is not true of voltage and step changes in load or RE supply can cause momentary local brownouts and voltage sag throughout the immediate network or potentially cause voltage spikes, increasing the stress on sub-stations and attached loads in a building.

The proposal is therefore that the point of connection of the renewable be located within or near the switch room since there is already a high density of high power cabling in that area.

The topology of the full building integrated Ethernet Network with Renewable Power Generation as described above is shown in block diagram form in Figure 4-9 below. The dashed lines on the figure represent data lines and black lines represent electrical power paths.

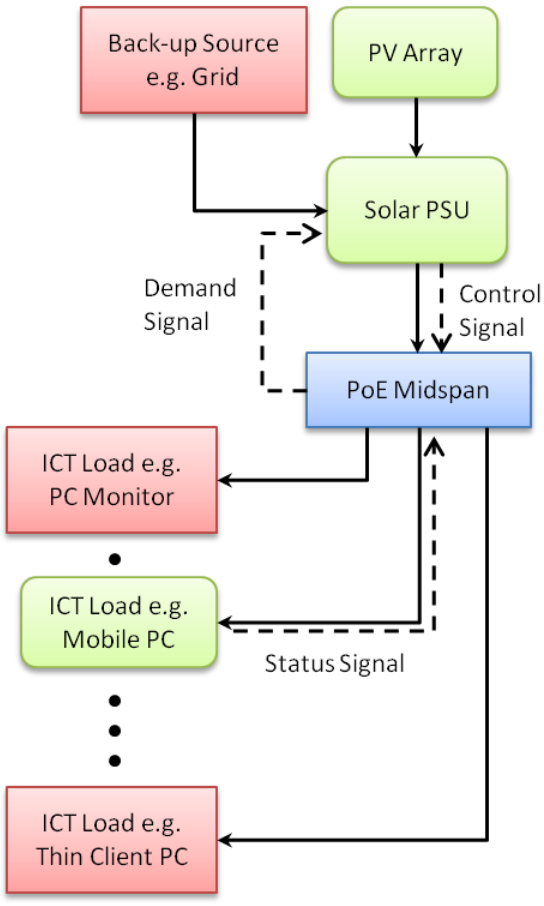

4-9 Schematic of Building Integrated Ethernet Network with Renewable Power Generation

The solar PSU component shown in the schematic simply represents a box containing sensory apparatus and any ancillary power conditioning devices or additional energy storage depending on the specific domain and topology.

4.9. BRIEF COST BENEFIT ANALYSIS

The intention of this section is to give a brief cost benefit analysis of Power over Ethernet in context of deployment in a commercial building. However, the starting point and reference baseline for the analysis is the incumbent AC power distribution mechanism and a summary description of the costs and features of this method is also necessary to give a comparison. This is not straightforward as is explained below.

4.9.1. Benchmark Costs of AC Electrical Services in Buildings

AC distribution in buildings is a very mature solution which is regulated by worldwide industry standards and supported by every appliance manufacturer. The capital and on-going costs of AC (or DC) distribution in buildings is difficult to ascertain for several reasons; the hardware cost of a socket and wiring is not the complete story since each socket should also bear a percentage of circuit protection and other switchgear capital and maintenance costs in addition to cabling installation and commissioning costs. A second reason why total cost of distribution is difficult is that installers and electricians are naturally reluctant to advertise their prices to competitors. Other less tangible costs of high capacity AC sockets in buildings are liability and insurance costs.

Data from a 10 year old BSRIA report was used to give the total cost of each AC socket in an urban commercial building in UK as around £75 including capital and installation costs but not including maintenance costs [BSRIA]. Adjusting for 10 years inflation at 5% gives a nominal figure of around £150 in hardware costs per AC distribution outlet at 2012 prices. The key assumption made for the present interpretation of this data is that the real market value of AC services in buildings hasn’t changed in the intervening

decade and is unlikely to change in the coming decade. Whether this is actually true or not is unknown.

At this point, an assumption must be made regarding also unknown on-going management and maintenance costs of AC in buildings. This is very difficult to define for only low power devices let alone quantify as a hard figure so the assumption made throughout this analysis is that total maintenance, management and associated costs relating to power distribution in commercial buildings on a per AC socket basis are equal to the amortised annual cost of the hardware necessary to deliver power to ICT and other low power digital appliances. The longevity of AC network cabling is also questionable but for the sake of analysis is assumed to be around 10 years in a commercial building. A further assumption is that device PAT testing adds £10 per year to the cost of actually using the socket.

In total, these assumptions put the annual costs of each AC socket at around £175 per year.

Note that the cost per AC socket is for delivery of electrical power only – no other function is included such as data transfer, monitoring or control.

Best practice AC is therefore the benchmark in dumb distribution networks in buildings.

4.9.2. Benchmark Costs of Ethernet in Commercial Buildings

As mentioned previously, provision for data in commercial buildings is expensive. Similar to the above analysis for AC, as well as the physical data cables usually used per device, each port should also include a portion of the costs involved in overall data switching and management.

As an example of switch room resources and costs, the CISCO Catalyst 3750 series 48-port fully managed Ethernet switch is a common enterprise class product in commercial buildings. Retail cost of this device plus its power supply is presently around £100/port from many distributers and retailers.

In a commercial building switch room, there is also usually redundancy in both switches and power supply to switches, conservatively (and without citation) assumed at £25/port.

A UPS back-up system is common in even small organisations, incurring an additional best guess of £25/port.

Installation costs of data cabling is also unknown but if the ratio of hardware cost to installation cost also given by BSRIA for AC (1:5) is similar to that of a data cable, the implied cost of data cabling is on the order of £100/port.

On-going data management in commercial buildings is big business (e.g. Atos Origin, HP, CISCO). Exact cost of data management on a per port basis for SME's and larger buildings is difficult to estimate (prices are not public) but is likely to be at least £100/port per year. Likewise, management, maintenance and insurance costs of power supplies and UPS systems associated with data networks are assumed to be £50/port per year.

If a further assumption is made that the life of an installation is roughly 4 years, the total cost of each functional Ethernet port in a commercial building is in the region of £212.50/port per year – 20% more than the annual cost of providing power.

As an intermediate summary of the costs in a conventional scenario (AC powered with Ethernet data), providing each ICT device with power and data functionality costs around £387.50 per year – not including the capital and other costs of the computing devices themselves.

4.9.3. Benchmark Costs of Power over Ethernet

A power over Ethernet (PoE) network consists of three components; a source of power, an Ethernet cable and a powered device interface (PD). The capital cost of PoE components depends on power level of the end-device since more mature products are lower power capability. However, costs of new high power components are dropping at a present rate of 20% per annum as the market gains momentum.

From recent market research across several vendors (2011) simply using online retailers e.g. Amazon, Dabs, Misco, and neglecting the cost of a CAT5e cable, the costs of PoE are:

- 13W PoE at around £20/port per year
- 25W PoE at around £70/port per year
- 51W PoE at around £130/port per year

The figures above assume a rack-mount power injector switch or midspan with maximum number of ports in the product class and a power compatible device interface.

By analysis of the above admittedly rough figures, 25W PoE is already price competitive with present best practice AC + Ethernet in new build or refit installations. 51W PoE is still new (2009) and so the market is still in early adopter stage. However, prices for such high power PoE hardware are presently dropping at 20% per year as the market gains momentum and so the price point where 51W PoE makes economic sense for certain applications may only be 2 years away.

4.9.4. Benchmark Costs of Advanced Appliance Control

PoE also allows advanced control of appliances; total elimination of standby losses in some cases as well as also allowing the advanced form of energy management proposed in this thesis. By comparison, implementation of this feature using another form of control e.g. AC relay switch with Wifi or Powerline would cost an additional £25 per appliance per year in hardware over a 4 year lifespan using one of several off-the-shelf products designed for this function. For advanced control of ICT appliances and considering the figures above, 51W PoE will be price competitive with equivalent AC solutions in less than a year.

Quantification of the added value in advanced control through integration of a renewable stream of energy is highlighted as future work.

5.1. SUMMARY

The implications of a standard unified data and power infrastructure for Ethernet enabled devices are wide and far reaching given the hundreds of millions of devices produced each year which could benefit from a single cable solution. Further, the decreasing power consumption of consumer electronics devices in general makes PoE an attractive and flexible solution since certification for AC installation voltages is not required.

The PoE system described in this chapter is a DC system. Although there may be little to no efficiency gains at present over AC, DC architectures and conversion devices are still relatively underdeveloped by AC standards and the indication is that significant improvements can still be made. Adoption of an IEEE802.3 amendment as a power bus instantly solves any interoperability issues since the Ethernet protocol stack is freely available for development and at low implementation cost. The result could be that as described, the management of power in ICT networks becomes a function of the network operator and as routine as monitoring data ports for continuity.

It is also clear from the above that the only instrumentation required to implement the carbon governor control on a PoE network is monitoring of the PV supply input to the network; all other signals are already available. The proposed solution is therefore almost totally a software one.

The potential for expansion of this network is also significant as was shown by the discussion of switch room UPS resources, network switch power supply methods and other ICT appliances.

There are 2 key problems in comparing PoE with other architectures. The first is a lack of a reference system, without which extended control features and added value cannot be appreciated fully. The second is a lack of public data regarding costs of AC and costs of installation and services which form the bulk of total figures.

5.2. REFERENCES

BERR, *Energy consumption in the United Kingdom, Update Pub URN 08/456*, Department for Business Enterprise & Regulatory Reform, 2008

BSRIA Application Guide AG 20-2/99, *Cost Benchmarks for the Installation of Building Services*, 1999

CISCO, *Stackpower White Paper*, http://www.cisco.com/en/US/prod/collateral/switches/ps5718/ps6406/white_paper_c11-578931.pdf, retrieved 2011

Counsell J M, Logan R, Stewart M, *A Novel Energy Management Philosophy for Building Integrated Renewable Systems*, 2nd International Conference on Microgeneration and Related Technologies, 2011

Darshan J, Microsemi Corporation, *Current Carrying Capacity Analysis of TR42.7 Update to IEEE802.3at*, Public document, http://www.ieee802.org/3/at/public/jan07/0107_TR42_1.pdf, Retrieved 2009

Energy Star, *Program requirements for Computers Version 5*, Retrieved 2009

Feynman R, *The Pleasure of Finding Things Out; The Best Short Works of Richard P Feynman*. Penguin Books, 2001

Hong J, *The Development, Implementation, and Application of a Demand Side Management and Control Algorithm for Integrated Micro-generation within the Built Environment*, PhD Thesis, University of Strathclyde, 2009

IBM, *Networking for a Dynamic Infrastructure: A Guide for Realizing the Full Potential of Virtualization*, Public White Paper, 2011

IEC/TIA, *Cabling Standards for Telecommunications Networks*, Online resource, www.ieee802.org/3/at/public/2007/01/0107_**TR42**_1.pdf , retrieved 2010

IEEE Std 802.3at-2009

ANSI/IEEE802.3-2009, *Carrier Sense Multiple Access with Collision Detection (CSMA/CD) Access Method and Physical Layer Specifications, Amendment 3: Data Terminal Equipment (DTE) Power Via the Media Dependent Interface (MDI) Enhancements*, ISBN: 9780738160436

IEEE Std 802.3az-2010

ANSI/IEEE802.3-2008, *Carrier Sense Multiple Access with Collision Detection (CSMA/CD) Access Method and Physical Layer Specifications, Amendment 5: Media Access Control Parameters, Physical Layers, and Management Parameters for Energy Efficient Ethernet*

Kim J, *Integrated Information System Supporting Energy Action Planning via the Internet*, *PhD Thesis*, Glasgow: University of Strathclyde, 2004

Moholkar A, Computer Aided Home Energy Management System, MSc Thesis, West Virginia University USA, 2005

Moore G, *Cramming More Components onto Integrated Circuits*, Electronics, Vol. 38, No. 8, 1965

Venture Development Corporation (VDC), *Power Over Ethernet (PoE): Global Market Demand Analysis, Third Edition, Executive Summary*, March 2008

Zero Client Product, ARCUS Z, http://www.arcustechnology.co.uk/pano-zero-client

Zigbee Alliance, *Zigbee White Paper*, http://www.zigbee.org/, retrieved 2009

CHAPTER 5 – CASE STUDIES

This chapter details prototype and case study deployments of the novel system in an operational environment to include the designed control described in previous chapters. The importance of this testing is apparent with the realisation that many aspects of the system are novel and as such required empirical evidence of functionality as opposed to simulation. Further, the relative scales of the components also directly affect the robustness of the controller; hence a live system trial was required.

5.1. INTRODUCTION

Design and development of the novel controller for this novel application necessarily made certain assumptions at the outset regarding the application.

First among these was the early assumption that mobile and other ICT equipment could subsist on the limited power supply offered by power over Ethernet distribution while remaining fully functional. A second important assumption was concerned with the capabilities and behaviour of a PoE network itself in normal operation and under various fault conditions imposed. In both cases, these technologies and capabilities underwent major revisions during this work and presented additional opportunities for control. The system hardware and architecture has therefore also undergone several evolutions as the concept network and control developed into its present form.

Similarly, methods of integrating an intermittent renewable source into this DC power network have evolved from simulation of this input to an actual BIPV array feeding an ICT network.

5.2. FEASIBILITY PROTOTYPE

The purpose of the prototype Building Integrated Ethernet Network with Renewable Power Generation (BIEN-RPG) system was to evaluate the, then, state of the art in low power computing combined with state of the art in power over Ethernet distribution for usability and reliability. The small prototype network would also provide a test bed for appliances and network to connect to the intermittent supply. Appliances and networking equipment were procured, installed and the capabilities of the network investigated. The complete network prototype is shown in Photograph 5-1 with the appliances consisting of a mobile PC, model Samsung NC10, 15" generic cold cathode fluorescent lamp (CCFL) type computer monitor and mobile inkjet printer, model Canon IP100.

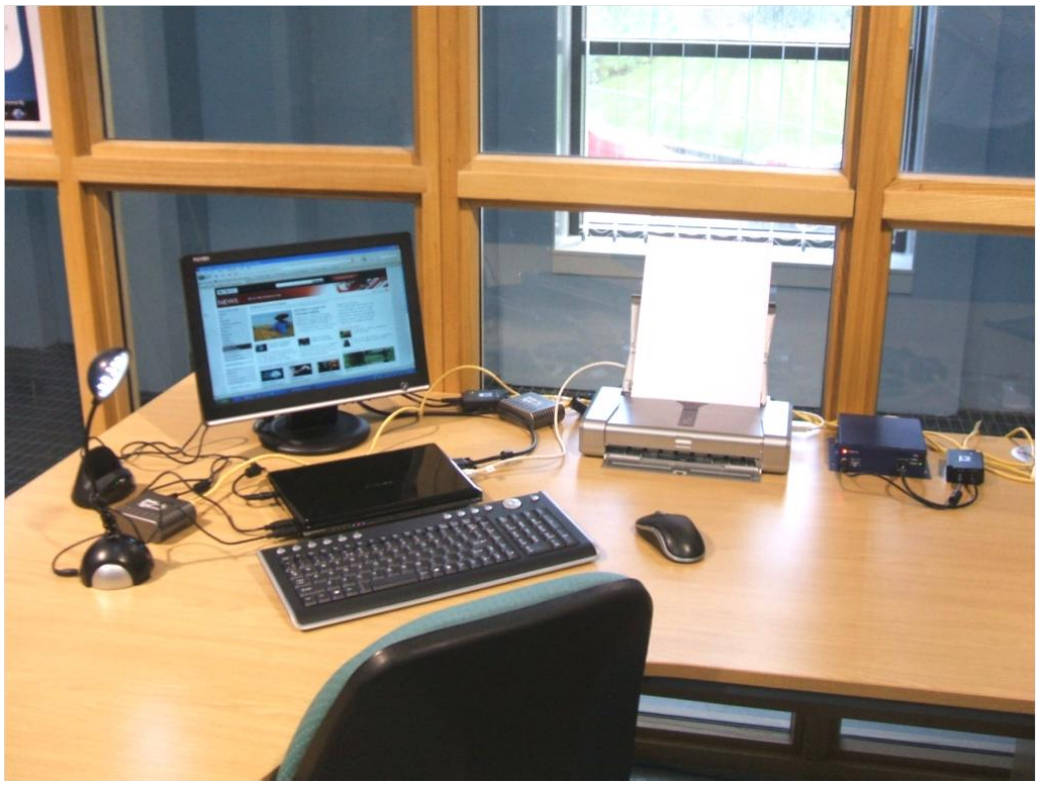

Photograph 5-1 Prototype PoE Powered Office Desk

The PoE network consisted of standard CAT5e cabling with power provided by an off-the-shelf unmanaged PoE Ethernet switch, model Netgear FS116P, providing up to 55W PoE load shared across 8 PoE enabled ports to IEEE802.3af (Type 1) specification [IEEE 2005]. Although unused by this particular application, a fourth port was populated with a PC104 hardware typical of a BEMS system to demonstrate interoperability. Each appliance was necessarily PoE enabled by use of a splitter of appropriate voltage since none of the appliances were natively PoE enabled. Given that the loads and network are indoor devices, connecting a live PV supply to the system created a bit of a logistical problem and so for this prototype, a simulated PV input was used and regulation provided by a managed central battery. Photograph 5-2 shows the battery controller and power supply regulator circuit which was implemented to control power to the system from a constant grid supply and the simulated intermittent supply.

The circuit designed used simple voltage feedback from an inexpensive digital voltage sensor to estimate state of charge and implemented a high gain bang bang type controller through solid state relay actuators to maintain the 24V, 28Ah lead acid (PbA) battery within a hysteresis band set by selection of resistance elements surrounding the amplifier. A time varying simulated PV control was implemented via a USB connection between the control circuit and a PC running a software control interface with signalling either manual or according to a simple fixed cycle.

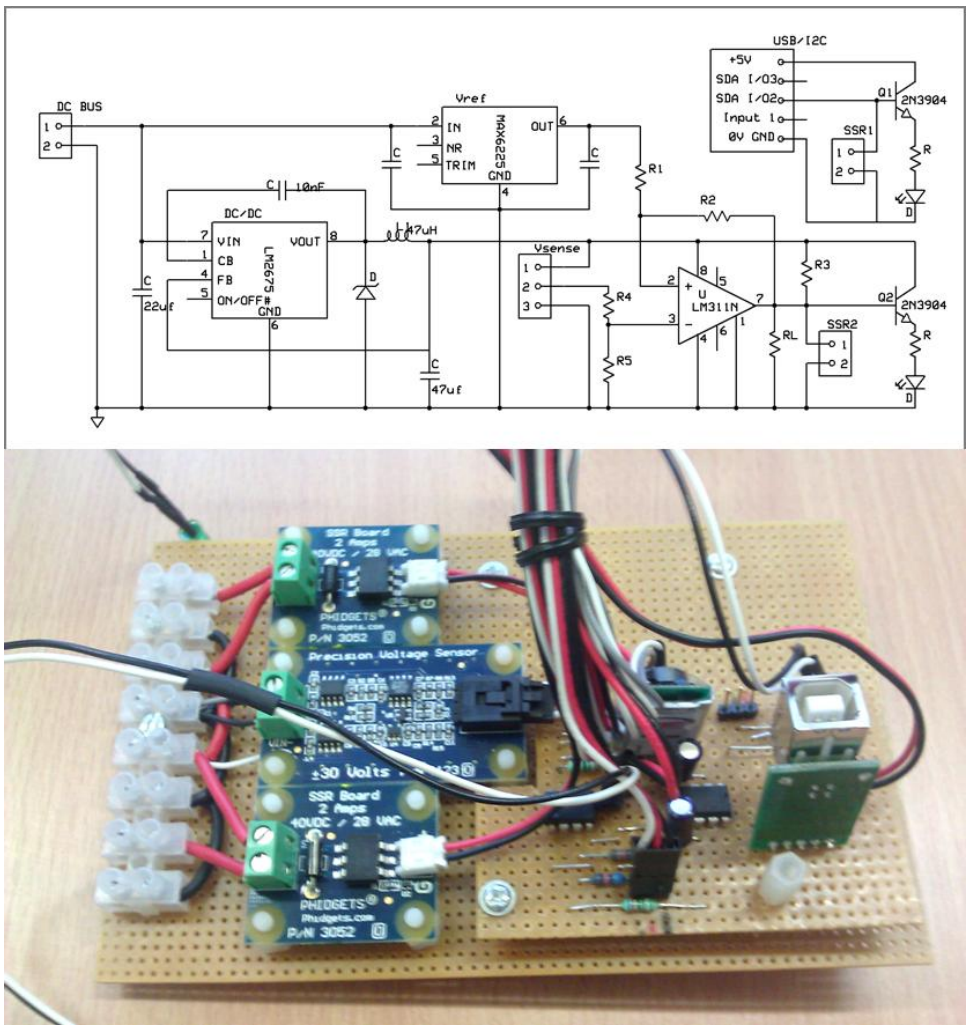

Photograph 5-2 Prototype System Control Circuit and PCB

The battery, AC/DC converters and control circuitry were installed in a computer case as shown in Photograph 5-3 (a) and (b) such that the prototype PoE network demonstrator was both functional and portable.

Photograph 5-3 Prototype Power Supply for PoE Network

5.2.1. Results & Discussion

Basic results from this system included verification of the power levels and efficiencies of the hardware as well as the behaviour of appliances and network elements under various fault conditions. The system also provided a simple Type 1 PoE compatibility test circuit.

Although the appliances worked normally, it was noted that the netbook charging cycle pushed power draw over the 13W PoE limit, causing a fault and cyclic reconnection to the PoE supply. This unacceptable behaviour could only be rectified by either increasing the PoE power supply limit or by interfering with the inbuilt software driver of the battery to limit its current draw. However, this latter option would also invalidate any warranty and was dropped in favour of evolving the network to incorporate the new Type 2 PoE standard.

Implementation of the prototype battery control method was not accurate or robust enough since only voltage was being measured and the simple model and control assumed a fixed hysteresis band which is unrealistic in a real system and battery under dynamic loading.

5.3. CASE STUDY DEPLOYMENT OF A FUNCTIONAL PoE NETWORK

In addition to the novel controller for demand management of ICT devices, there is also significant industry and academic attention on the capabilities and robustness of Power over Ethernet as a unified distribution and data medium in operational workplaces for a number of other applications.

The use of Power over Ethernet to power fleets of non-PoE enabled desktop and a great many other devices, although technically feasible, is largely untried in industry and to the author's knowledge no public documentation of such usage of PoE is yet available. Given that this technology is a key integral component of the proposed system, a trial was arranged with a high profile project partner to test and demonstrate use of a Type 2 Power over Ethernet network retro-fitted to a conventional fleet of thin client based machines over the existing CAT cable infrastructure and in an operational office environment.

Although the full measured results of this trial cannot yet be published for commercial reasons, the conclusion is that Power over Ethernet can easily be deployed in a 'plug and play' manner and is robust in operation since zero issues were reported by network administrators. It can also be taken that users were 100% satisfied since, apparently, they were unaware that any change in power supply configuration had taken place.

This trial was also a valuable exercise in PoE network design, component procurement and implementation as a retro-fit solution, giving confidence to the immediate applicability of PoE technologies with a view to implementing the demand controller and chosen desktop devices.

5.4. CASE STUDY DEPLOYMENT OF A FUNCTIONAL BIEN-RPG SYSTEM

Building on experience and lessons learned from the initial prototype and PoE deployment trial, the fully functional system intended to incorporate this knowledge with advances in power delivery capability with Type 2 PoE and with improvements to power consumption of common desktop devices. With a focus towards a readily deployable solution, the objectives of the design were modified to control energy storage in the devices themselves rather than in a centralised battery, thus the proposed solution could utilise a standard grid-connected BIPV array as a live energy source in conjunction with a fleet of low power but otherwise standard mobile computing devices. The key objectives of this design were:

- Deployment in a live office working environment
- Integration of a live PV source
- Implementation of the low carbon governor control

In terms of demand and network hardware, the aim of the design stage was to source ICT equipment which did not need internal modification and could be used with a standard (Type 2) PoE network [IEEE 2009]. The relative scale of the PV array against these components is critical since the control objective is to minimise import and export and so this aspect was identified for study against nominal network load.

5.4.1. ICT Network Loading

The working office in which this novel network was installed contained 2 operational desks plus a hotdesk station. ICT provision for each main desk consists of a business class laptop and second monitor.

The laptops, monitors and other ICT equipment chosen and used were as follows:

DESK 1

- Samsung Q330 Series Laptop i3 2.4GHz dual core (Win7)
- Samsung PX2370HD 23" LED backlit LCD Monitor
- Generic wireless keyboard & mouse

DESK 2

- Samsung Q330 Series Laptop i3 2.4GHz dual core (XP)
- Samsung PX2370HD 23" LED backlit LCD Monitor
- Generic wireless keyboard & mouse

SERVER STATION

- FIT-PC2 Single Board Computer, Atom Z550 2GHz single core
- BenQ V920 19" LCD Monitor
- Generic wireless keyboard & mouse

OTHER HARDWARE

- Netgear 8-port Ethernet Unmanaged Switch
- Microsemi 4-pair PoE+ Managed Midspan 6 port model PD-9506-ACDC/M

Splitters and Modifications

Note that none of the ICT loads are native PoE enabled and therefore PoE to DC adapters known as splitters were procured at a range of voltage outputs and from a number of vendors, indicating standard interoperability of these components. A selection of these devices used in the trial is given in Photograph 5-4 showing the relative scales of these devices.

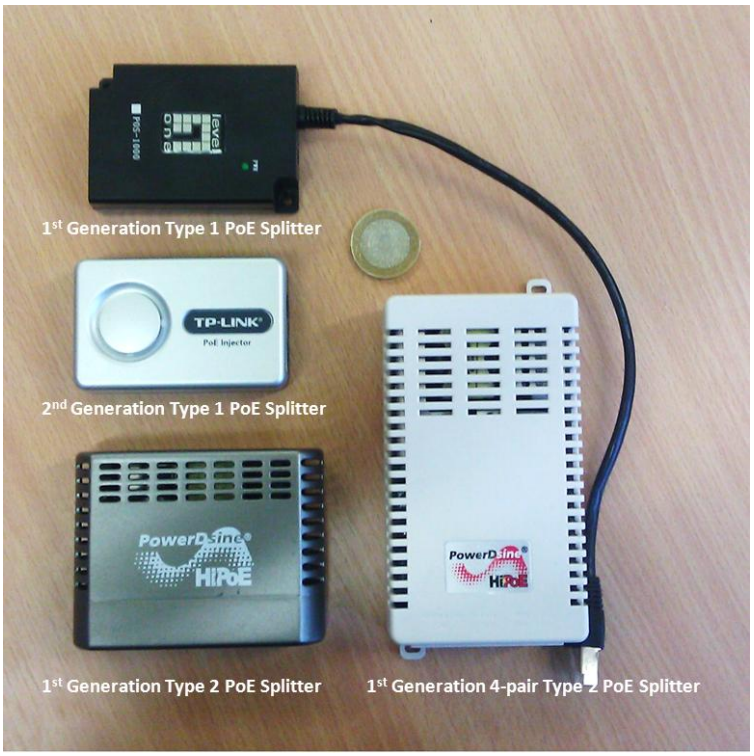

Photograph 5-4 Power over Ethernet Splitters

Although screens, server PC and other components were easily catered for with off the shelf splitter devices as shown above, a particular problem was noted for the laptops. Given that the high power 60W 4-pair splitter required was a new product line, it was only available in 12V and 24V output versions (though compatible with its target market of high power PTZ cameras) whereas the laptop's input voltage was 19.5VDC. Attaching a supply of even a few volts difference from rated device voltage to

appliances is not recommended and would result in shortened component lifespan and perhaps safety issues or a failure to charge the device fully. The solution was to step down this voltage from 24 to 19.5VDC while passing up to 3A using a modern compact high frequency DC/DC buck converter, model PTN78020W from Texas Instruments.

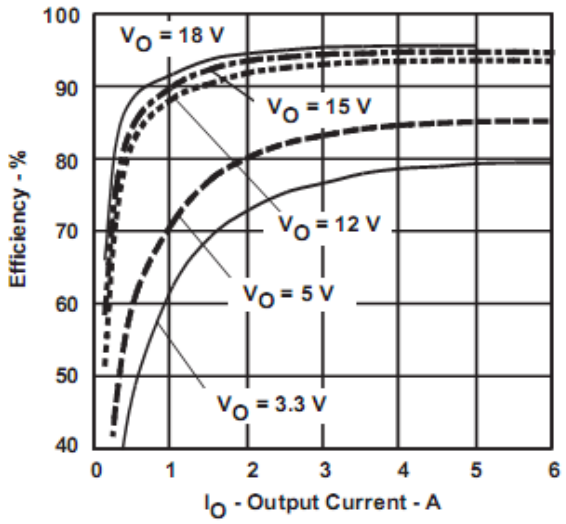

Figure 5-1 Conversion Efficiency Curves for PTN8020W DC/DC Converter [Source: TI]

The rating curves for this highly efficient 90W rated DC/DC converter as shown in Figure 5-1 from its datasheet. At 60W (3A) maximum load, losses from this additional conversion were therefore limited to 3W.

As is shown in Photograph 5-5, the complete device including external components and PCB mounting measured less than 1 cubic inch and was simply attached in series to the splitter output to give the necessary voltage to the end device.

Photograph 5-5 Miniature High Efficiency 90W DC/DC Converter PCB

Nominal values for power consumption of load and network devices are as follows.

Both Samsung laptops state consumption of 60W peak which is right on the 4-pair PoE+ limit. However, the working power consumption for these devices was measured at between 15-25W for light to heavy usage respectively.

The 23” screens were seen to consume 20 - 25W each but can be reduced to less than 15W through adjustment of screen brightness. Each desk therefore consumed energy at a nominal 45W for a PC and total viewing screen area of over 300 square inches.

The server PC and its 19” screen both consumed less than 25W together and so was powered via a single Ethernet cable and PoE port.

The PoE midspan itself is stated to consume 30-40W in operation with no load. This relatively high figure is simply due to the generic manufacture of these devices; a 12, 24 or 48 port version would likely still only consume 40W.

In summary:

Midspan	40W constant
Ethernet switch	2.5W constant
Server/ Screen	20W
23” Monitors	20-25W each
Laptops	15-25W real load, 48Wh Li-ion battery

Although these figures include adapter conversion efficiency losses of 15%, supply of power to PoE devices through the midspan also incurs a conversion penalty, estimated at a further 15%. The total nominal baseload of the network without the laptops was therefore around 110W with each laptop contributing from zero to 20W nominal and 60W peak.

5.4.2. PV Installation

A key objective was to utilise a real PV array in the network as an active part of its power supply. Although photovoltaics are a scalable and translational technology, an attempt was made to correctly size the array against its loading regime and the control method to be utilised. Since the control aims to balance supply and demand such that import/ export energy is zero as a function of time, the laptop power demand on top of baseload network demand determines the scale of array in such a way as to negate any variation in supply or demand. This is at odds to the convention of sizing a grid-connected PV-battery-load system for energy.

During the summer, an optimally aligned PV array at UK latitudes during very clear sky conditions will output a maximum of 70-80% of its rated output [Jones]. Assuming that laptop demand and battery charging and discharging cancels each other out; the total

network demand of 150W would suggest an array of around 200Wp if sized for summer peak.

The electrical characteristics of the chosen BP350J panels are given in Table 5-1. Four of these modules were used.

Electrical Characteristics[2]	BP 350
Maximum power (P_{max})[3]	50W
Voltage at Pmax (V_{mp})	17.5V
Current at Pmax (I_{mp})	2.9A
Warranted minimum P_{max}	45W
Short-circuit current (I_{sc})	3.17A
Open-circuit voltage (V_{oc})	21.8V
Temperature coefficient of I_{sc}	(0.065±0.015)%/ °C
Temperature coefficient of V_{oc}	-(80±10)mV/°C
Temperature coefficient of power	-(0.5±0.05)%/ °C
NOCT (Air 20°C; Sun 0.8kW/m^2; wind 1m/s)	47±2°C
Maximum series fuse rating	20A
Maximum system voltage	600V (U.S. NEC & IEC 61215 rating) 1000V (TÜV Rheinland rating)

Table 5-1 BP350J Electrical Characteristics

A PV array also has a minimum nominal output given by response during cloudy conditions. From Chapter 2, this is around 15% of rated output or around 30W during summer months for this scale of array and under very cloudy conditions.

The 200Wp array and its frame were installed on the roof of the university (Photograph 5-6) in 1s-4p configuration to give 15V array nominal operating voltage with the DC energy fed through a skylight into a corridor next to the office used and from there into the office area chosen for the demonstration. This very low level of voltage was dictated by the small scale of the installation hence very few grid-tie inverter products were available at such low ratings and all featured a 15VDC input from an array. Larger systems would benefit from wider inverter product availability, allowing a higher array voltage and reducing cable losses.

Photograph 5-6 PV Array on Roof of James Weir Building

5.4.3. Power Interface

The power interface and monitoring hardware was located in the office containing the network being powered. The panels were connected to the local grid via a small generic 12V, 250W inverter with MPPT functionality with pure sine wave output. As with all good quality inverters, the device has anti-islanding protection and other safety features built-in. The mismatch in scale between the inverter and the array is a common problem in PV installations with the solution usually being an inverter rated at about 90% of the array output, resulting in clipping during very sunny days in the summer. The inverter used in this small trial was the only product found with the desired features and small enough scale to be compatible.

With demand being monitored and reported to the control by the midspan, only one of the two supplies need be monitored to characterise all three. The choice of actively monitoring the PV supply instead of the grid input is therefore arbitrary and the choice made simply on cost and ease of integration with the system.

Although a number of researchers have tried to characterise a PV supply through monitoring of a single parameter, this would not be possible in this case since the array was connected to an inverter with MPPT, therefore both voltage and current were measured. Both sensors, generic voltage sensor and hall effect current sensor, were selected to feature a 5VDC supply as well as being range compatible with the application. This allowed both to be powered and interfaced with a simple low cost generic USB based data acquisition unit, giving 11bit noise free resolution and providing a ubiquitous, programmable low cost monitoring solution.

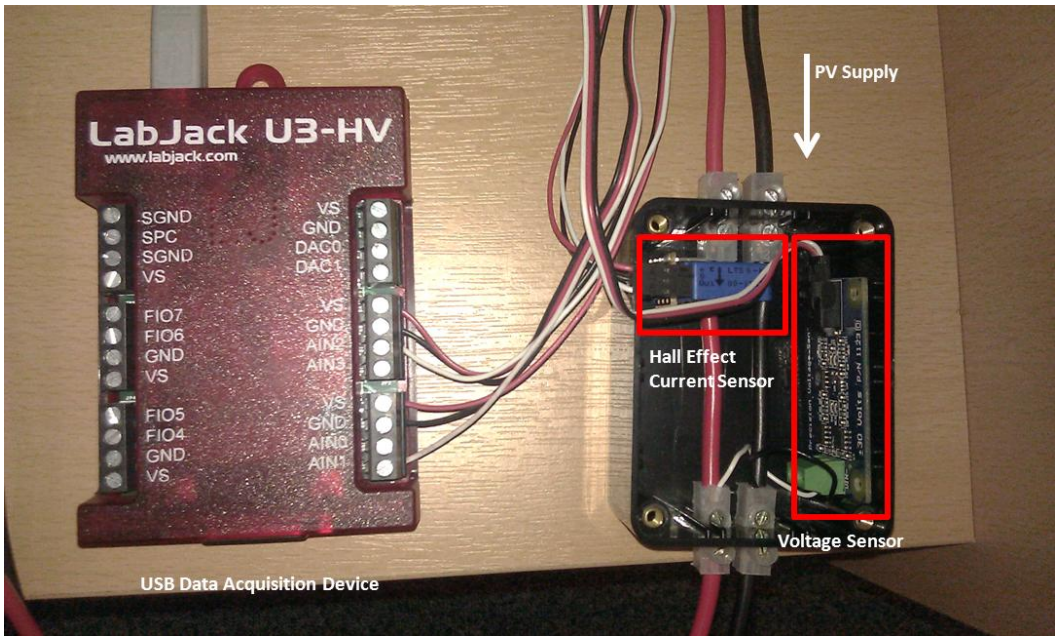

Photograph 5-7 Networked PV Data Acquisition Unit and 5V Sensors

The complete structure of the trial including the PV array, power conditioning interface, PoE distribution midspan, ICT loads and measurement instrumentation is shown in Figure 5-2.

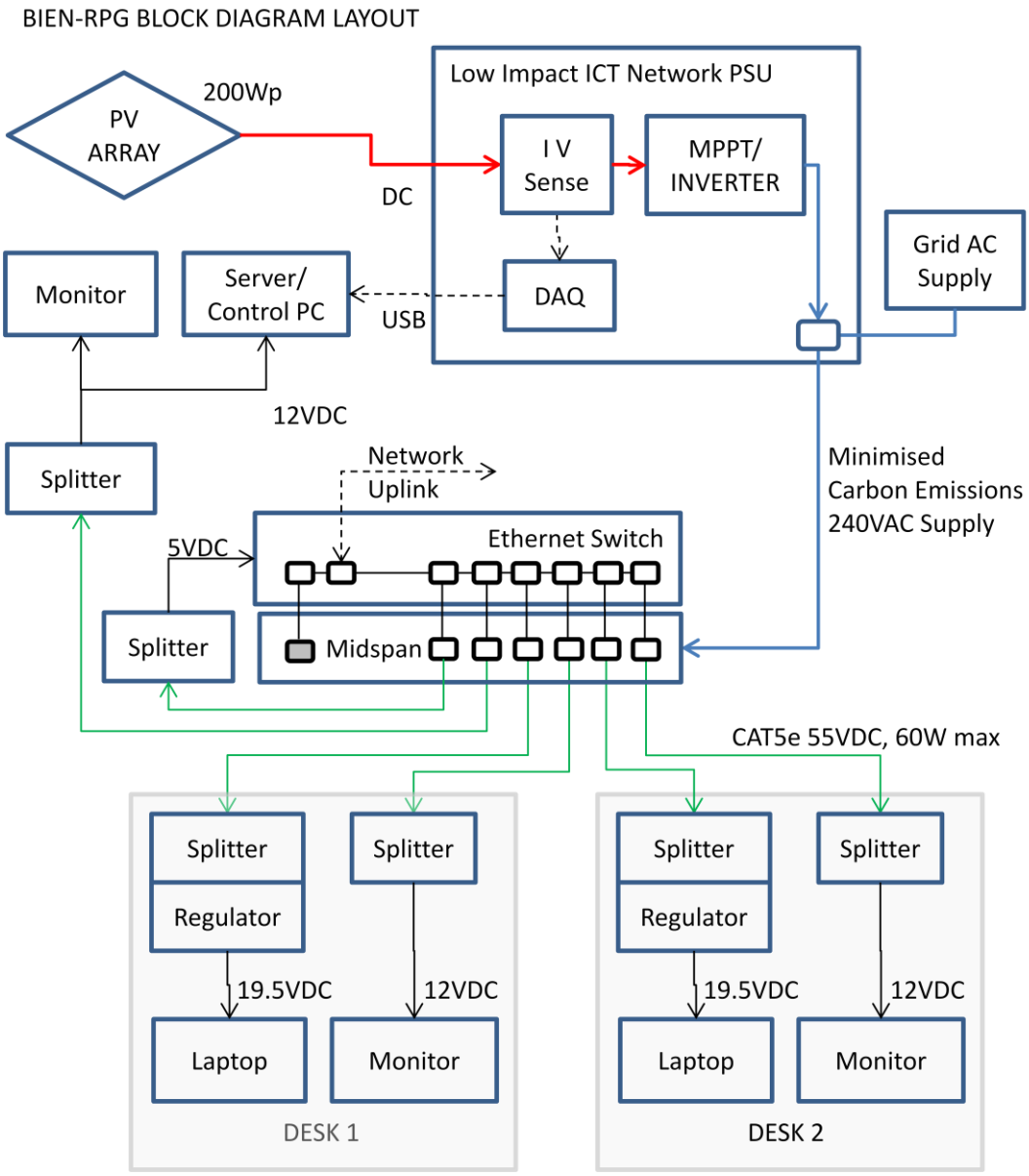

Figure 5-2 BIEN-RPG Trial Block Diagram

5.4.4. Network Installation

The PoE network and power equipment was installed in an occupied office in the James Weir building in the University of Strathclyde with deployment as shown in Photograph 5-8.

The top shelf of the ‘mini server room’ holds the server PC and viewing monitor, accessed via wireless mouse and keyboard and connected to the local IT network. Power to this dedicated PC/ monitor is provided by a single CAT5e cable from the PoE+ midspan.

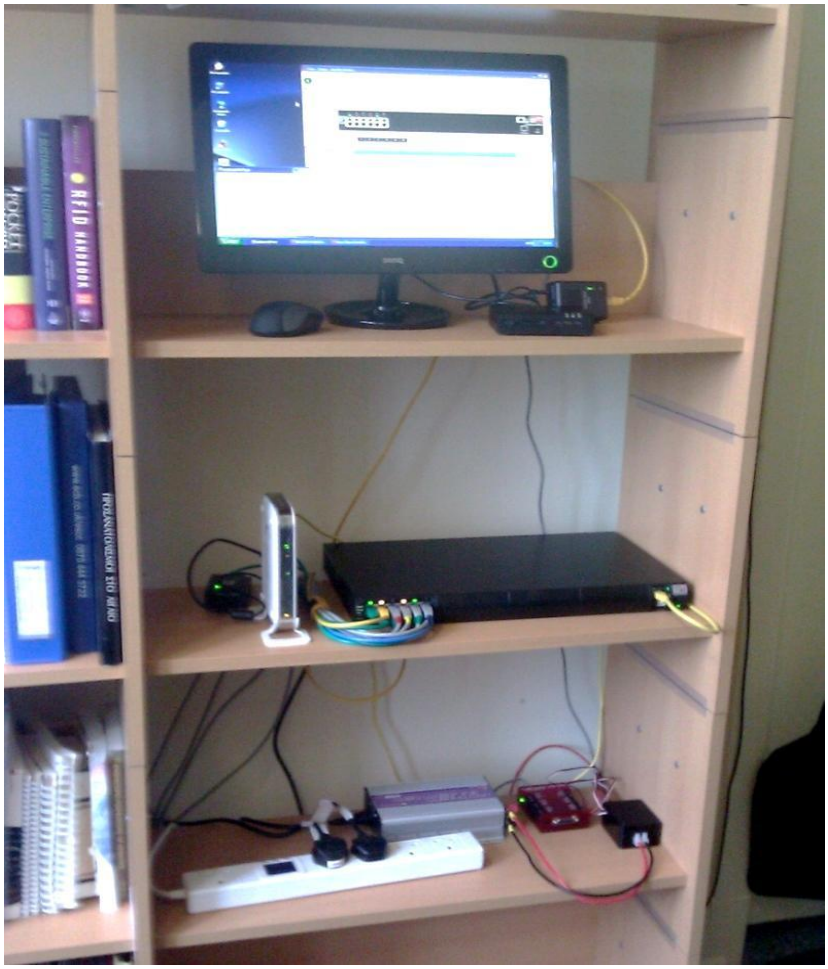

Photograph 5-8 PoE Trial Network Power Components in Situ

This combination of ICT equipment can also be used as a low power single cable desktop PC in its own right as shown in Photograph 5-9 and Photograph 5-10 illustrating the significant advances made in computing technology and miniaturisation as well as PoE capabilities. The middle shelf holds a standard 8-port Ethernet switch and midspan. The lower shelf comprises the power conditioning hardware and PV monitoring system for the network as described.

Photograph 5-9 Sub-25W PoE Powered Computer Workstation

Photograph 5-10 Back of Sub25W PoE Workstation Detailing Single PoE+ Cable Data and Power Supply

The desktop appliances consisting of a laptop class Samsung Q330 mobile device and a Samsung PX2370 23” LED monitor per desk were deployed and used as the main workstations for the office as shown in Photograph 5-11. However, given the higher power requirement of both, it was not possible to power these devices on one cable as with the server workstation and so a CAT5e cable per device was used.

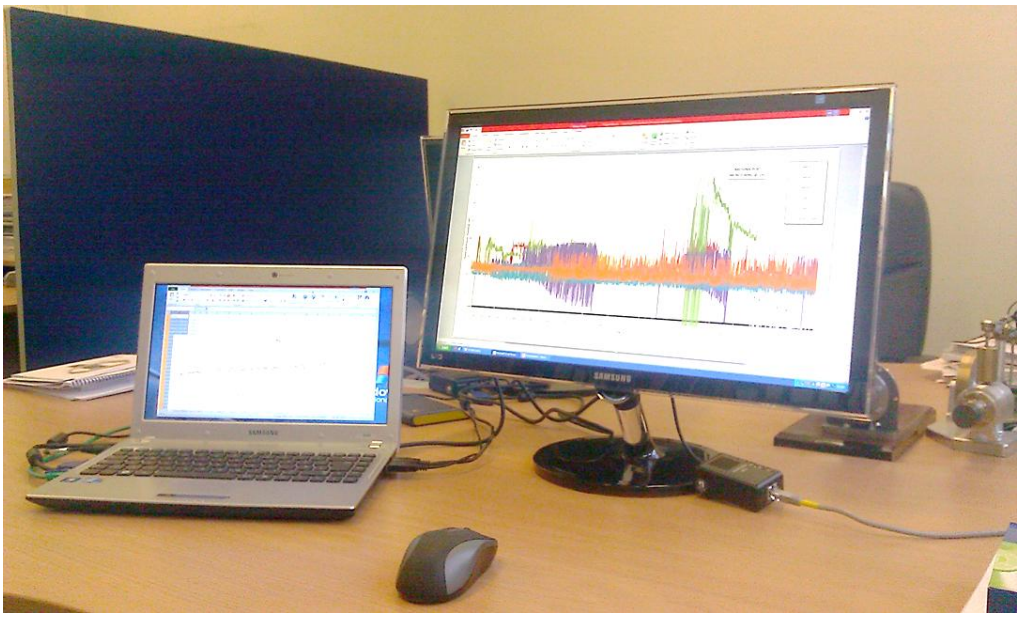

Photograph 5-11 PoE Powered Laptop and Monitor Computer Workstation

5.4.5. Low Carbon Governor Manager Program

The deliberate strategy in implementing the BIEN-RPG controller uses the already available CAT network and common ICT components for communication. The BIEN-RPG controller and network manager were coded in software (MS Visual C++ and .NET framework) and installed on the dedicated network connected server PC to run as a background network service. In order to implement the control, the manager program requires state of charge data from participating laptop PC’s on the PoE network and so client software was also written and installed on these participating machines to gather this data from already installed Windows operating system battery management

programs hence the client was only required to interface with these programs and transmit the data to the network manager. In addition to these two custom written programs, the midspan software (PowerViewPro) was also polled by the manager for power consumption on each of its ports. Power monitoring and control functionality at software level is standard in all managed PoE switches and midspans. The final piece of information required for control is a measure of power generated by the array. This was also polled by the manager via the standard USB connection between the server PC and the generic data acquisition unit situated close to the inverter and connection to the local AC network.

The software manager was set to poll all of the relevant network devices every second, perform calculations as necessary to determine action based on the coded control strategy set out in Chapter 3 and issue commands to the midspan, altering the power supplied through each port and hence also to the laptops. Continuous data connection to each device was established and maintained throughout. The BIEN-RPG Program Manager Interface is shown in Photograph 5-12.

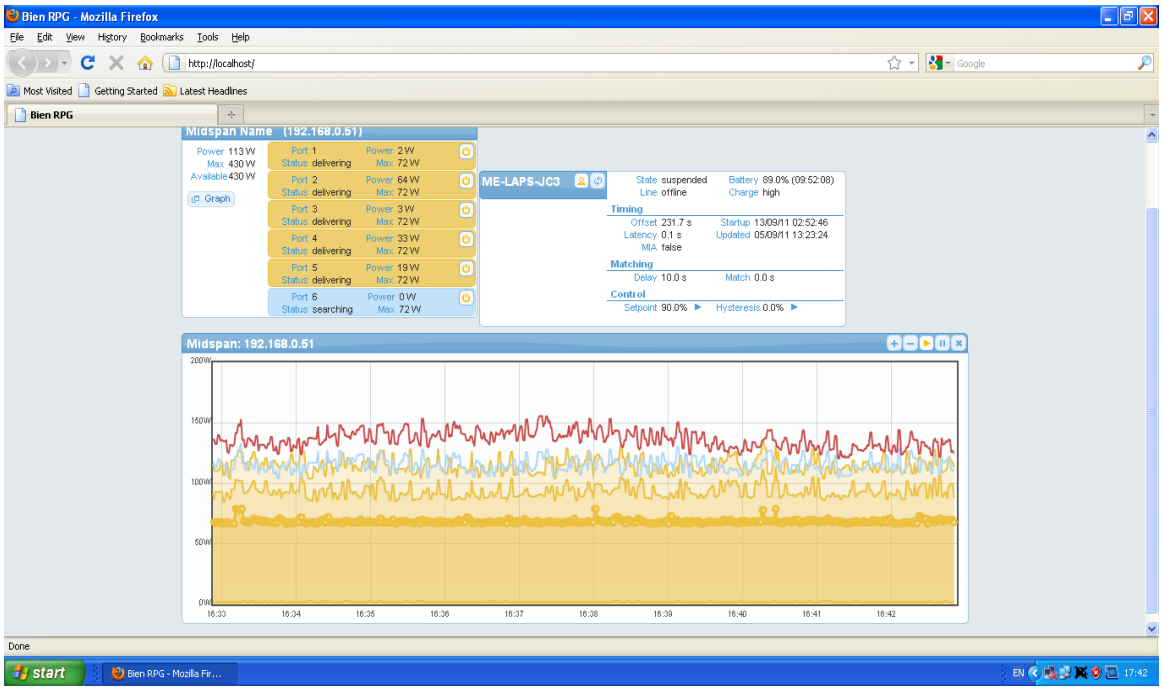

Photograph 5-12 BIEN-RPG Control Manager User Interface

The manager GUI is accessed through a standard web-browser window with the page display area sectioned into three parts. The upper left shows any midspans present on the network and lists the number and status of each of its ports (6 in this case).

The lower section of the GUI shows second by second power data from all of the devices detailed previously including the renewable supply. The 6 PoE loads on the network are shown progressively aggregated in yellow on the graph to give total PoE consumption in Watts. The red trace in the graph is PV power generated on secondary vertical axis. The upper right section of the GUI window shows attached participating loads matched to particular ports on the midspan. This section contains settings required to control individual device battery behaviour and limits from a central network location. In the example figure, a laptop, ME-LAPS-JC3, is attached to port 2 and has been given a battery set point of 90% state of charge to which the device is maintained. Other coded settings include the ability to reduce oscillation about this set-point through allowing a hysteresis band and the ability to delay control action and also allow for network latency effects.

5.5. RESULTS & ANALYSIS

Data was gathered from the system at 1Hz, detailing power at each port. This data was filtered to reduce noise with a 1min running average and the consumption of the midspan itself accounted for and added. Figure 5-3 shows the cumulative demand of the entire network as separated into constituent loads. The graph is presented with the dividing line between ‘baseload’ and controllable load (laptops) shown in black, hence baseload for the network is around 110W as expected.

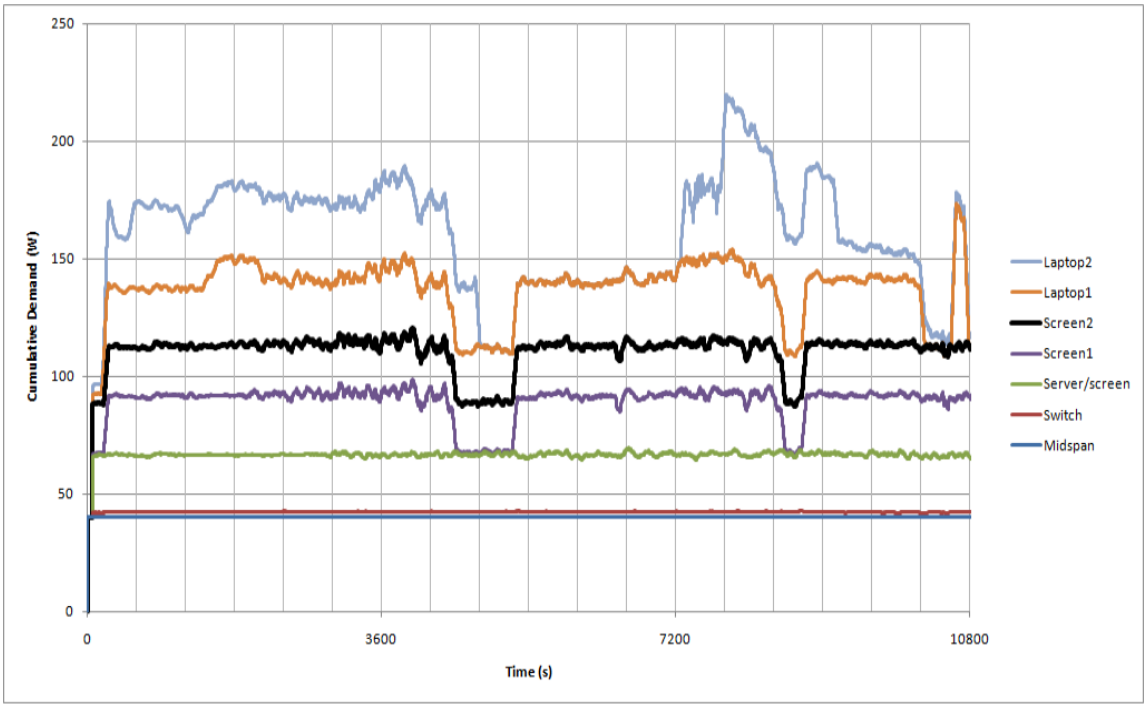

Figure 5-3 Cumulative Measured Network Demand by Device

Each laptop adds 20W nominal baseload to the network plus charging power when being powered from the network and disappears from the measured demand while using its battery. This is seen by considering the graph in three parts with the first section showing both laptops being used normally. The second section shows one laptop disconnected and running on battery back-up, hence zero demand for the device until the third period where it is re-attached and recharges, pushing network demand to a 220W peak.

Figure 5-4 shows the same baseload and laptop data but overlaid with output from the array installed on the roof of the James Weir building of the university campus in Glasgow. The day in question, 26th April 2011, was a fine dry day with a good deal of sunshine to begin with, clouding over somewhat later on. Given the time of year, the array was therefore only at about 75% generating capacity but still roughly within the band required to minimise import export by implementing the control. The scale chosen for the array against the nominal demand is therefore deemed a reasonable choice. This result would also suggest that the system will experience a nominal supply greater than baseload for 6 months of the year.

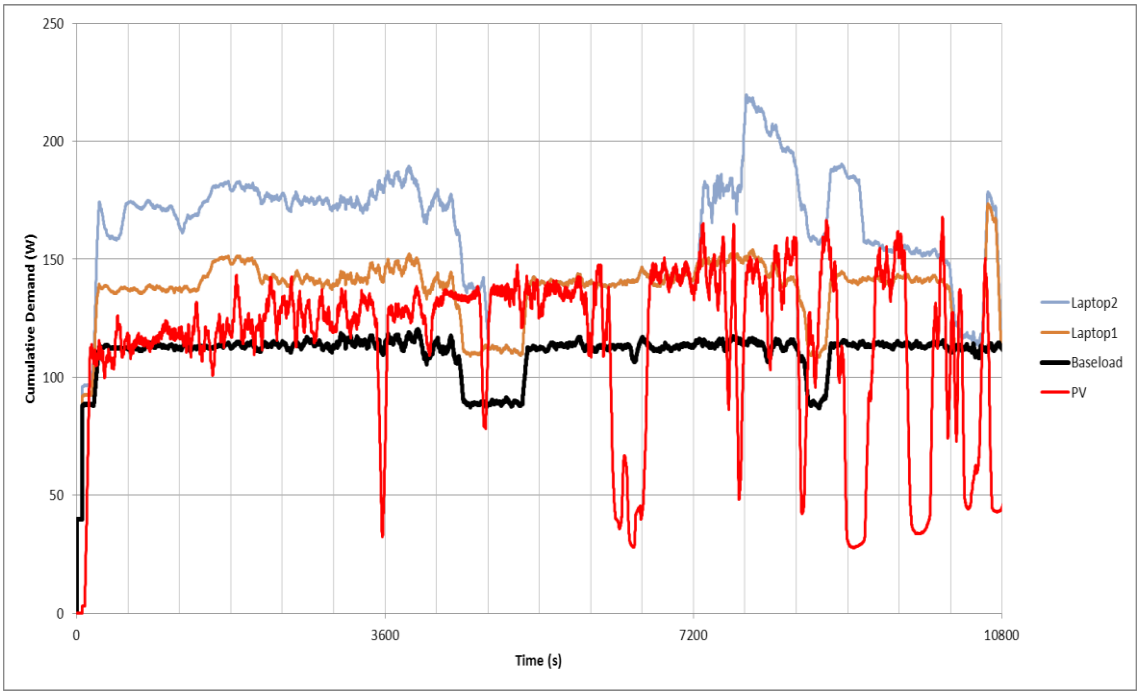

Figure 5-4 Comparison of Raw Network Demand and PV Availability

A more conventionally qualitative and scientific analysis of weather conditions on that particular day is given by Figure 5-5 from an online weather reporting service which gathers data at 5min intervals from locations across the UK [Weatherspark]. The data is from the Glasgow Airport meteorological station around 10 miles west of the array site and so can only be used as a very rough guide to local conditions.

In particular, the hourly cloud cover fractions reported for that day roughly correlate with actual data gathered but only in general terms. An issue is that this common form of weather reporting makes no distinction between 50% cloud cover due to lots of diffuse cloud and 50% erratic cover due to low level cumulus covering the array for 50% of the time. Each of these conditions has a profoundly different effect on output power as was discussed in Chapter 2.

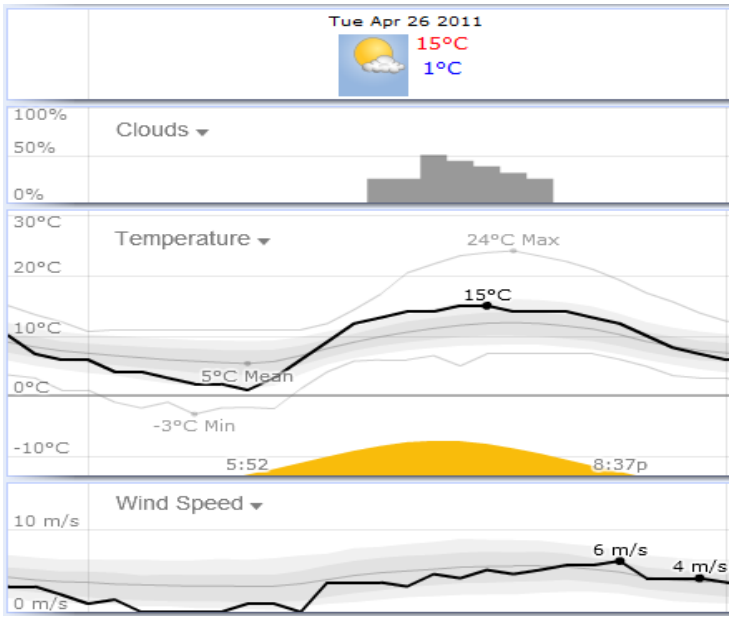

Figure 5-5 Comparative Historic Meteorological Data [Source: Weatherspark]

The second trace below, Figure 5-6, shows two periods of closed loop network control.

These are highlighted as red areas against open loop before, between and after these periods for contrast. In this controller test, the control set-point was set to zero i.e. aiming for total self-sufficiency for the network. The figure shows two traces; the power balance of the network at the single point of entry (the midspan) and PV generation during this time for comparison and reference. Note that PV generation was fairly constant for most of the test period.

The action of the control during the first controlled period resulted in demand reduction until import of energy was avoided. The second controlled period shows an artificially increased load so that export of PV was avoided. The remaining areas of the graph show periods where demand was not controlled for comparison.

In terms of energy, just under 1Wh import was avoided during the first active period with around half this amount of export avoided in the second. This amount of energy is consistent with what would be expected of one laptop being switched out of the network in the first instance and one being added to the network in the second as was actually

the case. Although this was a short duration test, the control is seen to manipulate network demand as intended to achieve the control objectives defined.

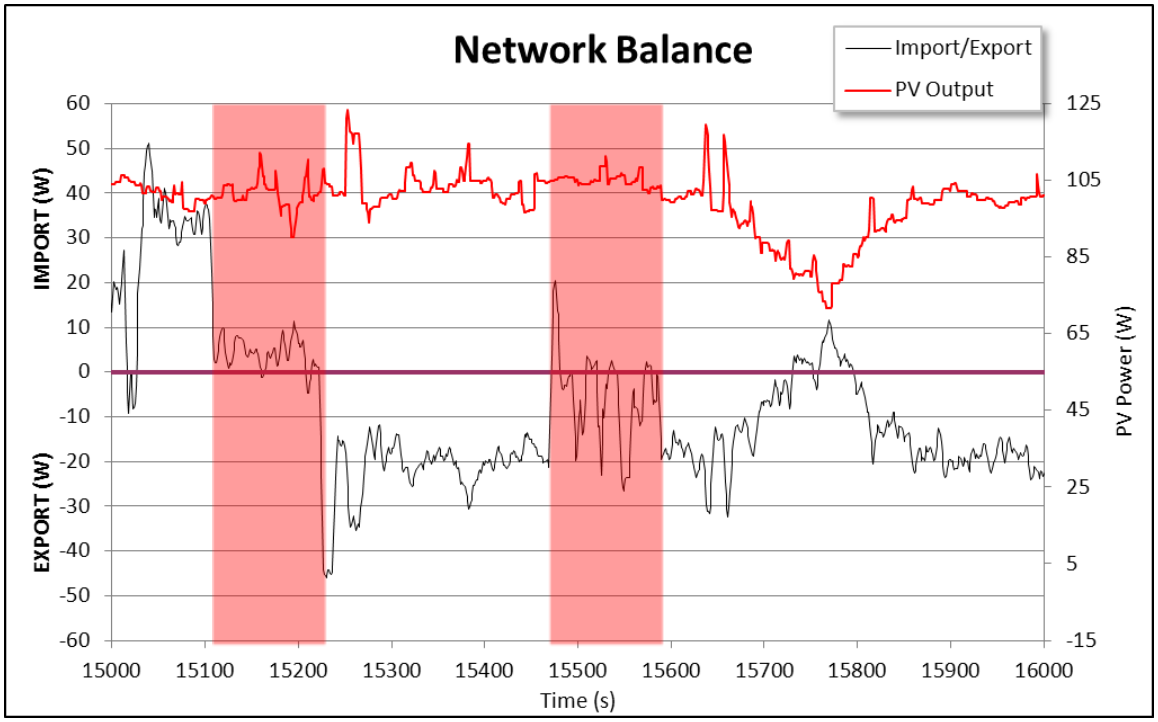

Figure 5-6 Closed Loop ICT Network Control Result

It can also be seen on the network balance test that closed loop control did not achieve true balance, as is shown by dither of the signal around the set-point during the active control periods. This is due to the quantisation effect of having only one controllable laptop in a small network representing greater than ~10% of total controllable load. Quantisation error can be reduced by increasing the number of controllable devices using the preferred implementation method described in Chapter 3. In general, doubling the number of laptops utilised by the control will have the effect of halving this error. Figure 5-7 illustrates this with comparison of quantisation error magnitude for two and four controlled loads respectively.

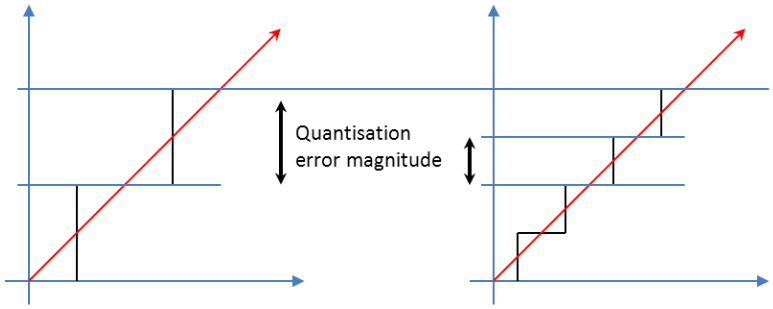

Figure 5-7 Illustration of Quantisation Error

Even with this very small scale system, controlling demand to match an intermittent renewable supply such that nearly all of the zero carbon local generation was utilised in-house was possible given the conditions of the test. Larger systems with more laptops would therefore be able to cope with a more volatile supply and to a more precise set-point.

5.6. SUMMARY

Three key aims of this trial were realised; an experiment in sizing of the system components for dynamic control, monitoring of demand and supply for the network as a whole and implementation of the demand control regime in a simple manner which does not interfere with normal operation of the laptops in question. The role of embedded energy storage as the mechanism for control was verified and shown to work even for this small system with the controller designed.

5.7. REFERENCES

IEEE Std 802.3af-2005
ANSI/IEEE802.3-2005, *Carrier Sense Multiple Access with Collision Detection (CSMA/CD) Access Method and Physical Layer Specifications, Amendment 3: Data Terminal Equipment (DTE) Power Via the Media Dependent Interface (MDI), 2005*

IEEE Std 802.3at-2009
ANSI/IEEE802.3-2009, *Carrier Sense Multiple Access with Collision Detection (CSMA/CD) Access Method and Physical Layer Specifications, Amendment 3: Data Terminal Equipment (DTE) Power Via the Media Dependent Interface (MDI) Enhancements,* ISBN: 9780738160436

Jones A, Underwood C, *A Modelling Method for Building Integrated Photovoltaic Power Supply*, Journal of Building Services Engineering, pp167-177, 2002

CHAPTER 6 - CONCLUSIONS AND FURTHER WORK

The key findings of this thesis are summarised in this chapter and an assessment also given of the potential impact of the work. The thesis concludes with recommendations regarding improvements to the control method.

6.1 CONCLUSIONS

Energy policies worldwide are encouraging corporations and other businesses to face the challenge of mitigating the environmental impact of rising electricity consumption by adopting a structured approach to demand reduction, conservation and energy management.

Demand and emissions reduction measures through improvements in building stock are an important initial step but these one-off gains are steadily eroded by growth in operational electricity consumption through increasing ownership and saturation of ICT and consumer electronics appliances in the workplace. Although these operational carbon emissions can be reduced by active demand management of appliances, overall impact is fundamentally limited by the high CO2 content of the electricity supply.

Investment in a building integrated renewable energy technology can reduce carbon intensity of electricity supply and further off-set demand but a critical lack of integration with demand management controls results in poor utilisation of this valuable resource. A more holistic and integrated approach to management of assets is therefore needed to fully exploit the potential of this low carbon source of electricity as part of a building integrated low carbon electricity management system.

How to control demand to utilise an intermittent low carbon resource in a reliable and robust manner is an important question answered in this work.

The primary objectives of this research were to:

a) Develop a demand management controller which reliably utilises a building integrated renewable energy resource within an ICT network without compromising appliance functionality.
b) Design and development of an integrated deployment strategy suited to the needs of stakeholders based on an interoperable approach using an ICT platform.
c) Demonstrate application of the controller in an operational office environment.

Key assumptions made in working towards these objectives are that, by its nature, availability of a building integrated renewable energy source is uncertain and similarly, demand in ICT networks which feature mobile computing devices is also naturally uncertain. These assumptions are deemed representative of building integrated renewable generation and networks of mobile demands in general.

However, neither of these assumptions is easily compatible with present demand management methods and so a novel approach to the control problem of reliably matching an intermittent building integrated source of renewable energy with uncertain demand in the building has been investigated and developed. As an alternative to traditional model-based predictive forms of demand management, the proposal of applying feedback control methods to the problem potentially brings far greater benefits than the conventional approach.

The objectives of the controller were defined as minimising import and export of electricity and minimising the environmental impact of the system. These two goals are defined as primary key performance indicators of the effectiveness of closed loop control over the system of building integrated assets from the viewpoint of the owner.

A feature common to all generating technologies is a level of emissions attached to electricity generated. From the perspective of an emissions conscious demand in a network consisting of multiple different sources, it is therefore desirable that the lowest carbon electricity supply be preferred over others. In a building integrated context

where ownership is of both a low carbon source and an emissions conscious demand, use of electrical generation from owned assets is even more important.

Control action is therefore required when full utilisation of the identified renewable by demands is not achieved. The error signal in this novel approach is carbon intensity of the fuel mix supplied to loads since this parameter is common to both grid and building integrated renewable energy supplies and, importantly, couples twin concerns of carbon emissions and electrical energy costs to the owner. This allows a SISO approach. Casting the control to reject both the real demand and the renewable supply as disturbances results in the control objectives as defined and further ensures that the control only acts when there is storage capacity and a renewable supply, hence security of conventional supply to loads is maintained. Modern control theory using feedback methods allows a simple, but not too simple, approach to capturing the essential dynamics of a system through model order reduction techniques. In present context, reduced order representations of energy storage, network elements and renewable supply allows plant description and control as a zeroth order system with a PDF type controller chosen as this form of controller can give superior nonlinear performance over other variable structure controllers. Nonlinearities exist in the control range in the form of battery saturation and current limitations and a method of maintaining control during these events was implemented.

A single input single output control brings a measure of inherent scalability to the system since, from the perspective of the input, demand always consists of an uncontrollable load element in parallel with a storage element. This is valid at the individual device level and also in a network of devices. The relative magnitude response of the aggregate controlled plant in a network context can be tempered by natural diversity and so in contrast to most alternative control methods, scaling the system up presents relatively few problems and can actually improve performance.

Two strategies for control of load elements were discussed; maintaining the set-point of all loads on the network equally at some chosen value and ranking individual storage elements for control selection based on state of charge. Although the former is recognised as the simplest implementation method, availability and response of the plant to instruction from the control cannot be relied upon and so the latter

implementation strategy allows refinement of the plant response to specific solar conditions and a more precise control in reducing quantisation error.

The relative scales of both building integrated renewable and available storage capacity are therefore identified as critical in ensuring robustness of the control. If sized correctly, the integrated system can optimise its own carbon emissions without advance knowledge of either supply or load over a wide range of conditions.

A significant failing in many demand management systems is deployment cost. The deliberate strategy adopted in the present case is focused on deployment as an integrated ICT product and so utilises state of the art in unified data and power distribution using already present building integrated Ethernet networks as the transfer medium and thus eliminating the need for expensive and proprietary alternatives. Adoption of IEEE ratified Power over Ethernet therefore ensures interoperability between components in a manner already familiar to building operators and IT managers, reducing maintenance costs.

In a new build office, this DC distribution method could reduce or even replace the need for blanket coverage of expensive AC infrastructure, drastically reducing investment in AC sockets and trunking.

Critically for this technology, its topology also allows retro-fit to existing Ethernet networks in buildings and importantly, the IEEE802.3 platform is under continuous development by industry standards authorities and is easily adapted to other potential control targets, eliminating the restrictions of vendor lock-in to a narrow range of hardware while remaining relevant throughout the long lifetime of the low carbon generating plant through a fast response to requirement changes.

The case study and results presented details full implementation of the concept building integrated low carbon ICT network in an operational office environment using the novel control, implementation methods and deployment technologies described above. Simulated and actual results from the control are highly encouraging and demonstrate closed loop appliance level control of a building integrated but grid-connected low carbon renewable source of electricity without compromising power supply to uncontrolled plant. The unified data and power deployment technology was seen to be

both robust in operation and highly valuable in providing relevant high quality sensory data from individual appliances, thus allowing a more refined control implementation strategy.

In summary, the novel demand management control developed in this work allows utilisation of electricity from a building integrated renewable asset in a reliable and robust manner to minimise emissions from electricity demand in offices and other ICT intensive areas, increasing the value of the complete integrated system of assets to the owner.

6.2 SUGGESTIONS FOR FURTHER WORK

This thesis has taken a holistic approach to integration of renewable energy in buildings. Given its novelty in several areas, the building integrated low carbon electricity network and closed loop control developed in this thesis are by no means the finished articles and several improvements and refinements are recommended which could improve control performance and thus resource utilisation.

The control set-point input represents the goal of a closed loop feedback system. In the present work, this was chosen to be an idealistic value of zero i.e. no transfer of energy across the system boundary. In reality, there will be an optimum import or export based on the relative carbon intensities of the sources and demands which may or may not result in an optimum zero energy transfer. By varying the set-point to represent this value, reachability and hence performance of the control could be improved.

Although the control as designed and implemented does not require advance knowledge of either supply or demand, prediction of future carbon intensity could improve effectiveness of the control. In addition to indicating potential sources of data regarding carbon intensity of grid generated electricity, a background study of the feasibility of using condition monitoring techniques to dynamically predict solar availability highlighted several potentially valuable research avenues in dynamic modelling of both the plant and in prediction of meteorological input conditions.

The relative scales of PV to energy storage to baseload demand in terms of both power and energy were identified as being critical to operational robustness of the control through natural daily and seasonal variations in demand, supply and storage capacity. Given that in the one-way network topology chosen, stored energy can only supply a single load, these ratios will change dynamically with conditions and therefore also optimum robustness. Although the scale of an array is fixed, the relative proportion of uncontrolled baseload can be tuned for system scaling at the design stage by adopting a 'new uses' policy to include other ICT devices such as the desktop monitor as usage of this device in particular is coupled to operation of the mobile PC. Similarly, the capacity of energy storage available can be augmented by incorporating other embedded storage devices such as UPS for example.

Internal to the control, the tuning constants of the governor reflect these requirements for robustness in a manner which also incorporates stability, sampling frequency and actuator bandwidth. Further work is identified in defining the range of these parameters to suit particular designs, perhaps using a genetic auto-tuning algorithm [Counsell, Zaher 2010]. Given the type of controller and relative degree of the system, sampling rate and rates of change of load are the primary influences on stability.

Some of the issues in appraising this system in terms of cost benefits were highlighted. These issues could be explored with further research.

Note that the control is not domain specific and dependant on Ethernet distribution; larger AC plant may be eligible for control if they can be acceptably modelled to be compatible with the controller and feature an Ethernet port for communications and an appropriate actuator. In addition to nominal sizing, there is also the opportunity to control fleets of embedded storage on a seasonal basis as well as daily and minutely, potentially increasing overall utilisation and value significantly. At present, a justified strategy for sizing of these components is not available.

6.3 PERSPECTIVE

The novel control and network topology as presented is aligned with corporate energy policy, CSR and other initiatives by allowing ICT asset owners to increase the value of their networks by minimising its carbon emissions and electricity costs through utilisation of a building integrated low carbon generating technology. Importantly, this is achieved as a closed loop system i.e. entirely managed by the asset owner and not reliant or dependent on any external third party. The control and topology proposed is also highly flexible and allows additional load, energy storage and low carbon generation to be added in ratio hence the structure is scalable and also highly adaptable since power supply to the controlled plant is not AC or DC domain specific. As a tool, the method described provides a means by which corporations can progressively reduce demand and emissions in a cost effective and transparent manner in the confidence that since the ICT network is utilised for control purposes, future interoperability is assured.

It is further suggested that this approach to demand management in general is also aligned with strategic energy policy on increasing the penetration level of distributed and building integrated renewables to reduce carbon emissions from large scale generation. Traditionally, a highly distributed, high penetration scenario has posed significant problems for network operators in maintaining stability due to increased uncertainty at lower levels in the distribution network. By actively matching building integrated renewable generation with local demand at this level, uncertainty in both supply and demand is reduced for all stakeholders with the beneficial consequence to the network operator in particular of increased local capacity factor, less strain on sub-stations and potentially avoiding investment in reinforcement and upgrades necessary through conventional DSM methods.

By applying a fundamentally different approach to the problem of managing electricity demand and emissions in buildings, it is hoped that the work contained in this thesis satisfy the desire for a readily deployable solution suited to industry's needs while also providing a platform for further research and exploration of other building integrated opportunities.

6.4 REFERENCES

John M. Counsell, Obadah S. Zaher, Joseph Brindley, *Auto-Tuning for High Performance Autopilot Design Using Robust Inverse Dynamics Estimation*, Fifth International Multi-conference on Computing in the Global Information Technology, pp.10-17, 2010

APPENDIX A ROBUST CONTROL THEORY

This section is given as a brief overview of robust feedback control theory as applied to the problem of matching an uncertain energy supply with an uncertain energy demand. Robust control is a branch of modern control theory which deals explicitly with uncertainties.

Two basic engineering assumptions in design of feedback control systems are that there is zero benefit in driving a system faster than it can respond and that past measurements are of no use. These assumptions result in a sensible starting point in design of a control for a real system that the actuator dynamics and the feedback sensor dynamics are such that they can be ignored. This is given in the following general rule of thumb for a closed loop bandwidth g which gives the time constants of both the actuator τ_a and the system τ_s as inversely proportional to this bandwidth:

$$\frac{1}{\tau_a} >> 3 \cdot g$$

$$\frac{1}{\tau_s} >> 3 \cdot g$$

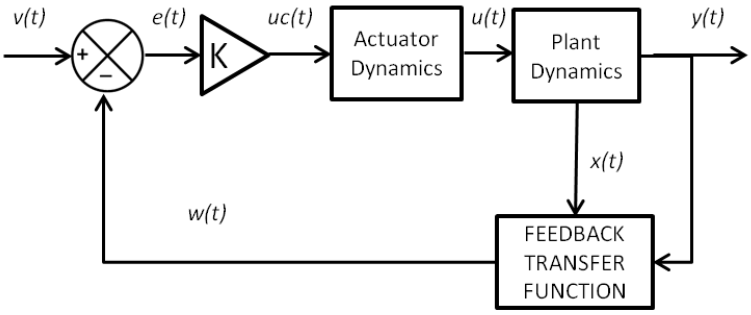

Figure A-1 Block Diagram of a Real Feedback System

For the feedback control block diagram of Figure A-1 these assumptions result in:

$$u_c(t) = u(t)$$

$$w(t) = f\left(y(t), x(t)\right)$$

Omission of these influences results in a more idealised representation as shown in Figure A-2.

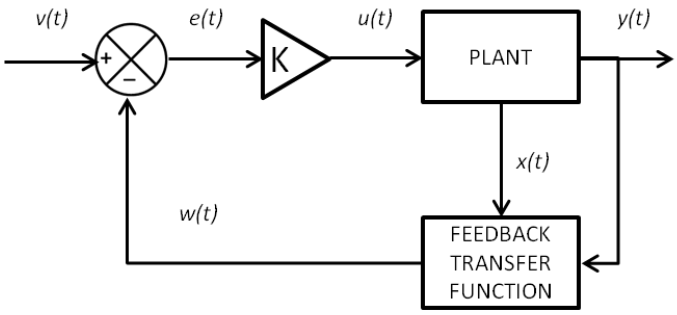

Figure A-2 Block Diagram of an Ideal Feedback System

Hence, real systems can be represented by idealised block diagrams in feedback control provided the system is not driven at too high a bandwidth.

For a simple first order plant model, the describing ordinary differential equation (ODE) is given by:

$$\tau \cdot \frac{dy}{dt} + y(t) = K \cdot u(t) \qquad \text{Equation A-1}$$

Where $u(t)$ and $y(t)$ represent the input and output time varying signals respectively, K is the gain and τ the plant time constant. In the Laplace domain:

$$L\left\{\tau\cdot\frac{dy}{dt}+y(t)=K\cdot u(t)\right\}\rightarrow\tau\cdot\left(sY(s)-y_0\right)+Y(s)=K\cdot u(s)$$

$$(\tau s+1)\cdot Y(s)=K\cdot U(s)+\tau\cdot y_0\rightarrow Y(s)=\frac{K}{\tau s+1}\cdot U(s)+\frac{\tau}{\tau s+1}\cdot y_0$$

Hence the Laplace form transfer function for a first order plant:

$$G(s)=\frac{K}{\tau s+1}$$

An idealised first order feedback controlled system is shown in Figure A-3in Laplace domain notation with control defined simply as some proportional gain K_p

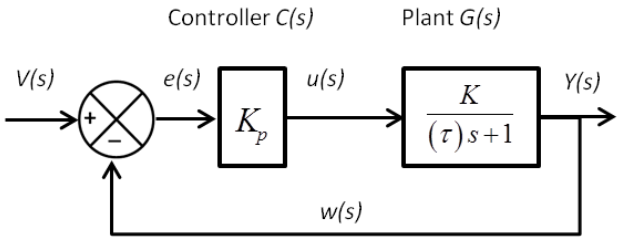

Figure A-3 Ideal First Order Feedback Control Loop Block Diagram

The describing equations around the loop of Figure A-3 are given as:

$$e(s) = V(s) - Y(s)$$

$$Y(s) = G(s) \cdot u(s)$$

$$u(s) = K_p \cdot e(s)$$

By substitution, the output signal is therefore:

$$Y(s) = G(s) \cdot K_p \cdot \left(V(s) - Y(s)\right)$$

$$Y(s) = \frac{K_p \cdot G(s) \cdot V(s)}{1 + K_p \cdot G(s)}$$

This gives the closed loop transfer function for the controlled system:

$$\frac{Y(s)}{V(s)} = \frac{K_p \cdot G(s)}{1 + K_p \cdot G(s)}$$

Tracking a Setpoint

According to final value theorem and in the Laplace domain, the tracking phenomenon occurs when $s \to 0$ and $Y(0) = V(0)$:

$$\frac{Y(0)}{V(0)} = \frac{K_p \cdot G(0)}{1 + K_p \cdot G(0)}$$

This equation tells us that providing $G(0) \neq 0$ and $K_p = \infty$ then $\frac{Y(0)}{V(0)} = 1$. This is Bode's principle of high gain [Bode H W, 1945]. However, if $K_p \neq \infty$, then the transfer function must always be less than one, thus:

$$\frac{Y(0)}{V(0)} = \frac{K_p}{1+K_p} < 1$$

The inability of the transfer function to reach unity at anything less than infinite gain in steady state represents divergence and a failure to track the setpoint. The most common solution to this problem is to add integral action to the controller.

Figure A-4 shows substitution of the proportional gain with an integrator in the block diagram. Note that this has the effect of raising the order of the closed loop system by 1.

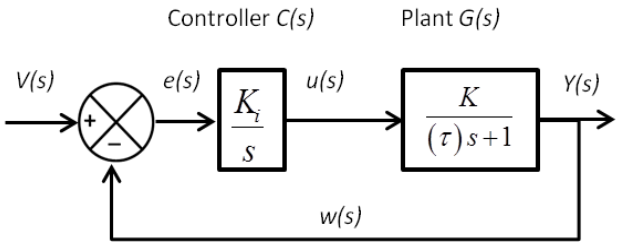

Figure A-4 Ideal First Order Feedback Control Loop Block Diagram

As before, derivation of the closed loop transfer function is given by:

$$\frac{Y(s)}{V(s)} = \frac{K_i \cdot G(s)}{s + K_i \cdot G(s)}$$

Again set $s \to 0$:

$$\frac{Y(0)}{V(0)} = \frac{K_i \cdot G(0)}{K_i \cdot G(0)} = 1$$

Hence tracking is achieved at all points within the closed loop bandwidth of the system.

Disturbance Rejection

A significant feature of feedback control methods is that of disturbance rejection. Disturbances to control can be present at the input or output to any of the system elements and represents anything in the system which distorts measurement and control in reaching and maintaining a setpoint. A disturbance $d(s)$ is added to Figure A-4 to represent such a disturbance and shown as Figure A-5.

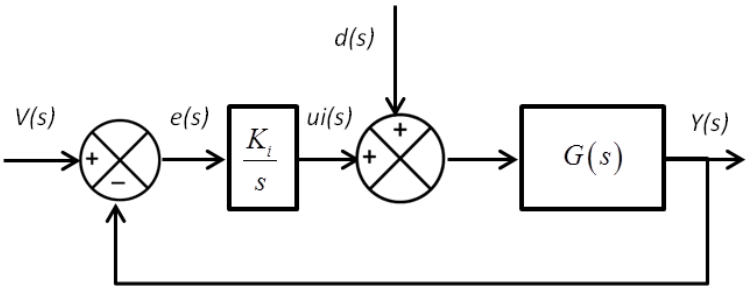

Figure A-5 Feedback Control Block Diagram with Disturbance

Analysis of Figure A-5 reveals that:

$$u_i(s) = \left(\frac{K_i}{s}\right) \cdot \left(V(s) - Y(s)\right)$$

$$Y(s) = u_i(s) \cdot G(s) + d(s) \cdot G(s)$$

Substitution in this case gives:

$$Y(s) = \left(\frac{K_i}{s}\right) \cdot \left(V(s) - Y(s)\right) + d(s) \cdot G(s)$$

$$Y(s) = \frac{K_i \cdot G(s)}{s + K_i \cdot G(s)} \cdot V(s) + \frac{s \cdot G(s)}{s + K_i \cdot G(s)} \cdot d(s)$$

Letting $s \to 0$ as before:

$$Y(0) = \frac{K_i \cdot G(0)}{0 + K_i \cdot G(0)} \cdot V(0) + \frac{0 \cdot G(0)}{0 + K_i \cdot G(0)} \cdot d(0)$$

The closed loop transfer function is therefore:

$$\frac{Y(0)}{V(0)} = \frac{K_i \cdot G(0)}{K_i \cdot G(0)} = 1$$

This equation is true for $G(0) \neq 0$ and $d(0) = C$, where C is constant, hence the disturbance to control is completely rejected.

Pseudo Derivative Feedback (PDF) Control

Phelan describes a form of controller which utilises the tracking integrator as described previously but also incorporates a derivative term from the feedback signal directly to the integrator output, hence its name [Phelan 1977]. Although the control can be used with second order systems, Phelan states that PDF control of a first order system results in zeroth order closed loop control i.e. proportional gain but no derivative term.

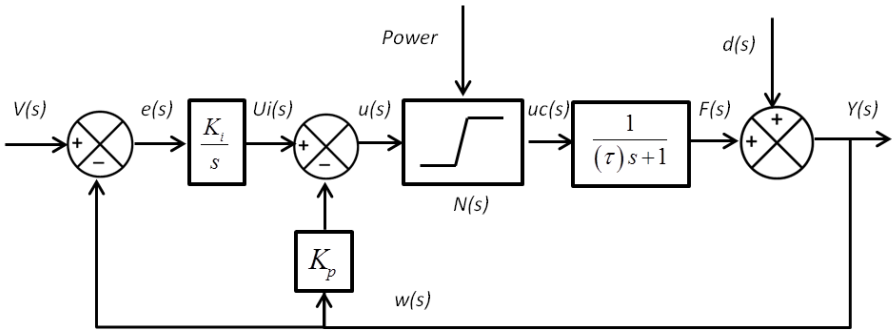

Figure A-6 PDF Controller for 1st Order Plant [Source: Phelan]

The structure of this controller for a first order plant is shown in Figure A-6 including a load disturbance $d(s)$ at the output. The loop equations for the figure above are:

$$u(s) = \frac{K_i}{s} \cdot e(s) - K_p \cdot Y(s)$$

$$e(s) = V(s) - Y(s)$$

$$uc(s) = N(s) \cdot u(s)$$

$$F(s) = \left[\frac{1}{\tau s + 1} \right] \cdot uc(s)$$

$$Y(s) = F(s) + d(s)$$

Substitution from above gives the linear output:

$$Y(s)=\frac{N(s)}{\tau s+1}\cdot\left[\frac{K_i}{s}\cdot\left(V(s)-Y(s)\right)-K_p\cdot Y(s)\right]+d(s)$$

And in transfer function form:

$$Y(s)=\frac{K_i\cdot N(s)}{\tau s^2+s+K_i\cdot N(s)+K_p\cdot s\cdot N(s)}\cdot V(s)$$

$$+\frac{s(\tau s+1)}{\tau s^2+s\left(1+K_p\cdot N(s)\right)+K_i\cdot N(s)}\cdot d(s)$$

Again, setting $s\to 0$, the disturbance is also seen to tend to zero.

For the regulation loop:

$$\frac{Y(s)}{u_i(s)}=\frac{G(s)}{1+K_p\cdot G(s)}=G_R(s)$$

The control then devolves back to the simpler structure given in Figure A-4 as both are mathematically equivalent. The closed loop transfer function is therefore given by:

$$\frac{Y(s)}{V(s)}=\frac{K_i\cdot G_R(s)}{s+K_i\cdot G_R(s)}$$

Phelan's description of load disturbance rejection is not restricted to a single instance however and the control developed for this work exploits this fact in rejecting two disturbances; the real device load represented by the load disturbance $d_1(s)$ and the grid supply through its relation with the PV supply $d_2(s)$.

$$d(s) = d_1(s) + d_2(s)$$

Stability

Stability is a primary requirement in control system design. In linear systems, if a bounded input signal results in a bounded output signal $x_a(t)$, the system is said to be bounded input bounded output (BIBO) stable.

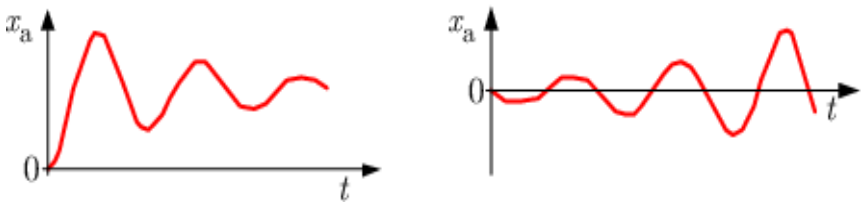

Figure A-7 Stable and Unstable System Response to a Bounded Input Signal

In the example of a PDF controller, stability depends on the values chosen for the gains and the system time constant as shown below.

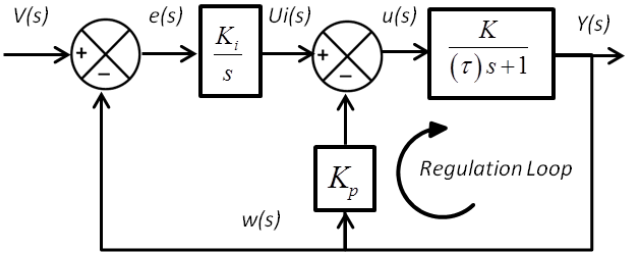

Figure A-8 PDF Controller Highlighting the Regulator Loop

Stability of the regulation loop of a 1st order PDF controller is given by:

$$\frac{Y(s)}{u_i(s)} = \frac{K}{\tau s + (1 + K \cdot K_p)} = \frac{Z_R(s)}{P_R(s)}$$

Where the numerator of the transfer function represents the closed loop transmission zeros and the denominator represents the closed loop poles. The solution to the characteristic equation $P_R(s) = 0$ gives the value of the closed loop poles.

$$P(s) = \tau s + (1 + K \cdot K_p) = 0$$

$$P_1 = -a \cdot \frac{(1 + K \cdot K_p)}{\tau} = -\frac{1}{\tau_c}$$

Where $\tau_c = \frac{\tau}{(1 + K \cdot K_p)}$ is the closed loop time constant and $\frac{K}{1 + K \cdot K_p}$ is termed the signal weighting function. A signal is bounded if there is a finite value for $\frac{K}{1 + K \cdot K_p} > 0$ such that its magnitude never exceeds $u_i(s) = UI$.

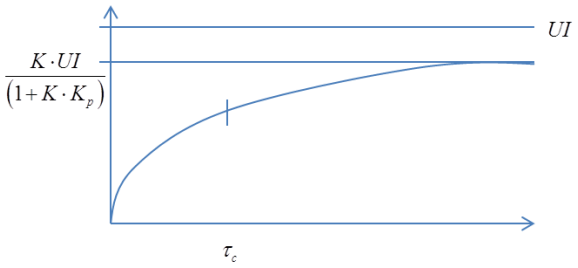

Figure A-9 Asymptotically Stable Response

This shows that stability is a system property of linear systems. If the above is valid then there can be no bounded input signal capable of driving the output to infinity and the system is BIBO stable. The parameter values chosen for K and K_p against the system time constant are therefore critical in ensuring that this is the case.

A linear system is said to be asymptotically stable if all of the roots of its characteristic equation lie in the left half of the s-plane. A system is unstable if its poles appear in the right half of the s-plane and is critically stable if it has at least one pole on the imaginary axis and none in the right half. These conditions are illustrated below and indicate that stability is sensitive to sampling rate through position on the $j\omega$ axis.

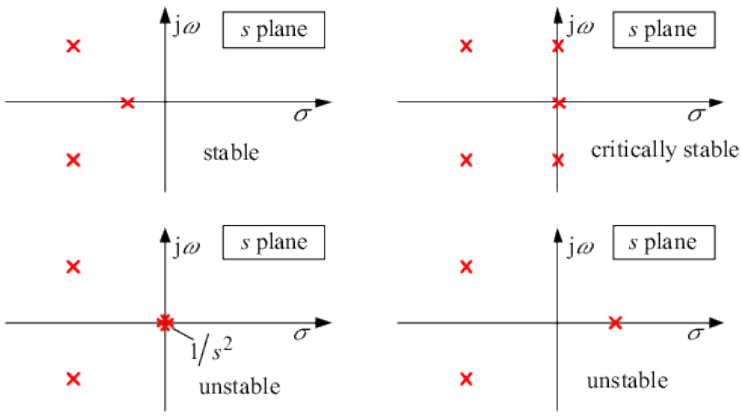

Figure A-10 S-Plane Stability Definitions

Although unnecessary at this stage, other methods of deriving stability criteria in algebraic form include Routh-Hurwitz and Nyquist methods.

The PDF controller is unique in several respects. It incorporates the desired behaviour of variable structure controllers (VSC) at limits and tracking stability of high gain proportional integral (PI) at the setpoint and as such is an improvement on both while being simpler to implement and visualise than loop shaping optimisation alternatives.

REFERENCES

Phelan R, *Automatic Control Systems,* 1977

Bode H W, *Network Analysis and Feedback Amplifier Design*, (1945)